Fall 12-16-2022

Thermoplastics 3D Printing Using Fused Deposition Modeling on Fabrics

Maxwell M. Blais
University of Maine, maxwell.blais@maine.edu

THERMOPLASTICS 3D PRINTING USING FUSED DEPOSITION MODELING ON FABRICS

By

Maxwell M. Blais

B.S. University of Maine, 2019

A THESIS

Submitted in Partial Fulfillment of the

Requirements for a Degree of

Master of Science

(in Mechanical Engineering)

The Graduate School

The University of Maine

December 2022

Advisory Committee:

Bashir Khoda, Professor of Mechanical Engineering, Advisor

Masoud Rais-Rohani, Professor and Chair of Mechanical Engineering

Douglas J. Gardner, Professor of Sustainable Materials and Technology

THERMOPLASTICS 3D PRINTING USING FUSED DEPOSITION MODELING ON FABRICS

By: Maxwell M. Blais

Thesis Advisor: Dr. Bashir Khoda

An Abstract of the Thesis Presented
in Partial Fulfillment of the Requirements for the
Degree of Master of Science
(in Mechanical Engineering)
December 2022

The creation of objects with integrated flexibility is desired and this can be achieved by additive manufacturing on fabric. We propose to use a textile fabric as a flexible joint and create to create an entire object with smaller parts called segments. Such a novel technique will bring integrated flexibility and folded assemblies using extrusion based additive manufacturing machines. The proposed process allows segments to be created flat one at a time on a continuous fabric, which will be suitable for flat to folded assemblies and eliminate size limitations of the 3D printer. Techniques considering object segmentation were used to unfold 3D models of objects into 2D patterns based on paper folding. The unfolding of models was specifically designed to allow manufacturability of the segmentations with no impedance from the 3D printer's frame, where minimal segments were also desired.

Three different textile fabrics based on cotton plain weave, plane weave acrylic, and polyester 200 denier ripstop fabrics were considered in investigations of the interfacial strength created with additively manufactured polylactic acid. Both treated and untreated fabrics were prepared simultaneously so that parts can be printed on top of them at a predefined spatial location. The

interfacial strength of additive manufactured parts printed on the fabric were also tested as a function of print process parameters, fiber morphology, fabric properties, as well as surface modification of fabrics.

The highest interfacial strength between additive manufactured materials and fabric was desired and tested for. Both adhesion peel testing and stress pull testing is used to determine the strength of the interface between the fabric and deposited additive manufactured parts. Results found that the interfacial strength reached a maximum of 5.18 $\frac{\mathrm{N}}{\mathrm{mm}}$ and 0.435 MPa. For a conceptual square shelter design a series of triangular panels were created on fabric to be assembled into the shelter. It was conceptually determined that the resulting interfacial strength could keep a 40-kilogram large triangular, panel of this shelter, held upside done from removing from the fabric, given its own weight. From this result, it was determined that the interfacial strength is strong enough for use with the creation of large heavy objects that require flexibly in them for hinges. Rough and thick fabrics were found to promote interfacial strength the greatest with higher bed temperatures, this was because of mechanical interlocking being promoted. Pre-treatments of the fabrics were found to help with interfacial strength as well and have potential with higher environmental temperatures, but not as much as mechanical interlocking. Adhesion forces desired between fabric and 3D printed parts can be tailored per specific large object as needed, per segmentation, using this information. The proposed manufacturing method helps fabricate multifaceted large single objects with localized optimum process parameters and objects with integrated flexibility. The additive manufacturing on fabric method of object fabrication addresses the anisotropic nature of additive manufactured parts by allowing parts of the object be created separately from each other. This allows each part to be tailored for specific mechanical properties to achieve desired mechanical properties for the entire object. Mechanical strength,

optimization of weight, interfacial strength, specific features or properties, and the ability to fold for storage or transportation of these objects could be tailored per application.

ACKNOWLEDGEMENTS

Thank you to Scott Tomlinson for the help through the years through both support with work at the center and thesis work. Without your support, I am unsure where the research would be at this point. Thank you to the Advanced Structures and Composites Center along with Natick for financially sponsoring my project as well as giving feedback on the direction the research should take. Thank you to my parents Stacey and Ted Blais for encouraging me in the right places and always behind me when it came to going for a Master's degree.

I would like to thank my advisor Bashir Khoda for pushing me to further this research and proving to me that this research was indeed greatly valuable. Their pushing for me to branch out and present my work to both conferences and local schools has been a great learning experience on how to make people care about what you care about. I would also like to thank my committee members Masoud Rais-Rohani as well as Douglas Gardner for taking the time to help me with my work. Masoud also helped push me into testing the mechanical strength of parts in a specific situation.

TABLE OF CONTENTS

LIST OF TABLES

LIST OF FIGURES

LIST OF EQUATIONS

LIST OF TERMS AND ABBREVIATIONS

Object – The entire product created by additive manufacturing or other manufacturing methods, is made of many parts

Part – A section of the entire product created by additive manufacturing or other manufacturing methods, typically is one of many created parts that are joined together to make the object

Additive Manufacturing – Also known as 3D printing, specifically fused deposition modeling unless otherwise specified

Interface – The bonding area between an Additive Manufactured part and fabric

Unfolding – The process of making a 2D pattern from a 3D model, normally used in making paper models

Segment – When unfolding a 3D model to 2D unfolded patterns groups of panels or parts next to each other can be considered as segments or patches, in some cases individual parts can be considered segments

PLA – Polylactic Acid, a common filament material for additive manufacturing

ABS – Acrylonitrile Butadiene Styrene

PA – Polyamide

FDM – Fused Deposition Modeling, the common method of additive manufacturing

CAD – Computer-Aided Design, also known as 3D modeling in some cases

TPU – Thermoplastic Polyurethane elastomers

TPS – Thermoplastic Styrene elastomers

CB – Carbon Black

CNT – Carbon Nano Tubes

PET – Polyethylene Terephthalate

PES – Polyester

CNC – Computer Numerical Controlled

PMMA – Poly-Methyl Methacrylate

PVA – Poly Vinyl Alcohol

DI – Deionized water

2D – Two Dimensional

3D – Three Dimensional

CHAPTER 1

INTRODUCTION

1.1 Background

The creation of large objects using additive manufacturing is desired for a variety of applications given additive manufacturing's ability to create prototypes and variations of designs quickly and affordably compared to other manufacturing methods. The use of folding origami designs to create shelters with both a folded and erected state leads to the desire to improve upon the design with additive manufacturing. However, when creating large objects by additive manufacturing creating a single large part can have a variety of complications. The major issue of additive manufacturing a large object is that there are few large 3D printers that can be used to create such large objects. Segmentation of the object into smaller parts could be done to allow smaller 3D printers to be able to create the large object but requiring post-manufacturing work to put all the parts together.

In this research, parts are additive manufactured on top of fabrics to adhere the two together and create an interfacial layer. The interfacial strength was then tested to determine if it sufficient for use in creation of objects with flexibly and create large objects. These large objects are segmentized and unfolded to allow the 3D printer the ability to create objects on one piece of fabric without colliding with previously created parts on the fabric. These parts would then be created on top of the piece of fabric where they will bond to the fabric creating an interface between them. Once all additive manufactured parts are created on the fabric all excess fabric could be cut off and the part folded up into itself to assume the shape of the desired object or to make the parts easier to transport. The ability to create all parts one at a time but keep them all connected allows smaller 3D printers to create large objects while lowering the amount of post-

manufacturing needed. Depending on the segmentation, interlocking parts could be included lowering any connective parts that would need to be created to keep the object erected in its desired shape.

1.2 Creation of Large Objects by Additive Manufacturing

The creation of large objects using additive manufacturing involves the creation of a singular large object or the creation of this large object as small, segmented parts to be connected afterward. However, there are problems with both methods.

For the creation of a large singular object, the accessibility to a large 3D printer to create an object of large size is very low given how few large 3D printers exist currently. Large additive manufactured objects will also be anisotropic given the printing method of the material which may not be desired. Objects will also be created with large bead widths and layer heights which may create a part of lower quality than expected, bed widths and layer heights being related to the amount of material deposited by the 3D printer each layer. Thermal deformation also has a big impact on larger additive manufactured parts and could cause unwanted deformation.

The creation of a large additive manufactured part by segmentation can have problems with the saliency of the object as the segmentation requires some changes to the object overall. Each segmented part can be set up to be created on any size 3D printer as desired. Being able to curate how each part is created can be used to solve the problem of anisotropy that a large singular additive manufactured object would have. Segmentation into smaller parts has problems when trying to combine all the parts into the desired large object as considerably more post-manufacture work would be needed.

1.3 Applications for Additive Manufacturing on Fabrics

The use of additive manufacturing on fabrics should allow small 3D printers the ability to create large objects. This is done by having segmented and unfolded objects created using Graph theory to allow one part to be printed at a time on a piece of fabric at specific locations on the fabric. Once all pieces are printed on the fabric all excess fabric can be cut away and the parts can be folded into place. The pieces fold into the large object that is desired with less post-manufacturing than creating all segmented parts separately. This also allows the object desired to not be anisotropic and the ability to have the object fold up into a state easy for transportation. Additive manufacturing on fabrics allows a new method of creating large additive-manufactured objects. It is also meant to combine the fields of textiles and additive manufacturing to create new objects not normally possible with additive manufacturing alone.

1.4 Motivation of Research

The motivation of this research is to explore the ability to create large additive manufactured objects with small commercial 3D printers. To create large additive-manufactured objects without the anisotropic properties that a single additive-manufactured object would have. Additionally, it explores the ability to have the finished object change to a folded state that would be easier to transport.

1.4.1 Scaling up to Large Scale

Additionally, large objects made by additive manufacturing on fabric with a large 3D printer could also have benefits depending on what is desired and is available. A large 3D printer could create much larger singular parts as desired and likely could print all the parts desired at once instead of one at a time. This would allow the large 3D printer to create a large object without the undesired anisotropic properties and the potential ability of a folded state of the object for

transportation. This method has not been tested on a large-scale 3D printer yet but is one of the goals of the research going in the future.

CHAPTER 2

LITERATURE REVIEW

2.1 Introduction

Additive manufacturing allows products to be created fast, the ability to create complex objects, also while being cost-efficient. The 3D printers also allow flexible and complex changes in design and are easy to operate for production. Additive manufacturing can be used to create products related to electronics, military, architecture, furniture, prototyping, education, and as construction products. However, currently small, fused deposition modeling (FDM) 3D printers are the common printer used for additive manufacturing. Because of the size limitations of these small printers, they are often not useful for the creation of large objects or objects with flexibility in them. This would require the use of a large-scale 3D printer to create full-scale objects as desired at low cost, or the segmentation of parts which would require a great deal of post-manufacturing. Incorporation of these large printers has various problems with the greatest being that large 3D printers are not common. Large 3D printers, becoming more common with several manufacturers. These printers can accommodate large objects as desired however the price for them is far more than many small companies could afford. [1]

Additive manufacturing on top of fabrics to create a composite has been a topic of research for the past few years with Korger et al., Grimmelsmann et al., Sabantina et al., and Pei et al. being notable early research papers [2] [3] [4] [5]. Interfacial strength, or adhesion strength, measured in $\frac{\mathrm{N}}{\mathrm{mm}}$, is obtained using the peel adhesion testing method DIN 53530. The literature review indicated that the materials used, pre-treatments applied to the fabrics, and process parameters affect the interfacial strength of the additive manufactured parts to the fabric. Research in these papers involved found different that combinations of fabrics and deposited materials from the 3D

printer acquire varying results. Changes in nozzle height from the print bed was also found to be a great factor, as well as other 3D printer process parameters. Testing of different fabrics and deposited materials when the fabrics were washed found the changes in material properties of the fabric affect the interfacial strength of samples. Different combinations of different fabrics and the creation freedom of printing different 3D shapes and composites explored the potential of creation products not normally possible with traditional manufacturing as well [2] [3] [4] [5].

In this research, the goal is to use traditional paper unfolding to segment 3D objects into 2D unfolded patterns. The 2D models are then additive manufactured one part at a time on top of fabrics to join them during manufacturing and add flexibility within the object allowing. This allows the ability for the object to change between a flat and an assembled state as desired. The process is envisioned to create large objects with small 3D printers that wouldn't normally be able to be created, this could also help with other applications as well as the potential of ease of transportation. Otherwise, the added flexibility to objects can allow the potential to create products that are not normally possible to create without additive manufactured on fabrics. This research builds on prior work dealing with 3D to 2D unfolding of models and testing of the interface between additive manufactured parts created on fabrics and the type of fabrics. The testing of the interface between additive manufactured part and fabric is specific to the kinds of fabric used, the pre-treatments used on the fabrics before part creation, the process parameters of the 3D printers used, and the strengths of the 3D printed parts themselves.

2.2 Additive Manufacturing on Fabrics

2.2.1 Kinds of Fabrics and Filaments Used

Different combinations of textile materials and filament polymers were used in adhesion peel tests. Of these fabrics two polyesters, a combination of wool and polyester, wool, and cotton

fabrics were tested, with the thicker woven polyester (PES) fabric having the highest interfacial strength at the interface. Polylactic acid (PLA) filament was found to promote the highest interfacial strength when used to create the sample compared to acrylonitrile butadiene styrene (ABS) and polyamide (PA) 6.6. From this testing, it was determined that PLA would be the preferred option for the polymer filament going forward and the thicker fabrics that promote physical form-locking between fabric and polymer. Maximum adhesion strength at the interface between fabric and 3D printed part was found between the PES fabric and PLA at 3.5 $\frac{\mathrm{N}}{\mathrm{mm}}$, [3].

Maximum elongation tests were performed on the composite created by additive manufacturing NinjaFlex filament on fabrics, different additive manufacturing patterns were used for samples. When additive manufacturing on fabrics the z-distance, the distance between the nozzle and the print bed of a 3D printer, cannot always remain the same because of the thickness of the fabric on the print bed. For fabrics with substantial thicknesses the z-distance must be set higher than normal to prevent sample creation failure from the fabric being moved by the nozzle or material backing up in the nozzle.

Two polyester fabrics were tested with one being particularly elastic and flexible than the other with both being warp knitted fabrics. Cyclic loading tests were done at a speed of 80 mm/min for 10 cycles and elongation tests were done by stretching samples to 108% elongation. Four different samples were tested as to determine any difference in maximum force at break between for different morphologies. This involved fully solid parts, parts with square grid-like holes, honeycomb holes, and circular holes as shown in Figure 2.1. A grid style part was created with the z-distance normally used on the print bed and the less elastic fabric had the greatest strength before a break given a maximum force of about 450 Newtons. Maximum force of any composite was found to be much greater than the additive manufactured part itself, which was around 50

Newtons for the same elongation. Figure 2.2 shows the maximum strength of the samples when exposed to 108% elongation or when the samples broke. All composite samples created on fabric broke in this experiment while all samples not created on fabric had to be stopped at 108% elongation. The purely additive manufactured parts were able to be elongated by a significant amount compared to those created as composites. The use of different patterns of additive manufactured parts and different fabrics could be tailored to get desired mechanical properties of the product depending on the application [6].

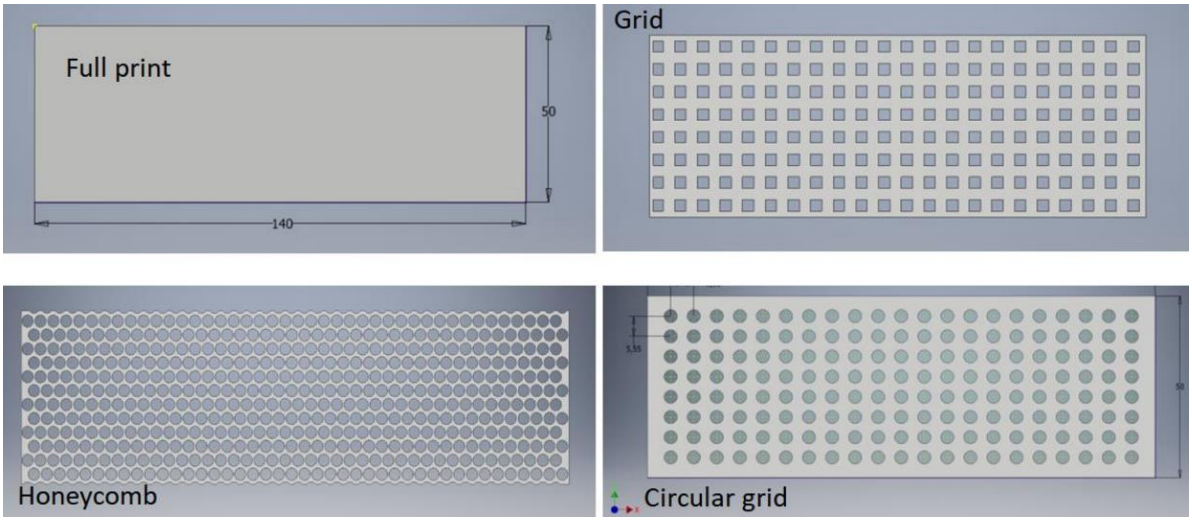

Figure 2.1: Patterns of samples created by 3D printing on warp knitted fabrics [6]

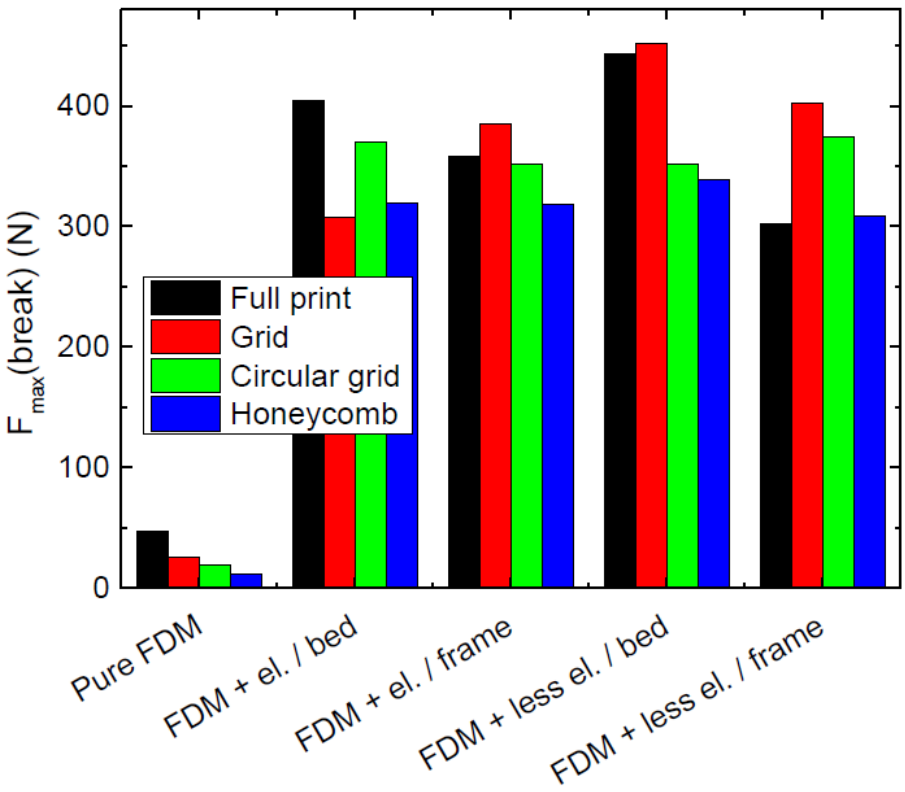

Figure 2.2: Maximum force at break or at maximum elongation of composite samples, this was true for the pure FDM created samples, FDM referring to the additive manufactured parts, el. and less el. referring to the elastic and less elastic fabrics, bed and frame referring to the additive manufacturing of samples at standard z-distance or using one farther away from the fabric [6]

Polyester, cotton, and wool were peeled adhesion strength tested, using the DIN 53530 standard, with various thicknesses with PLA and Ninjaflex filament printed on them. Thicker fabrics did better, and this was concluded to be because of the form-locking connections of the additive manufactured polymer to the fibers on top of the textiles as well as the inside of the textile structure. The Ninjaflex polymer performed relatively well with the PLA counterparts in terms of adhesion strength, potentially allowing the creation of bendable applications given the polymer's high flexibility. Results of the samples are shown in Figure 2.3, where a trend of higher interfacial strength the thicker the fabric used is observed.

Influence of the chemical properties of the textile were found to also affect interfacial strength, specifically referencing the hydrophilicity or hydrophobicity of the textile. The washing or lack of washing, and plasma treatment of the fabrics are desired to change the properties of the fabrics going forward. This shows the potential of pre-treatments, such as washing, to fabrics before sample creation as to increase the interfacial strength [2].

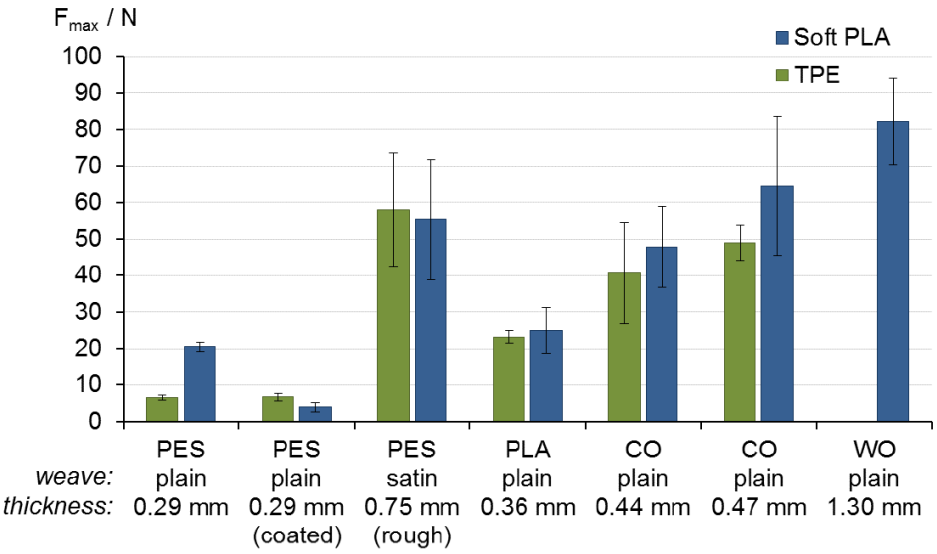

Figure 2.3: The maximum adhesion forces of FDM parts to fabric, 350 mm x 50 mm, on different woven fabrics – polyester is PES, polylactic acid is PLA, cotton is CO, wool is WO [2]

Thermoplastic polyurethane (TPU) elastomers, like Ninjaflex filaments, were found to have higher adhesion than thermoplastic styrene (TPS). This is specifically for knitted or woven textiles that were made of given the polyester, cotton, and aramid fabrics as shown in Figure 2.4. Fabrics material and type do not appear to be large factors in determining adhesion, but TPU is found to have better interactions with certain textiles. Figure 2.5 shows the results of the adhesion forces, found using standard DIN 53530 and EN ISO 2411 for the various fabrics, TPSs, and TPU. The TPU polymers exhibit good wettability, adhesion, and a more polar character that is appropriate for the textiles. Use of TPS leads to lower interfacial strength but

was found to still provide sufficient strength when used to create parts knitwear. This proves that rough knitwear assists greatly in adhesion strength for all deposited materials. This is because of the high porosity of the knitwear fabric, compared to other fabrics, allowing the molten polymer to penetrate and create form-locking bonds with the fabric leading to high adhesion strength. If the elastic stretch of knitwear was about the same as the adhesion forces the additive manufactured part will stay on the fabric. When testing multiple TPS polymers TPS1 had better adhesion forces to TPS2 likely because of the lower melt viscosity of the compound and lower Shore hardness, a measurement of the materials resistance to indentation, allowing the material to flow deeper into the fabric. The two different printers using a filament diameter of 2.85mm and 1.75mm may also have affected these results, because the material would have a different thermal gradient within it, but that is undetermined [7].

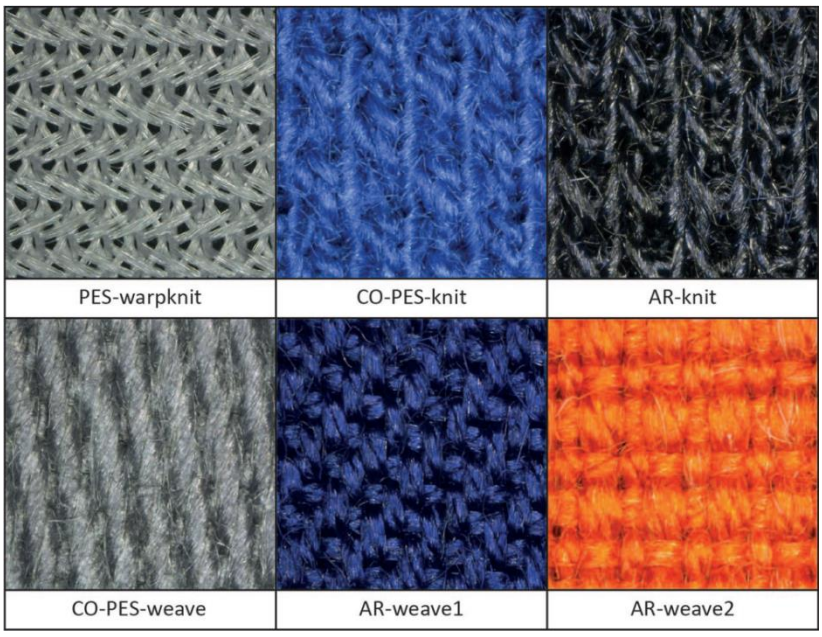

Figure 2.4: Microscopic pictures of fabric substrates used [7]

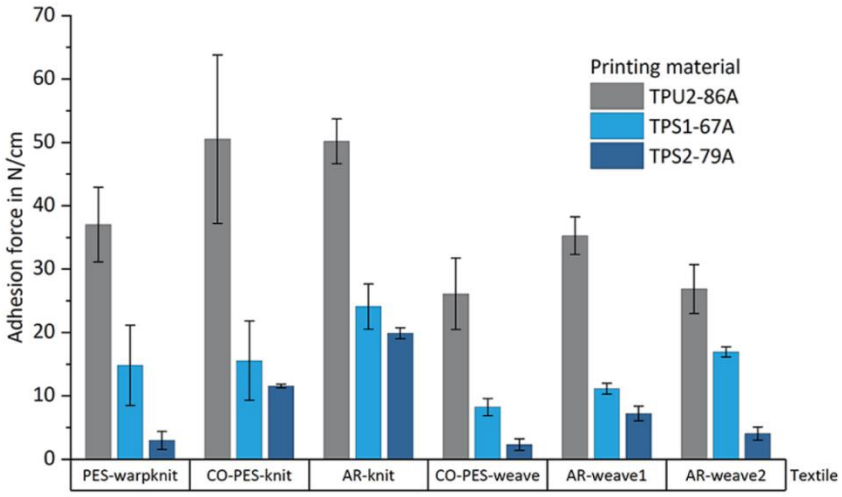

Figure 2.5: Adhesion forces of TPE additive manufactured parts on different knitted and woven workwear and sportswear fabrics [7]

Given the findings that printing flexible NinjaFlex on top of rigid PLA has better adhesion than PLA on NinjaFlex it was determined that different filaments and fabrics are far more complicated. For the most part to characterize the interaction between fabric and filaments would require mechanical, morphological, and chemical understanding. Understanding these physical properties of both the fabrics and the polymers would be desired to tailor interfacial strength.

Wetting, diffusion, and pressure are very important for layer-to-layer 3D prints and should also be just as important when printing on top of fabrics. Good wetting properties with hydrophilic fabrics also seems to promote adhesion as well. Warp and weft count, roughness, as well as greater thickness of the fabrics increased interfacial adhesion [8].

Various samples were created with different combinations of fabrics and additive manufactured materials to test the interfacial strength of these different combinations of materials. Nylon on PA 66 fabric, PLA on PA 66 fabric, PLA on PLA fabric, nanosized carbon black (CB) and PLA nanocomposites on PLA fabrics, and carbon nanotubes (CNT) and PLA nanocomposites on PLA

fabric were tested. The adhesion testing method used was the SS-EN ISO 1139:2010 standard in this case, at a rate of 100 mm/min. Fabric was also mounted to the print bed using double sided tape. The results of the sample testing found that the polymer textile combination was important. Specifically, the PLA and PLA nanocomposites had a high adhesive force when they were deposited on top of PLA fabrics. Tearing of the fabric or breaking of the deposited layers would be common for these samples. The polar-ester groups in both the adhesive and adherent along with a diffusion theory, diffusion of chain like molecules into the fabric, help to explain the high adhesion strength observed [9].

Of polymer filaments tested when additive manufacturing parts on top of fabric PLA was found to have the best adhesive results to the fabric compared to nylon and ABS filaments. Results were qualitatively found by using the Likert scale to manually measure and assign attributes with ratings from 1 to 10. PLA had great adhesion with little warp while still having high print quality and flexural strength. For fabrics woven polywool promoted the highest adhesion with woven cotton and knit soy fabrics also performing well. A fabric known as Bendlay was also tested resulting in potentially good results [5].

Tensile testing was done with additive-manufactured PLA parts on top of polyethylene terephthalate (PET) fabrics and the fabrics themselves to determine the strength of the composite. However, the additive-manufactured part on the fabric has lower strength than the fabric itself. This was determined from tensile testing composite of the additive manufactured part and fabric showing that the composite had a weaker tensile strength than the fabric itself. Delamination of the additive manufactured part during testing is the main source of this strength lowering of the composite, this occurred because of poor adhesion at the interface between fabric and additive manufactured part. The improvement of textiles properties could be obtained using

flexible filaments and the improvement of the adhesion at the interface of the fabric and the additive manufactured part. Figure 2.6 shows the PET fabric tested on its own as well as a composite, the time the PLA delaminates can also be observed as point (2) on the graph.

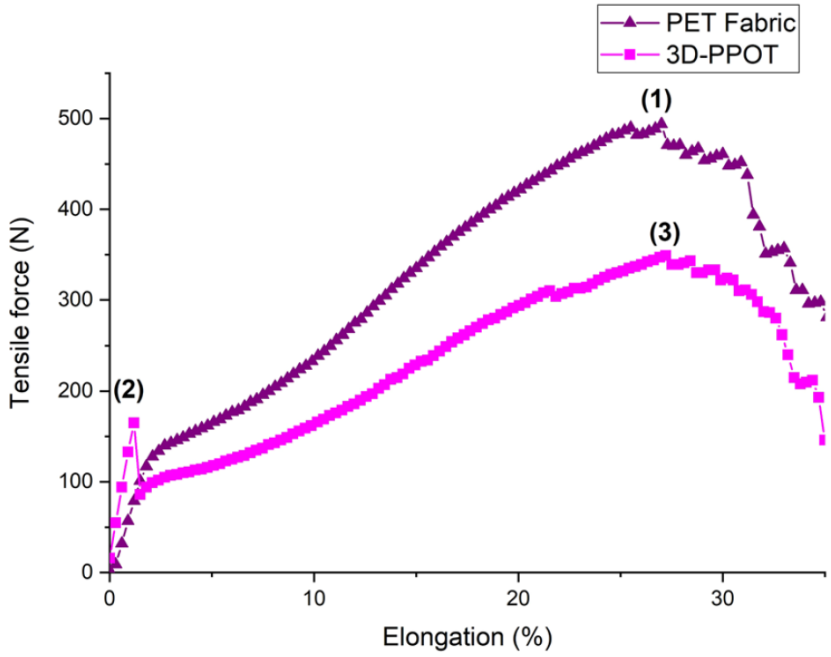

Figure 2.6: Tensile force-elongation curves of fabric samples (1) PET woven fabric, (2) maximum strength of the PLA on the PET, (3) the maximum strength of the PET after the PLA delaminates [10]

2.2.2 Primer Coatings and Pre-Treatments of the Fabrics

Pre-treatment, such as coatings, washings, and other treatments were done to change the material properties of fabrics intended to have parts additive manufactured on them. This was to observe the change in the adhesion at the interface between additive manufactured parts and fabrics, as well as potentially help with specific applications. Polymer pretreatment coatings were added to the fabric before additive manufacturing on top of them was tested in previous literature in which PLA, ABS, PMMA, and PA coatings were tested. Additive manufactured parts were created on top of these coatings included the use of PLA and ABS filament materials. All coatings

increased the contact angle of the fabric greatly from the original contact angle. The DIN 53530 standard was used to determine interfacial strength and was evaluated using the ISO 6133 method for more than 20 peaks. A cotton fabric with a thickness of 0.21 mm was used with a printing z-distance of 0.28 mm, as to compensate for fabric and coatings. However, despite the 5% solid content used for all coating solutions and identical coating procedures PLA coatings were found to be thicker, likely because of the higher temperature required to create the solution making the solution dry faster.

A low z-distance of -0.02 mm, which was the normally used z-distance when creating parts on the print bed and not on fabrics, was used for creating parts on untreated fabric. Z-distance being the distance set between print bed and nozzle, which is different per printer and may be changed for some tests to account for thickness of fabrics. This found that the material placed by the 3D printer was found to be much rougher, after being removed, and have much higher adhesion than compensating for the fabric. PLA filament put on PMMA and PLA coatings were found to have the highest adhesive forces at the interface between fabric and 3D printed parts, as shown in Figure 2.7. Overall, the adhesive forces found were very low making it possible to remove the 3D printed part by bending the composite. Both filament materials were not found to penetrate the fabrics in any case even with no coatings. Adhesion results between the additive manufactured part and fabric were found to be increased significantly for some of the fabrics. This means that for fabrics with low interfacial adhesion, given base process parameters, could have coatings applied to them to significantly increase their adhesion strength [11].

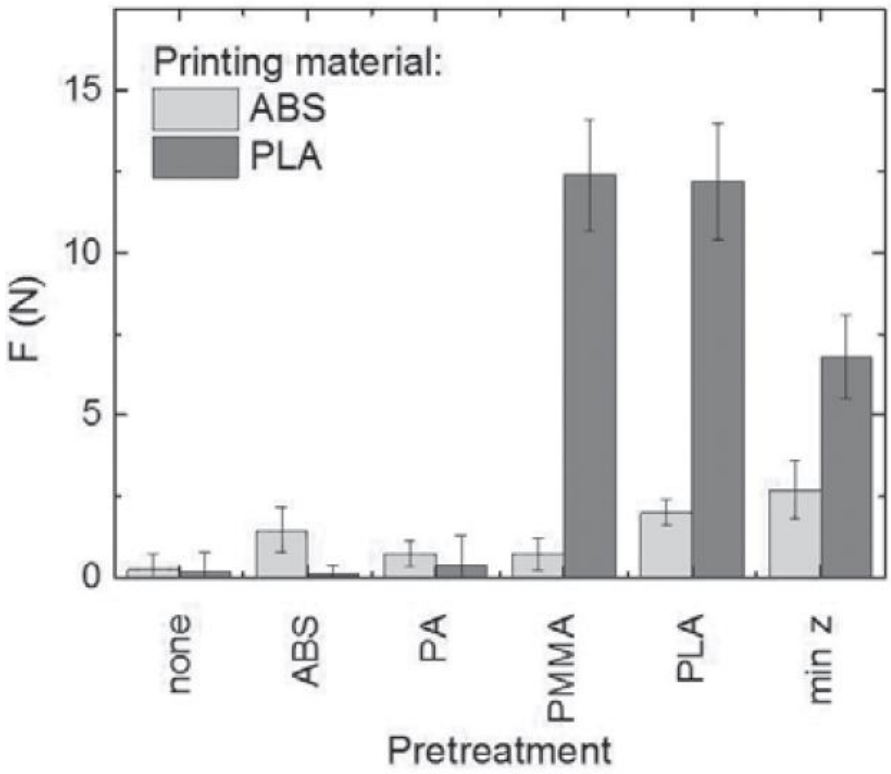

Figure 2.7: Adhesion forces of ABS and PLA when additive manufactured on cotton fabrics with different polymer coatings, and with a small z-distance with no coating [11]

Multiple pretreatments were tested on top of cotton fabric as to determine which one would increase the interfacial strength the greatest. The adhesion testing method DIN 53530 and evaluation method ISO 6133 were used to find the adhesion strength. Of the pre-treatments of the fabric tested the application of waterproof spray, acetone bath, and rubbing 250 and 750 times to standard DIN EN ISO 13427 lowered and ironing the strength of the adhesion at the interface with these pretreatments. Pretreatment of NaOH, the washing of the fabric, hair spray, ironing after sample creation, and laser treatment all were found to not affect the adhesion greatly or slightly increased it. The only pre-treatment of the fabric that was found to increase interfacial strength, from the untreated baseline, was the glue stick pretreatment. The interfacial strength testing results can be observed in Figure 2.8 [12].

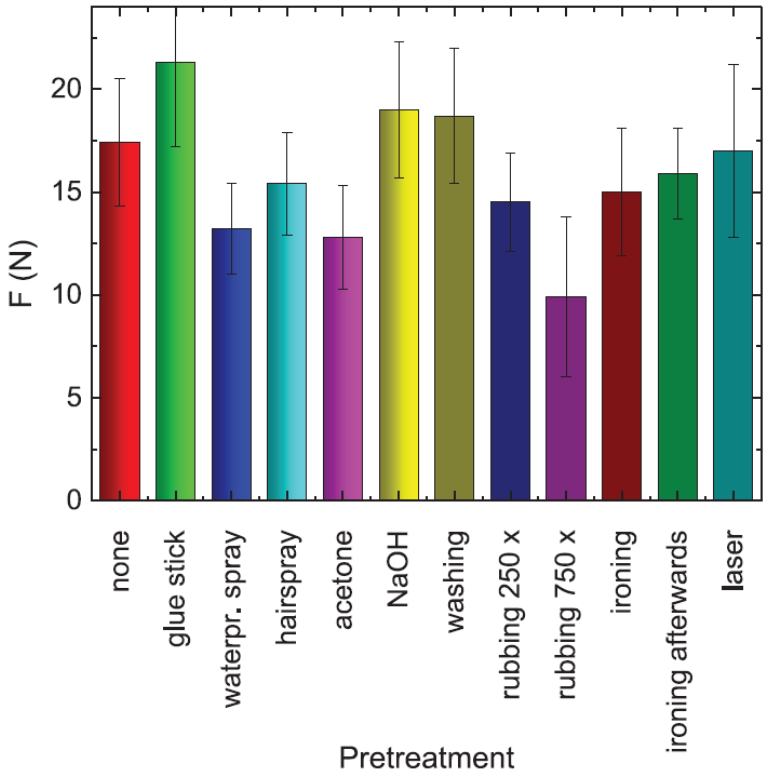

Figure 2.8: Adhesion forces measured for different pretreatments of the fabric substrates for additive manufacturing [12]

Contact angle analysis found that the 750 times rubbing had the highest contact angle while NaOH treatment the lowest, with glue stick treatment being roughly the same as the untreated fabric. The linear rubbing was done according to the DIN EN ISO 13427 standard with 400 grit abrasive paper. Results from the contact angle analysis confirms the Korger law [2] that the more hydrophilic a sample fabric is the higher adhesion forces. Tensile testing was done for created composite samples, using various pretreatments, using the EN ISO 13934 standard for tensile testing, using rectangular shapes instead of bone shaped ones. Results, shown in Figure 2.9, found that all pretreated composite samples had higher tensile strength than the untreated fabric, with no clear correlation to any one property [12].

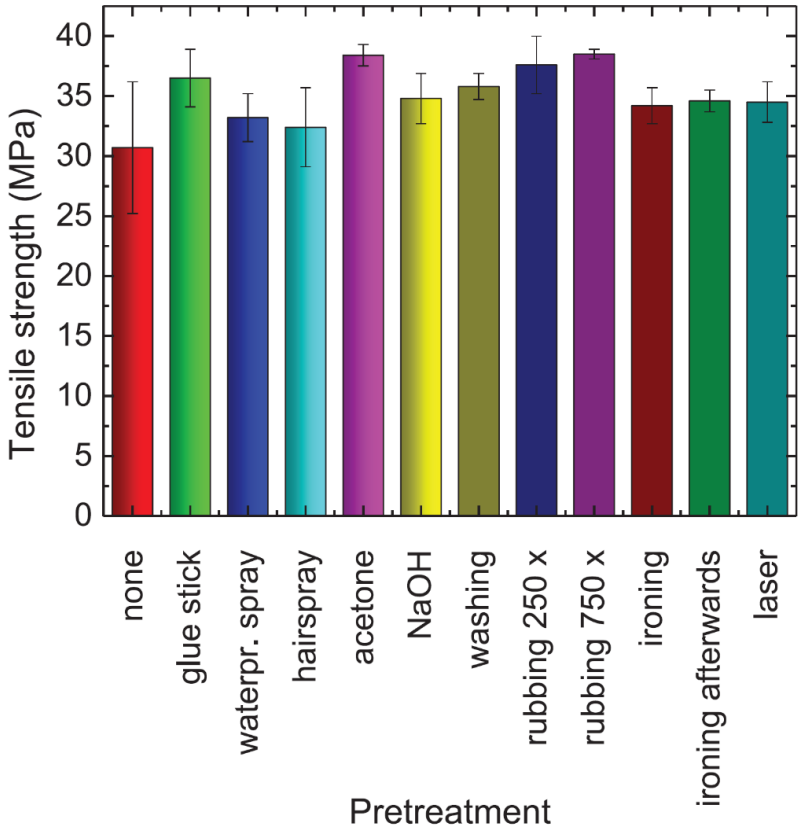

Figure 2.9: Tensile strength measured for different pre-treatments of cotton fabrics [12]

Chemical pre-treatments and polymer coatings on fabrics were found to increase adhesion proving again that Korger law, where hydrophilic surfaces promote adhesion, is true. For filaments with high viscosities, and fabrics with low thickness and roughness, a polymer coating applied to the fabrics was found to be to be the better solution than to force interpenetration of the deposited material with the fabric. This is comparative to samples where low viscosity and high pressure on untreated fabrics induce very high interfacial adhesion from form interlocking. Differences from a physical, mechanical, morphological, chemical, and surface energies of materials all matter when additive manufacturing on fabrics [8].

Separation force and abrasion resistance tests were conducted with different kinds of printed woven fabrics. Roughness and hairiness of fabrics form interlocking connections with

wettability of the textile also appeared to be a factor. The surface energy can be controlled by washing or performing plasma treatment of the textile before printing on it. Washing of fabrics included samples put at 60 °C for 45 min and adding the enzyme amylase and the Kieralon CD washing agent also known as BASF. Plasma treatments of samples were done under carbon dioxide, argon, and nitrogen rich environments where settings were 600 W and 250 sccm for 30 seconds. The plasma treatments were also done using low pressure at 50 Pa, and a 2.45 GHz microwave discharge

Cotton was used and it was found that washing greatly increased adhesion forces with Figure 2.10 showing the adhesion strength results for washed and unwashed fabrics. Cotton twill warp caused fabric destruction when removed making adhesion strength impossible to measure, but clear that it had the highest adhesion strength. Effectively the surface energy of the fabric was greatly enhanced causing better adhesion, but this was not universal for all cotton fabrics and was not true for the polyester (PES) fabrics. The finish on the fabric is likely the cause of much of the adhesion strength for these PES fabrics compared to the other cotton weaves, and washing the fabric causes it to be removed [2].

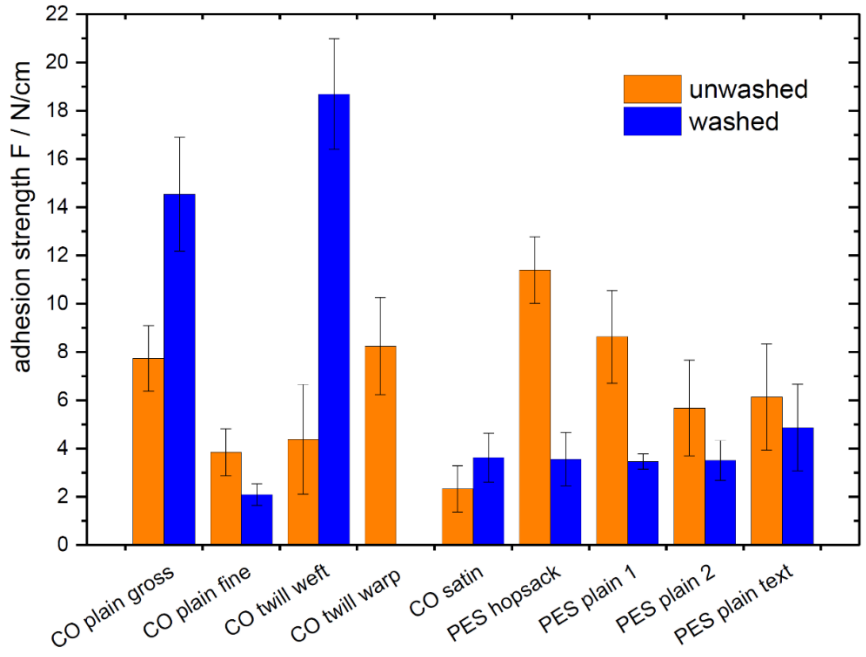

Figure 2.10: Adhesion strengths of additive manufactured PLA on different washed and unwashed cotton (CO) and polyester (PES) fabrics [2]

Plasma treatment, with argon and nitrogen, drastically reduced adhesion strength for soft PLA and was apparently found to have only a cleaning effect but no polar groups were created. Carbon dioxide plasma treatment, however, was found to promote hydrophilicity and wetting behavior and could be enhanced for texturized yarns. Carbon dioxide plasma treatment also led to almost two times higher adhesion strength compared to untreated samples. Very little work or results were shown on the carbon dioxide plasma treatment so future work on this pretreatment may be desired. Abrasion resistance tests found that the addition of PLA structures helped greatly against abrasion. From this, it could be determined that wettability is important. Wettability can be controlled by washing or desizing the finish off the fabric, adding finishings or coatings, or by using plasma treatment of the textile before manufacturing of the part [2].

Printing parameters, physico-chemical, and mechanical interactions like form-locking at the interface affect the adhesion strength. Generally, form-interlocking is the most important but for

smooth fabrics as polymer coatings are desired to help with adhesion. Specific thermoplastic elastomers are of interest in which filaments like Ninjaflex are desired but are hard to print. Selected thermoplastic elastomers were tested as print polymers for FDM printing on fabrics. Adhesion properties, washing, and abrasion resistance of a given plastic is desired for use on garments.

Additive manufacturing on fabrics using workwear textiles is desired for applications for textiles and products used in daily work, and this would involve the washing and abrasion testing of the samples. Washing of the fabric samples is done after they have parts manufactured to determine if the additive manufactured parts could maintain their adhesion after extended use. Samples were washed following the industrial washing standard EN ISO 15797. 10, 25, and 50 washing cycles are performed on the samples and then the DIN 53530 standard was used to test the interfacial adhesion strength between the manufactured parts and fabric. Samples were then either line dried or oven dried, without additional drying samples were observed to be of lower quality.

To test the performance of the TPU and TPS materials additively manufactured on warp knitted and densely woven cotton fabric. Initial testing of washing the fabrics with rectangular strips printed on them found adhesion strength was reduced by 40% at most after the first 10 washing cycles but future washing cycles appear to not further reduce adhesion. Although lasting damage can still be possible given enough washing, current results appear to show that an acceptable amount of adhesion is kept after washing.

Various other geometries, besides the rectangle testing samples, were then tested with different print heights to determine if the prints could withstand the washing process. Heights from 5 to

25 mm were tested on an AR-knit textile with a TPS filament polymer. After 15 washing cycles at 70℃ there was no detachment from the fabric found for any of the samples.

Polyester-based TPU was found to be constantly rubbed off the textile during abrasion testing with the increase of Martindale abrasion test cycles, following the EN ISO 12947-2 standard, after 20,000 rubbing cycles. This was unexpected given that polyether based TPU were fine up to 40,000 cycles and generally polyethers perform worse than polyesters in abrasion tests. This is likely because of the lower hydrolytic stability of the polyester based TPU given the exposure to temperatures over 230℃ in which with the combination of moisture can degrade the material. Although the material was dried before printing a moisture content of less than 0.05% cannot be maintained during the printing process causing the material to degrade, making the polyester TPUs desirable for workwear applications. Moisture content is also found to negatively influence print quality as not oven drying the filament before additive manufacturing is found to show a reduction in print quality for each part created since the drying, as shown in Figure 2.11. This is true for the TPUs and TPS with the softer materials performing the worst. TPS materials, however, can be processed more easily given the lower hygroscopicity, ability to absorb water into their surface, but has disadvantages given the loss of material during Martindale abrasion

testing cycles. Washing was found to not affect the adhesion of the materials to the textile, however [7].

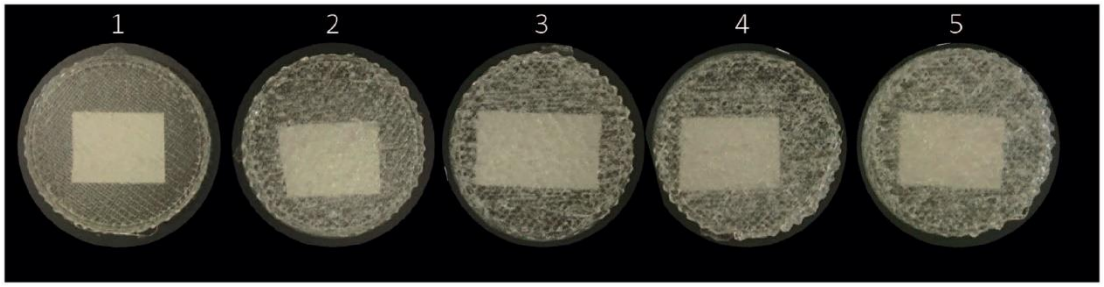

Figure 2.11: Sequence of TPU samples directly after drying increasing in moisture content

To help with smart textile creations, NinjaFlex was additively manufactured on top of PEDOT:PSS-coated polyester fabric and cotton fabric. The peel strength found for both the coated polyester and coated cotton fabrics to the NinjaFlex was found to be 4160 $\frac{\mathrm{N}}{\mathrm{m}}$, and 3840 $\frac{\mathrm{N}}{\mathrm{m}}$, respectively. The peel test involved standard SS-EN ISO 11339:2010 using a tensile testing machine according to standard ASTM D5034. Samples were also tested for durability given washing in a domestic laundry washer and dryer; this was done according to type 3A reference washing for textile testing in standard ISO 6330:2012. From washing tests, it was found that NinjaFlex was able to increase its bending lengths, by 1.03 and 1.39 mm, and otherwise did not affect the properties of both composites very negatively. Overall, the results were sufficient for application usage, while also having high adhesion strengths, at 4.16 $\frac{\mathrm{N}}{\mathrm{mm}}$, found using peel testing. These high adhesion strengths were likely attributable to the coating added to the fabrics given how it would have been expected that thin polyester fabrics would have been. However, it is unclear if the testing was with the coating at all so it is possible that there was no testing done with the PEDOT:PSS coating [13].

A washing process and the addition of conductive fillers was done to the PLA and it was not found to affect the tensile properties of the PLA but the washing did affect the stress of the fabric negatively. Otherwise, the PLA was found to have good durability after the washing process, before and after conductive fillers were included in the PLA [10].

Dog bone tensile testing samples were created where two layers of jute fabric were sandwiched between three layers of additive manufactured parts. This was done to test if the tensile strength of a dog bone would be increased by having the sample print with the fabric laid down in-between sections. Various flame retardants, and other pre-treatments, were tested to see if they would affect the strength of the composite of additive manufactured parts and fabric as well. These flame retardants used where a Flamebar S3 and a Hi-Tack 71. The results of the PLA and flame retardant covered jute fabrics are compared against each other with a purely PLA sample as a control in Figure 2.12. The coatings and pre-treatments used were all on jute fabric with J-M being the sample washed in ionized water, and J-R the sample covered in a flame retardant. Then J-MR the sample washed in ionized water then covered in flame retardant, J-A the sample covered in mist aerosol adhesive, and J-RA and samples covered in flame retardant and adhesive [14].

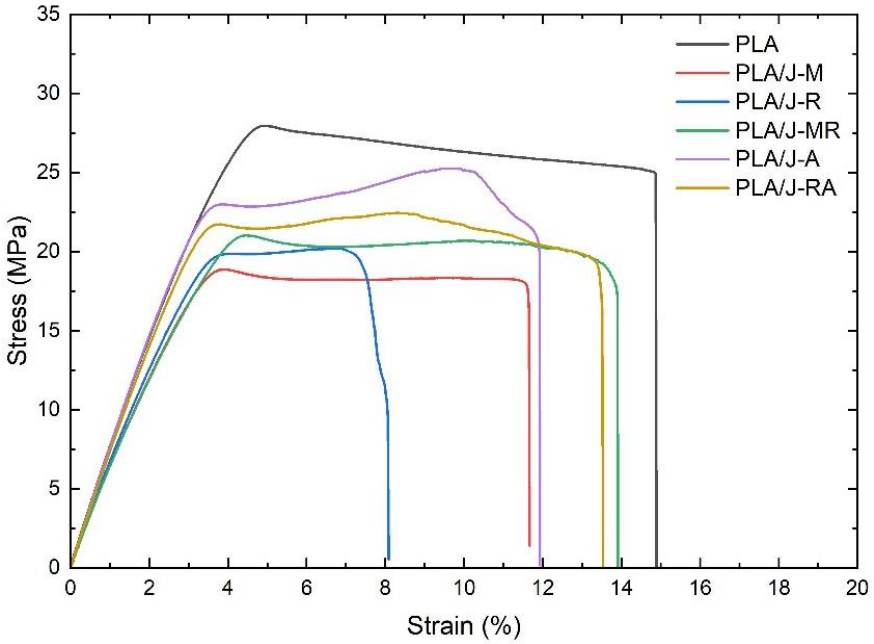

Figure 2.12: Stress versus strain graph of PLA and PLA composites created with jute and various flame retardant coatings [14]

The flame retardant and adhesive treatments to samples was found to increase the composites strength overall compared to untreated ones, as well as give it desired flame-retardant properties. Different treatments or different fabrics could potentially lead to higher mechanical properties as current results are very promising. However, outside of treatments all composite samples with the fabrics performed worse than the solid PLA samples. This is likely attributable to the jute hindering molecular motions during sample creation, and is likely true for all mechanical strength of composites made of additive manufacturing on fabrics [14].

2.2.3 Process Parameters

The process parameters refer to the 3D printer settings used when additive manufacturing on top of the fabrics. Testing was done with various changes to the process parameters to determine how each setting could potentially change the adhesion strength of the interface. The infill or fill direction used when additive manufacturing on fabrics is one of the more important process

parameters. This is specifically on how the direction of the inside or fill of the first layers are orientated with the warp direction of the fabric, where each fabric tested has a warp and a weft direction perpendicular to each other. This is because the peel samples tested in accordance with the DIN 53530 adhesion test standard have the long edge parallel to the warp for all samples in this case. Samples were created with PLA filament and woven cotton fabric. Results found that the short pathing, 90 degrees from the warp direction, along the weft, had the highest adhesion strength as seen in Figure 2.13. From the results it was shown that printing along the long edge with the warp produced the smallest amount of adhesion strength. Using a 45- or a 135- degree fill angle both produced a similar adhesion force between the 0- and 90-degree angle results representing the lowest and highest adhesion strength.

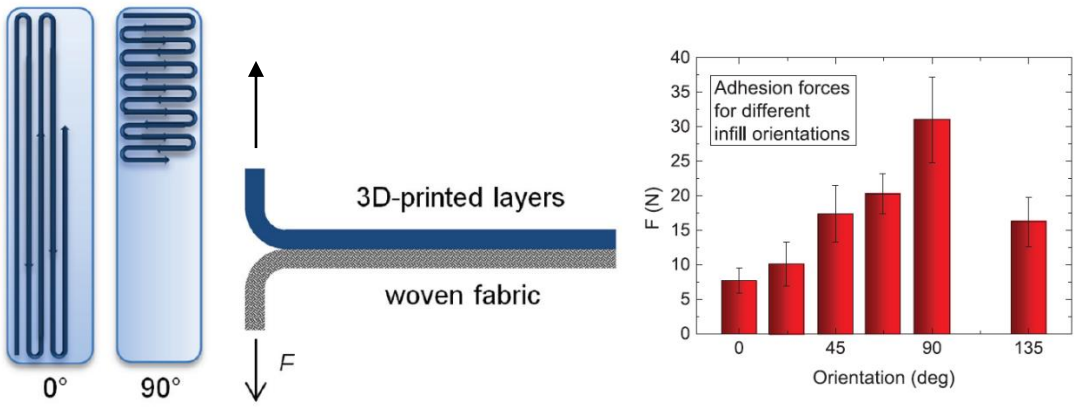

Figure 2.13: Visualizations of the fill orientations, how fabric samples are tested, and the adhesion force results for different fill orientations of additive manufactured samples [12]

Tensile strength testing was done for the same infill sample composites using the EN ISO 13934 standard, which found that all samples had about the same tensile strength regardless of fill angle. Future testing with fill angle would involve the testing of additive manufactured parts along the weft direction with different fill orientations. Currently, only the samples along the

warp have been tested and it is likely that results would greatly differ if the long direction of samples was changed in orientation to the fabric.

The roughness of the fabric and the surface area in contact with the fabric has a great effect on the adhesion strength and the additive manufactured surface in contact with the fabric. To test this, samples were additive manufactured on fabric. The first and second layers were measured for roughness with a confocal laser scanning microscope. Results found that the higher fill angles closer to 90 degrees, towards the weft direction of the fabric, had much higher roughness than any other fill orientation, as shown in Figure 2.14. Where Ra is the average roughness, Rq is the root mean squared roughness, and Rz is the average distance between the highest peak and lowest valley per sampling length. This would likely mean that the interfacial strength that is increased when changing orientation along the weft is likely because of the higher roughness the additive manufactured parts encounter when being created on fabric. [12].

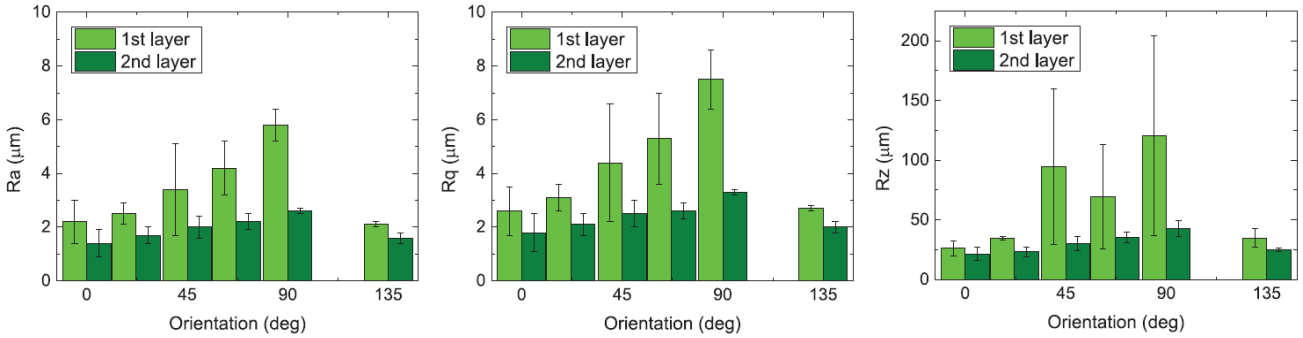

Figure 2.14: Roughness values Ra, Rq, and Rz measured for different infill orientations of additive manufactured samples on fabrics [12]

Layer thickness used for the first few layers appear to affect the adhesion strength to some degree, with thicker layers producing higher strength. However, the z-distance, the distance between the nozzle and the printing bed, was found to be one of the most influential properties. The lower the z-distance is set inside the fabric the higher the adhesion strength that would be

obtained at the interface between the additive manufactured part and fabric. However, if the z-distance is set too low the fabric would be moved by the nozzle. In this case the fastener for the fabric, usually tape, to the print bed would fail and then cause the part to fail being created. Optimal z-distance for the thicker fabrics, a thickness of about 0.55 mm for each, was found to be where the nozzle is 0.2mm inside of the fabric. An exception was the 0.52 mm thick wool fabric which performed well with a z-distance at the surface of the fabric itself. Fabrics that were 0.2 mm thick or thinner performed the best when additive manufacturing parts on them using the z-distance normally used when not additive manufacturing on fabrics to accommodate them. This means the nozzle would be fully inside the fabrics in these cases. A visualization of the interfacial strength found for various additive manufactured parts on fabric samples created with different fabrics is shown in Figure 2.15. From the results it could be determined that there was a strong form-locking physical bond being promoted by the z-distance, with no indications of chemical bonding present [3].

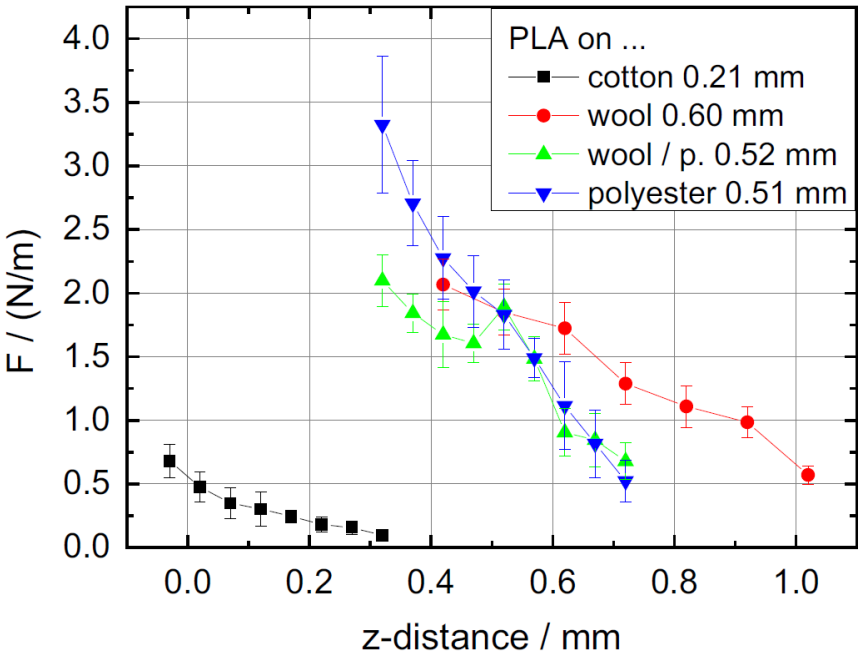

Figure 2.15: Adhesion strength for additive manufactured samples created on fabrics with PLA filament at various z-distances, fabrics thicknesses are listed next to their names [3]

More testing with z-distance was done finding that the nozzle presses the polymer more into the open pores of the fabric the lower it is. This was done with PLA on various cotton fabrics. Additionally, it became clear that the adhesion strength would level off after a certain z-distance, as the fabrics would clog the nozzle given the roughness it would be experiencing from the fabric. With thicker fabrics producing higher adhesion forces, the nozzle could be put farther into the fabric, as shown in Figure 2.16. The removed additive manufactured parts from the fabrics were also visibly different with the closest z-distance to the print bed having samples as shown in Figure 2.17. This proves that the lower z-distance has higher adhesion because of the higher encountered roughness, the fibers left on the polymer also show a clear increase in the adhesion strength.

However, temperature of both the nozzle and print bed matter a lot more than z-distance for promoting adhesion. This is shown in Figure 2.18 where the higher bed and nozzle temperature

obtains higher adhesion strength with a farther z-distance than the lower temperature [15]. For most testing methods, a nozzle and bed temperature of 210℃ and 70℃ is used for PLA when creating parts on fabrics. This makes testing with higher and lower temperatures significant in understanding exactly how temperature affects adhesion [2]. From this, it can be determined that the adhesion strength is greatly dependent on the bed and nozzle temperature as well as the z-distance together. Specifically, the decreasing of the viscosity of the PLA during additive manufacturing by the higher temperatures raises adhesion greatly with assistance from the lower z-distance. Future work will include more investigations into how the adhesion can be improved specifically with the modification of the filament viscosity, nozzle size, and first layer height [15].

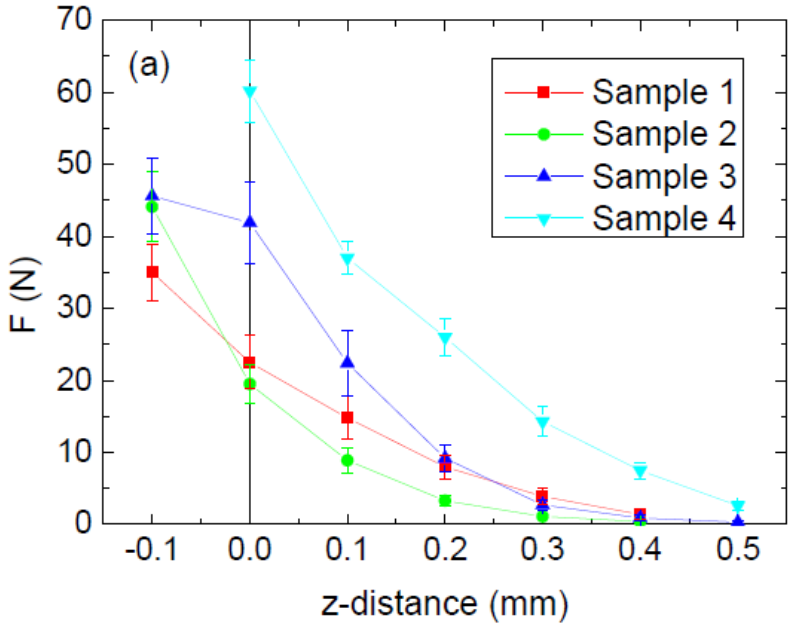

Figure 2.16: Z-distance versus adhesion force of PLA on various cotton fabrics of increasing thicknesses, with sample three leveling off after a bit [15]

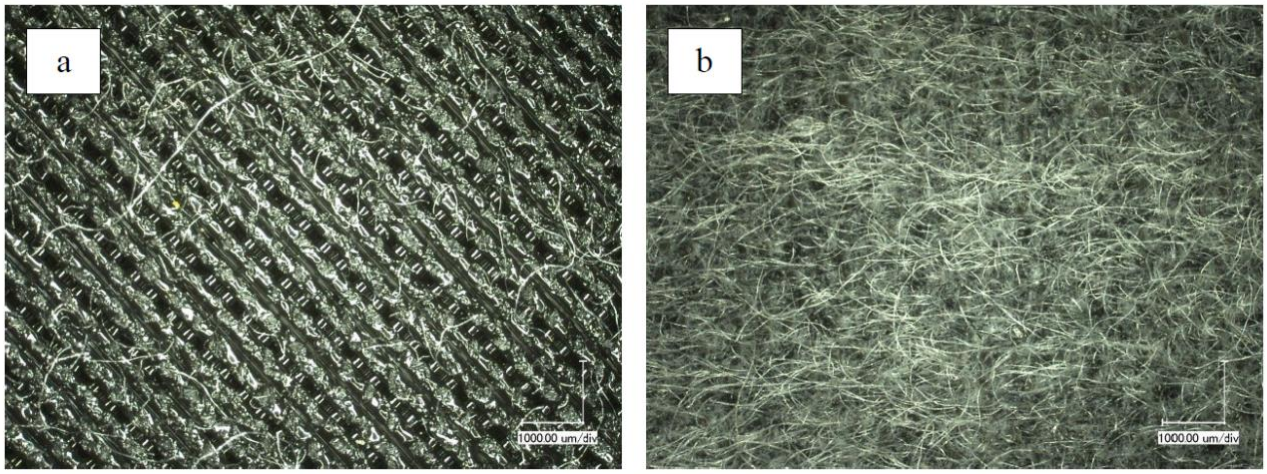

Figure 2.17: Close up of sample three after adhesion tests (a) maximum z-distance, (b) minimum z-distance [15]

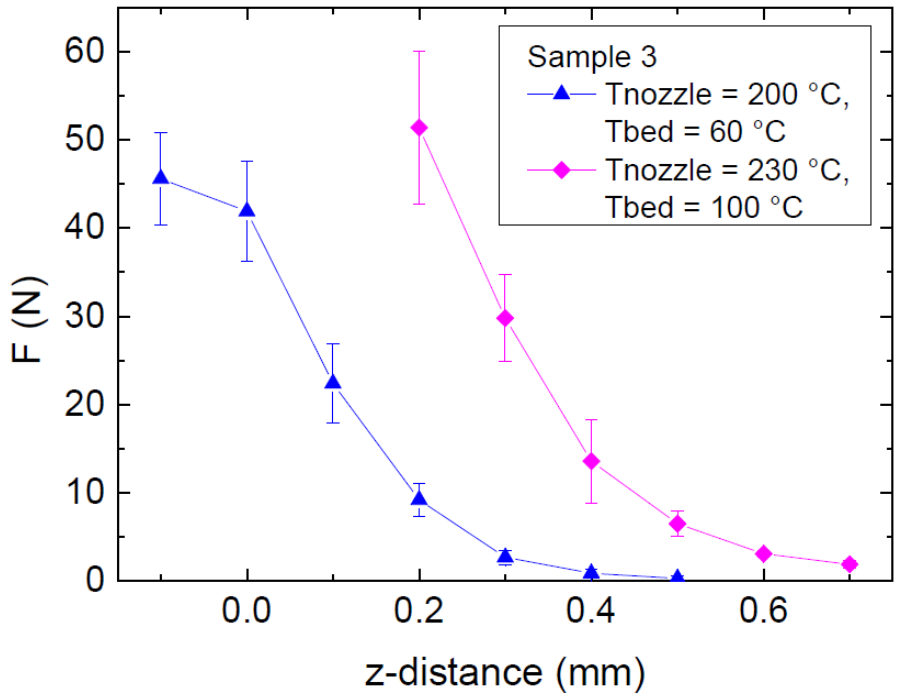

Figure 2.18: Z-distance dependance of the adhesion force of PLA on fabric sample three with different temperatures [15]

Tests done with Nylon and PA66 fabric found that the interfacial strength of the interface increased with higher nozzle temperature and had a quadratic effect depending on the printing speed. Diffusion theory explains that polymers adhere to each other by diffusion of chainlike

molecules, which leads to a strong bond between adhesive and adherent. Higher nozzle temperatures were also found to lower the strength of the additive manufactured parts showing that the higher temperatures can cause higher brittleness. Bed temperature was only tested to 70°C and results found that if the bed temperature did not surpass the glass transition temperature of the fabric the temperature mattered little. This would mean higher adhesion forces start to appear only at higher bed temperatures. Figure 2.19 shows the adhesion strength versus process parameters and how they affect each other when used for additive manufacturing Nylon on PA fabric [9].

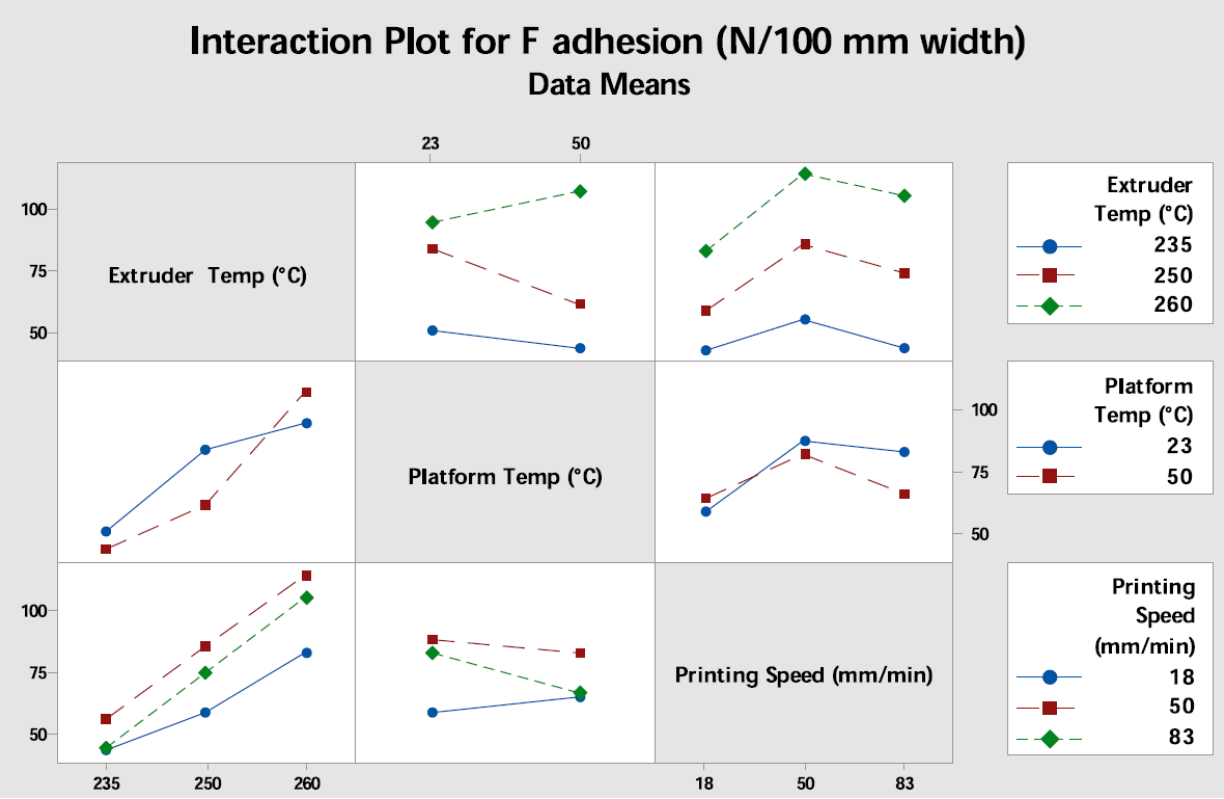

Figure 2.19: Interaction plot for the adhesion force versus extruder temperature, bed temperature, and printing speed of the 3D printer when depositing Nylon onto PA66 fabric [9]

Adhesive properties of printing on fabrics were tested using tensile, bending, and peel test standards. Specifically, we have been focusing on the adhesive peel testing of samples to obtain

the highest adhesion strength possible, and a lot of parameters must be tested one at a time to determine their influence. As an example, a Bolt Pro 3D printer was used along with a X400, and process parameters are set to specific values to test the changes in adhesion attributable to various properties and parameters. The z-distance was specifically chosen to be 0.15 mm with a fill orientation of 45 degrees for all samples. Adhesion tests were performed using the DIN 53530 standard using a Zwick Roell testing device. Otherwise, adhesion strength testing was based on the EN ISO 2411 standard of the adhesion strength of coated fabrics using an Instrom testing device for adhesion testing after washing. These two different testing methods were used based on testing at different locations but are similar. The standard sample sizes for test prints on fabrics are 100 mm x 17 mm x 1.2 mm for the DIN standard and 150 mm x 20 mm x 1.2 mm in the ISO standard. Layer thickness is set to 0.2 mm and for each case the adhesion forces are recalculated to 10 mm print width each for better comparison, obtaining comparable values between the testing methods [7]. Of these static settings chosen most if not all in the middle of two extremes previously tested. These middle settings are used to create a baseline sample to compare to in the case of parameter or pre-treatment testing.

To test the strength of the interface between additive manufactured part and fabric another testing method was developed for adhesion testing outside of the DIN and ISO standards. In this case a 25.4 mm diameter plug of plastic is created on top of the fabric and pulled off the fabric using a general tester. The ultimate force required to remove the plug is then recorded and compared to other samples. This could be considered the tensile strength of the interfacial adhesion [16]. Issues with this testing method involve the failure of the additive manufactured part during testing before the interface would fail, as well as not being based on any previous adhesion testing standard.

A study of the adhesion between the textile and polymer composites was done as well as theoretical investigations on the adhesion inside of a 3D printed part itself. Essentially the study is a summary of previous work in the promotion of interfacial strength when additive manufacturing on fabrics. The study concentrated on embedding fibers and textiles during the 3D printing process without specialized equipment. Where short fibers were not embedded into the feedstock before object creation or other introduction of fibers into an additive manufactured part during manufacturing.

Printing directly on open-pore fabrics with PLA is often found to work well enough in terms of adhesion for applications, such as for filtering, electroluminescence, and use with their mechanical strength. Bed temperature was found to be an important factor with higher bed temperature promoting better adhesion. Orientation and weft density of the woven fabric was also found to be important. Flexible filaments were found to work the greatest on hairy woven fabrics given the lower viscosity of the materials during printing. ABS was found to perform worse than most filaments given its higher viscosity, with PLA working much better for common filaments used. The distance between the nozzle and fabric, as z-distance, was found to be an important factor as well. A summary of these parameters being that proper low viscosity and high pressure makes the additive manufactured material penetrate the fabric to form an interlocking connection on thick and rough fabrics.

In the literature it was reported that the extrusion or nozzle temperature was more important than the envelope temperature for bonding between 3D printed lines. In a different study it was found that sintering, the removal of pores, occurred between layers for only a short time before temperature was reduced below sintering temperature where envelope temperature and convection mattered for the bonding. Welding time between lines of deposited filament is

important for strength between these lines. Higher extrusion speeds and temperatures appear to be preferable to lower defects and higher bonding strength. Annealing of parts could also be a solution. Despite the research done on these subjects however it is not certain if wetting, diffusion, or other factors are the best for adhesion to fabric or other printed layers. Pressure caused by z-distance was found to be very important in promoting interfacial strength when printing on fabrics, in which wetting could be almost entirely forgotten, but temperature could assist [8].

Samples additive manufactured on fabrics and additive manufactured parts by themselves had results that found the environmental temperature was more important than nozzle temperature for increasing interfacial strength. Specifically, the environment, such as the print bed and ambient temperature, had an influence on bonding potential greater than nozzle temperature. Otherwise, the bonding strength between layers of material can be difficult to establish a direct relationship to specific process parameters outside of temperature. As an example, high bonding quality occurs when there is a low convection coefficient of the surrounding area, a large area of contact between layers, and a small height to width ratio of the material being put down during additive manufacturing [17]. The initial difference in results for environmental testing could potentially show that environmental temperature control may be desired in the future for additive manufacturing on fabrics.

Recently work with contact areas related to pressure between layers was modeled in which the melt pressure at the nozzle was attributable to viscosity, flow rate, layer width, and height. Small layer heights are important the contact area increases with previous layers the smaller the layer heights are, making wetting almost unneeded. Further testing of samples with printing speed and after-treatments, such as chemical, ultrasonic, or annealing treatments are also desired.

Additionally, air buffers were said to be observed between 3D printed parts and fabrics and so may be desired to be limited [8].

Improvement of the adhesion between the 3D printed PLA between different layers of itself and the fabric was found to improve the tensile properties of the both the PLA printed layer and the composite of PLA and fabric. Specifically increasing the platform temperature of the 3D printer was found to lower the tensile strength of the PLA. Additive manufacturing in a cross direction along the short edge was shown to have better stress at rupture attributable to better bonding with the fabric. Platform or bed temperature, fabric orientation, and weft density influence the tensile strength and deformation of the deposited PLA from stock material properties [10]. Specifically, the print bed temperature was found to be important in enhancing inter-molecular diffusion between two layers or a layer and the print bed [18].

2.2.4 Unfolding Methods

When creating large objects using small 3D printers that cannot normally be created because of the small size of the printer, segmentizing the 3D model of the object is desired. Specifically, the 3D model must be 3D to 2D unfolded and each of the faces created by the 3D printer. The unfolding specifically makes a spanning tree, this tree is desired to be one single plane without any overlapping. This section is about previously researched unfolding methods for 3D models to acquire a spanning tree, or otherwise methods of segmentation, from various models.

A large object was desired to be created using a 3D printer from a previous study. For the additive manufacturing of the large object a clustering algorithm based on grain segmentation was used to segmentize the object. The modified K-means clustering algorithm combines the angle between centroids of faces to partition the object into a K number of grains. The algorithm then chose certain faces centroids randomly as seeds and created different segments with the

surrounding faces along with a smoothing technique to achieve equal sized parts. K-mean facet clustering algorithm is specifically used with honeycomb tessellation to capture functional variation per segment. A similarity index is done to keep the parts alike and was found that overall support material and print time were reduced. However, this did not include pre and post processing which made the part creation. The segmentation of an object can be found in Figure 2.20 [19].

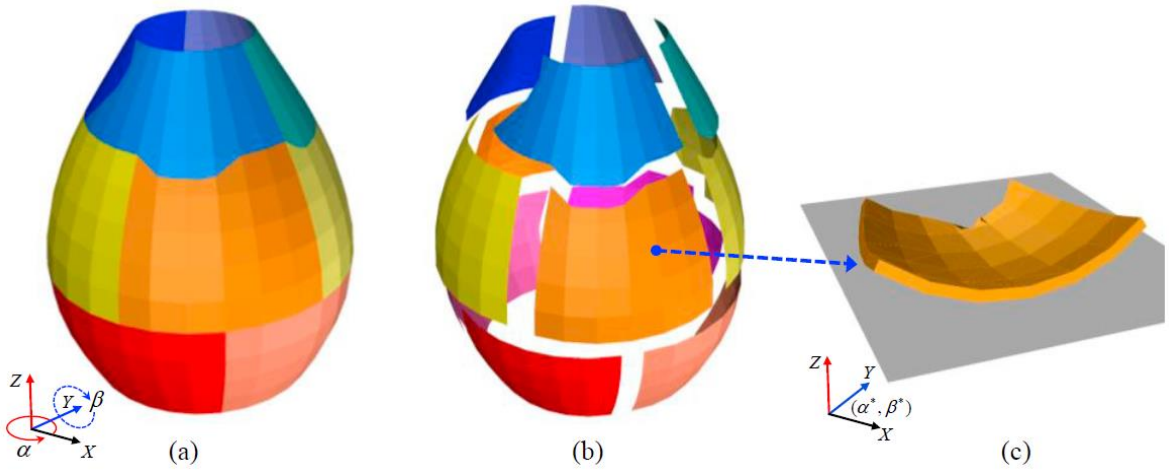

Figure 2.20: Large object desired to be additive manufactured using a 3D printer (a) segmented object, (b) exploded view, (c) reorientation of specific part for manufacturing on a print bed [19]

To improve the surface quality of shell models and the reduction of supports a surface segmented method is proposed based on spectral clustering. The spectral clustering was used to segment the surface into several parts to be printed separately. The method uses triangle faces in a 3D mesh of nodes made of the centers of faces, in a graph, where the distances between the centers of two adjacent triangle faces are edges in this graph. Surface features including surface quality and support structure volume for each triangle on the 3D mesh surface are extracted to form a similarity matrix. Area balance cut (ABcut) is a proposed algorithm that can be used to cut the graph by considering the minimum loss function and maximum area in each sub-graph where a

Laplacian matrix is design based on the similarly matrix and ABcut. After clustering the 3D mesh surface into clusters, boundaries between clusters are optimized to generate smooth boundaries. Figure 2.21 shows the segmentation of a part by the proposed method with the smooth parts shown in part (c). Case studies comparisons to a traditional spectral clustering method found that the surface segmentation increases the surface quality and reduces the amount of supports needed drastically [20].

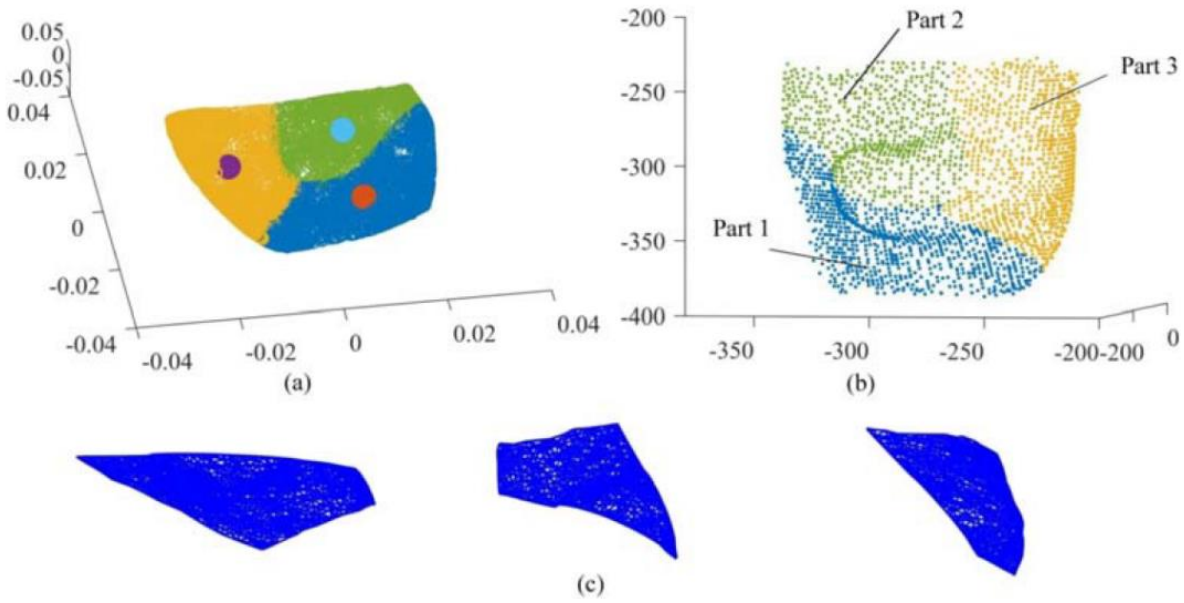

Figure 2.21: Part segmented using clustering method (a) Feature space obtained from original triangle surface, (b) generated results by the proposed method, (c) segmented results after smooth boundary is generated [20]

A mesh saliency approximation, for the segmentation of polygonal meshes, was presented to outperform existing methods of saliency segmentation, specifically when segmentizing 3D objects with protrusive parts. The method specifically involves a multi-scale approach to the adaptive approximation to the saliency of a polygonal mesh that integrates the three factors of part saliency. An automatic part-type mesh segmentation algorithm is used with low time complexity and high-quality outputs that matches with the theory of human visual perception.

Specifically, this segmentation can be used to segmentize parts to be additive manufactured while keeping important features. While being optimized to have the lowest number of segmentations, and segmentize out protrusive parts from a model. This allows all segments to be solid and have good mechanical properties on their own before combining parts to create the desired object. This is desired because if a segment is created too small or weak it will break or fail to be created before being combined into the full object. Figure 2.22 shows the presented method on the right compared against two previous methods on the left and middle. Of note is that the presented method segments the objects in solid parts much more than the other methods [21].

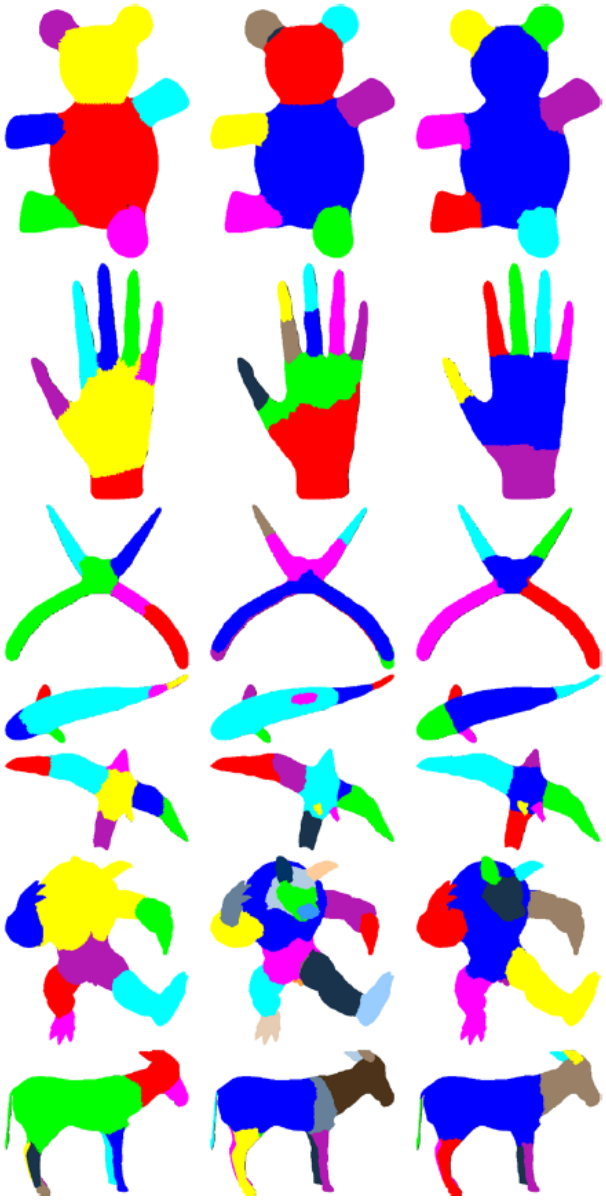

Figure 2.22: Colorized segmentation of objects with three different methods, each color is a different segment, (left) randomized cuts, (middle) shape diameter function, (Right) presented method [21]

Decompose and pack or DAP program combines shape decomposition and packing. DAP tries to decompose an inputted 3D or 2D shape into a low number of parts to fit within a certain space to be efficiently packed. Each shape segmentized with this program has a packing position, specifically for packing and transportation, as well as an assembled state. The solution search is top-down and iterative with a coarse decomposition of the original shape; a set of docking tests

are done per iteration to find the best way to match the boundary of a part. The packing tests are similar to the game of Tetris given on how parts are created and stored in the designated packing volume. The balance between splitting the part into smaller pieces and making these pieces packing friendly is the problem of this paper in which pyramidal primitives are used to solve this problem. Pyramidal shapes are terrain-like with a flat base as to decompose parts into few pieces and allow them to be packing and 3D printing friendly given the flat base all parts will have. The dapper program has no prior forms but is the result of simultaneous shape decomposition that is modified as it goes. The method doesn't work well with a thin geometry, as the thin geometry would be considered the same volume as much larger parts. DAP brings up a new class of optimization problems as printing volume, print time, pack-ability, and functionality matter. Future work will help with the pack-ability of the method. Warping of small parts from printing them is common and prevents exact assembly of all parts. Figure 2.23 shows 2D examples of the DAP program segmenting a part for transportation [22].

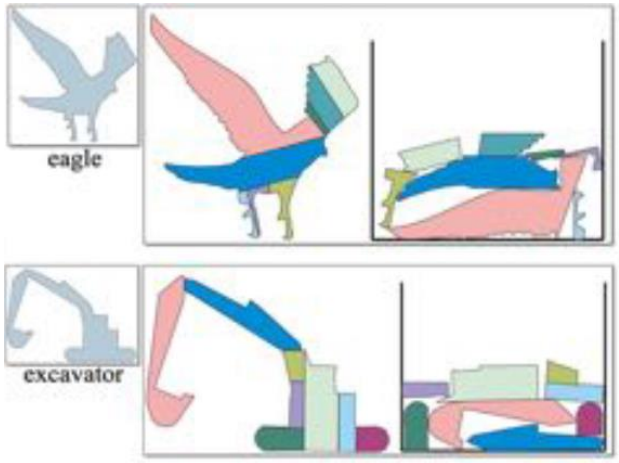

Figure 2.23: 2D results from DAP showing the constructed part and the packing after refinement [22]

Additive manufacturing technology has been changing and objects must be segmentized optimally to fit inside the print volume of the 3D printer. To solve the optimization problem for

segmentation a framework called Chopper is proposed. Chopper decomposes a large object into smaller parts to have these small parts fit inside the print volume while keeping the meaningful features of the object. This would mean the seams between different segmented parts are not interrupting any important features. Small and weak parts would be avoided so that the strength of each segment and the entire object could be kept. Connections at the interface between two parts would also be made to allow easy assembly of parts into the desired object with as little glue as possible. Chopper uses beam search to find a binary space partitioning tree that partitions the model into several parts.

In Chopper, the optimization of number of segments, not interrupting important features, manufacturing time, strength of segments, and ability to assemble with different connectors is done. The Chopper framework attempts to create the best segmentation for a specific 3D printer print volume and part as it can. If the segmentation is not as desired the user can also input which areas are important to prevent seams from being created there. This segmentation may also be useful for smaller parts as an ability to minimize support material and allow the creation of hollow parts. Figure 2.24 shows some examples of Chopper segmentation [23].

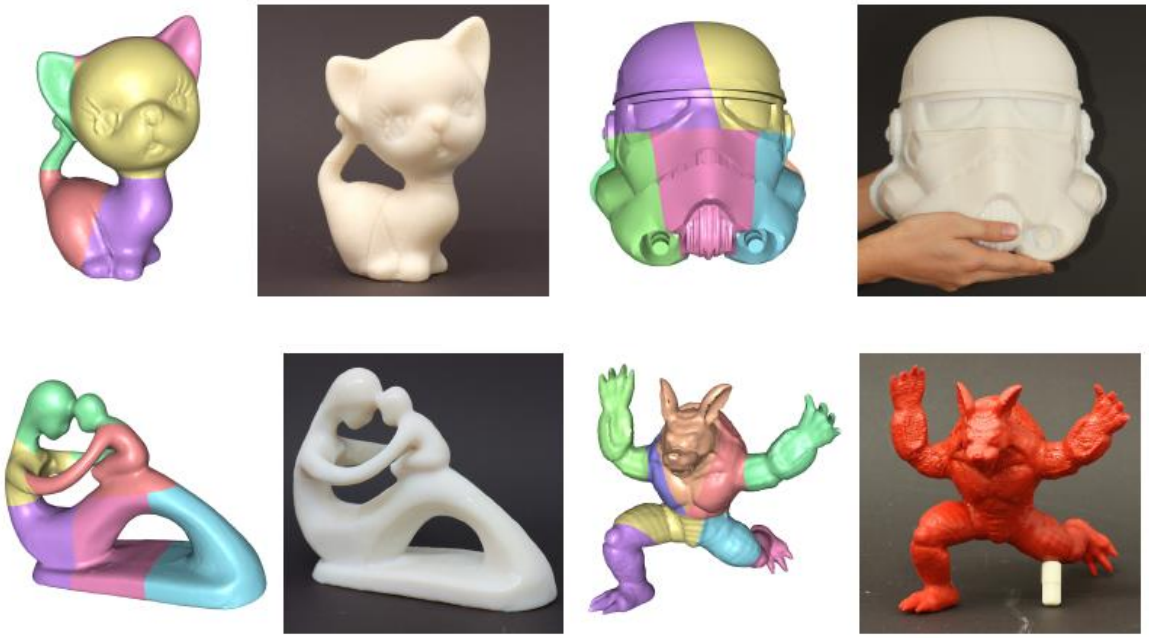

Figure 2.24: Partitioned models by Chopper with their additive manufactured results [23]

Computational methods to help with the designing and construction of reconfigurable assemblies for furniture are presented in works by song et al. These methods allow the creation of products that can be reconfigured into one of two configurations with each having their own function. Three main parts of the methods are compatible decomposition, creating a joint connection graph to model the solution space of the reconfigurable assemblies, and formulating the backward interlocking and multi-key interlocking models to optimize over iterations. Reconfigurable furniture is then created to prove the usefulness of the methods. Three major challenges exist for this; cost effectiveness, compatible joint connections between designs so parts can be reused, and that all component parts should connect solidly and there should be no wobbling in the part. No gluing or nailing can happen between parts as the structures should be able to be disassembled and reassembled at will.

To solve these challenges, first it must be known that co-decomposing multiple structures into parts that can be called as a dissection problem. Second, there needs to be compatible joints on

all sets of parts so that they can be reused to create different assemblies. Mechanical interlocking is used to accomplish this by immobilizing every part in an assembly except for one part as to allow disassembly. To solve the three challenges, first co-decomposition is formulated as an optimization over dynamic bipartite graphs. Second, a joint connection graph is created to model the connection between parts for multiple configurations. Third, a creation of backward interlocking and multi-key interlocking models to connect parts into assemblies. This allows for the creation of reconfigurable assemblies by interlocking assemblies and creates them using additive manufacturing as well as other methods. Results end up with something like the reconfigurable chair, shown in Figure 2.25, which can also be set up as stairs. Previous work by others have created modeling systems where new models are created from parts from existing models [24].

Figure 2.25: Additive manufactured step ladder chair made of nine parts that can be assembled as either a step ladder or a chair [24]

There are two ways to unfold a convex polyhedron without overlap, that being by star unfolding or by source unfolding. Both unfolding methods can be generalized to use a geodesic curve instead of a source point. A source point is a singular point on the shape that has the shortest paths to vertices of the shape, and the geodesic curve is used to replace that singular point with a curve along the surfaces. Unfolding is the cutting of the surface of a polyhedron so that the polyhedron can be flattened into a plane creating a single polygon. The finding of simple non-overlapping unfoldings is the main goal. Finding out if every convex polyhedron can be edge unfolded, with cuts only along edges, is also very important [25].

Initially created for texture mapping, an algorithm for hierarchically decomposing 3D meshes was presented for the segmentation of 3D models into smaller segments. Segmentation of models in this algorithm is done in four parts. First distances are assigned between all pairs of faces in the 3D mesh, the initial decomposition is done and assigns a probability of belonging to each segment. Then a fuzzy decomposition is computed by refining the probability values using an iterative clustering method. The exact boundaries are then constructed between the components and change the fuzzy decomposition into the final one. This segmentation is faces based which allows the model to be segmentized, then deformed, and not need to be segmentized again. Face based segmentation saves processing time by not needing to be redone after every deformation of the model. This algorithm is used specifically to avoid jagged boundaries, over segmentation, as well as keeping the segmentation after deformation of the model [26].

To make models initially designed using computer aided design to create 3D models has previously been common with use of computer numerical controlled (CNC) machines. When it comes to creating parts, additive manufacturing can have a problem when creating large parts, because of the build envelope of the 3D printer used. However, the creation of paper models to

create the same 3D models can be done with low effort and can create large models given properly sized paper. A 3D model can be put into a program to create a cutout-sheet unfolding, where the sheet can be printed, cut out, and glued together to create the desired model as paper. This is also true for making shoes or clothes, with fabric, as a 3D shape needs to be created correctly from a 2D one. Specific tabs are created in these paper unfoldings to allow locations inside the model to be glued without being visually noticeable, an example is shown in Figure 2.26 [27].

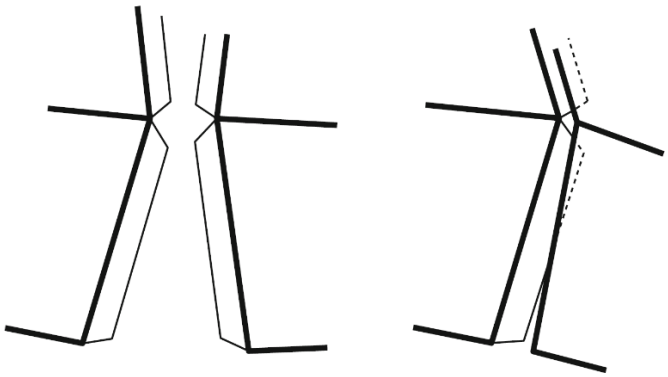

Figure 2.26: Glue tabs the cutout of the model would have allowing to parts of an unfolding to be glued together (left) tab to tab gluing (right) tab to face gluing [27]

To create this cutout sheet for paper models there are a few 3D to 2D unfolding methods. The first involves a spanning tree between faces of a 3D model. This spanning tree would originate from one face and connect to the surrounding faces, considering each face as a vertex of the graph, and each connection to the neighboring face is an edge. Unfolding the model means the deleting of edges between faces until the edge connections of the spanning tree are the only ones left, which ends with a 2D graph of the model. An example of a spanning tree can be found in Figure 2.27 for a polyhedron [27].

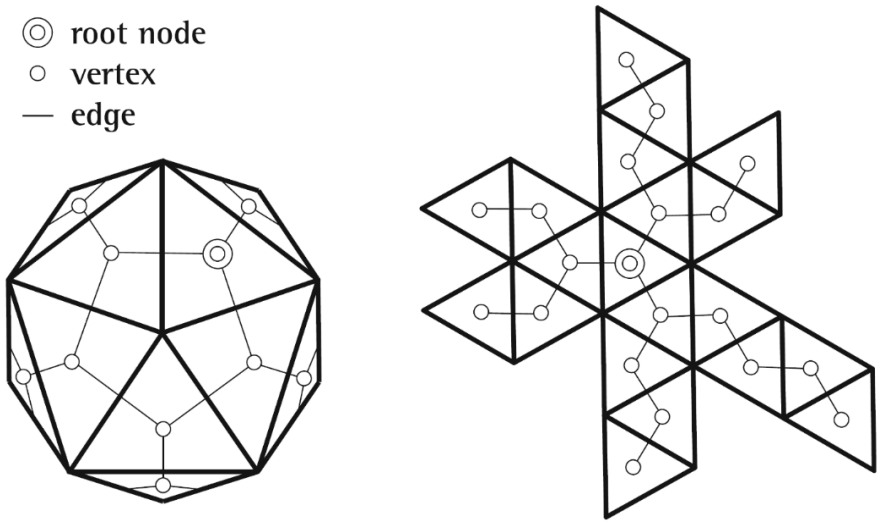

Figure 2.27: Unfolded polyhedron shape with spanning tree graph [27]

Unfoldings of models can be very different from each other even with the same model, as unfoldings with overlapping faces especially are the most undesired. For a polyhedron a non-overlapping unfolding always exists, but for shapes that are concave there does not exist a case where there is no overlapping. In this case multiple parts of the unfolding are required. Smoothing or simplification of the model may also be required to properly unfold the model. Model creation can take multiple hours, as care must be taken in specific folds. Producing smaller folding angles and overall less nodes in the unfolding, can allow models to be much easier to create. This is specifically true for potential multiple branching paths the models could unfold to otherwise, making it optimal to have the least amount of branching paths for ease of folding and creation. Pepakura is commercially available to do unfoldings of models and can be used to create unfoldings for almost any 3D model. The program specifically works with a symmetry strategy but allows a lot of options for the user to adjust the final layout as needed. Finding the global optimum for a specific unfolding is found to be a NP-complete problem for each shape, but a user with good intuition could get a result close to optimal. A partly unfolded 3D model of a duck is shown in Figure 2.28, it has been unfolded using a program but has not

been laid flat yet to show the shape of the model. Generally the shape of unfolded models cannot be guessed when they are in their flat shape [27].

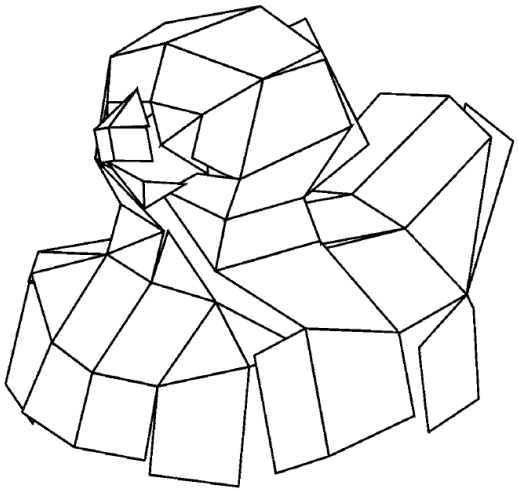

Figure 2.28: Partially unfolded 3D model of a duck, visualization of how the model unfolds from its original shape [27]

A heuristic approach to unfolding 3D triangular face meshes to 2D without major shape distortions as to make 3D paper models was created. The heuristic approach to unfolding these shapes involves the use of topological surgery, where the edge sequence on the boundary of the unfolding is encoded using symbolic representation. A genetic-based algorithm allows the unfolded mesh to fit as a single patch. The approach was found to be distortion-free as the unfolded patterns do not need to be distorted to prevent self-overlapping. This also corresponds to an open problem involving unfolding polyhedra into a single 2D unfolded section. Problems with the solution found was that all possible combinations of edges to be cut must be checked until a solution is found, which may be too computationally expensive depending on the 3D shape. Meshes up to 500 faces are the limit for the unfolding algorithm. When compared to previous methods using minimum spanning tree the proposed method allowed the creation of

unfolded models in singular unfolded segments or patches. The ability to have a singular patch unfolding can be exceptionally useful for certain applications [28].

Face and leg models were first put into different mesh tools to simplify them given their complexity. Simplifications of 90%, 99%, and 99.5% of the two models were found to be acceptable depending on the software. A head and elbow model were used for unfolding after being simplified in both Meshlab and Instant-Meshes, Instant-Meshes creating the more desired conventional mesh type. It was observed that the Instant-Meshes simplification produced was the most accurate in its simplification than the other methods, as well as creating a mesh made of uniform sized shapes which is desired for unfolding. The instant filed-aligned method was used inside the Instant-Meshes program. This simplification of models is desired because the finer and more detailed the mesh the harder it is to unfold them 3D to 2D.

The simplified models were then unfolded in Pepakura, Blender, and SketchUp. Sketchup was found to be unable to unfold cylinders and the like and so needs trial and error from manual operations to unfold which is not desired. Initial unfolding is a bit inconsistent, so a manual strip-based unfolding is done to simplify the unfolding of round objects like the sample head. Pepakura and Blender can unfold all kinds of models into flat shapes by splitting parts into their own segments as needed. Pepakura patterns can be easily separated and saved in multiple file formats and overall are found to be much easier to use for long term 3D to 2D unfolding work. Figure 2.29 shows the 2D unfolding of the Instant-Meshes simplified elbow using Pepakura, Blender, and Sketchup. The Pepakura and Blender unfoldings are desired given the lower amount of segments or patches that are created [29].

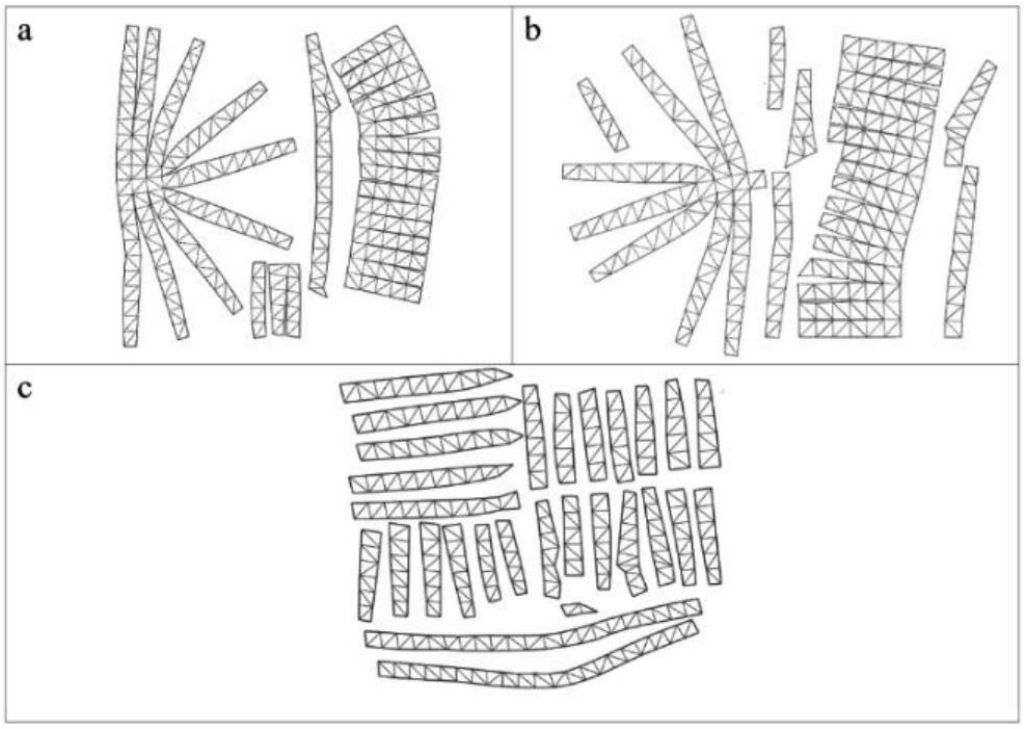

Figure 2.29: Unfolding of the Instant-Meshes simplified mesh of an elbow with manual segmentation (a) with Pepakura Designer, (b) with Blender, (c) with SketchUp [29]

Use of CLO and GRAFIS software was used to create shirts and other textiles with a 2D sewing pattern generated. These programs would use a specific 3D model of a person and create flat, unfolded clothing that could be cut out of fabric material and sewn together. Additive manufactured parts can be created on the fabrics to fit to a person while being the correct size and the ability to stiffen the textile. This could involve the creation of knee braces or protectors as shown in Figure 2.30 or for other applications where hardened surfaces on textiles are desired. This would essentially allow the creation of textile products the ability to stiffen the final product as needed with additive manufactured parts on top of the fabric. A sound dampener also could be created given a specific shape on fabric. Personal training or protection equipment could be created to fit a specific person's body [7].

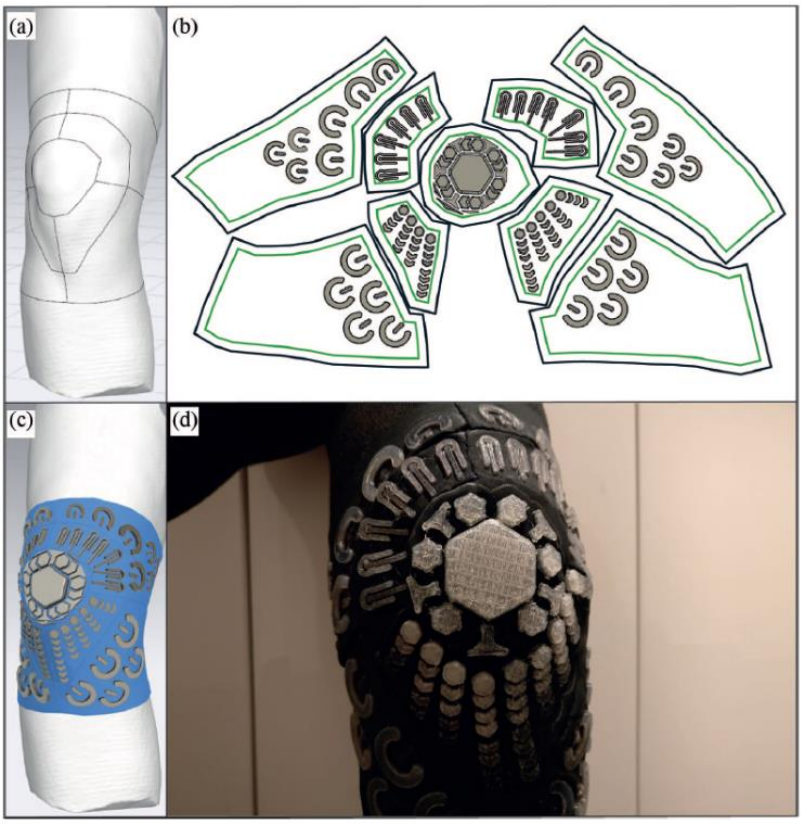

Figure 2.30: Knee brace created by additive manufacturing on fabrics (a) added seam lines on scanned knee in CLO, (b) 2D sewing pattern with modeled 3D objects in place, (c) final simulation of production on scanned knee in CLO, (d) finished product [7]

2.2.5 Applications

Engineers have been urged to look for new technologies to manufacture objects while being fast and flexible to changes in design, easy to deploy, while also being cost-efficient. Conventional manufacturing was found to cost a great deal to set up production lines, while CNC machines take a long time to create parts while having considerable cost and producing a lot of waste. This makes small production runs and prototyping not viable given these methods. Additive manufacturing however uses the required amount of material to create an object and is good for rapid prototyping and development of parts given the creation of parts is faster and more cost-effective than traditional methods. Being able to create complex geometries with the flexibility to quickly be able to create new parts are some of the main advantages of additive

manufacturing. Electronics, military, architecture, furniture, prototyping, education, and construction are examples of some previous fields additive manufacturing has been used [1]. For this research, we will be focusing on what additive manufacturing on fabrics can provide for applications, however.

Additive manufacturing on fabrics can have many applications ranging from attaching functional or aesthetic parts onto clothing to potential engineering applications. However, before getting into the specific applications additive manufacturing on fabrics can have, we will talk about recent research on the use of stereolithography (SLA) resin printers in this field. The potential of using SLA resin printers to manufacture directly on fabrics was presented as a proof of concept, as in the past FDM printers were only thought of for this task. Many textile surfaces were tested for this purpose and additive manufacturing on most of these textiles was done with little issue. Additive manufacturing on smooth surfaces and coatings was found to be an issue, however. Compared to FDM 3D printers, SLA printers can manufacture finer structures down to 0.01 mm. This would also allow the ability to create more complicated parts than previously done on fabric; parts could also be created without supports. However, only expensive resin could be used, which could make FDM printers more suitable for certain applications.

Initially cylinders were created as test prints and cured as needed. Contact angle and thickness of nanofiber material was done. A new zero level was determined because of the textile thicknesses. It was observed that roughness determined a great deal of effect on adhesion, with higher roughness producing higher adhesion at the interface. Hydrophilic samples also performed very well from looking at the samples using a fabric with a contact angle below 90. A strongly hydrophobic thin sample did however perform well which was unexpected, potentially showing that the hydrophobic materials in the sample could potentially promote adhesion.

Microelectromechanical systems could be possible with this form of printing and integration with textiles.

Fabric was also found to soak up resin in the printing process which could be squeezed out with isopropanol, but is a complex process and leaves resin in the fabric. Samples printed on fabrics were to investigate the feasibility of printing with SLA printers on fabrics and other surfaces, many surfaces were tested. Almost two thirds of the textiles tested were able to be printed on reasonably. The double-sided tape did not stick to the fabrics as well as the print bed. Resin also slowly dissolves the tape adhesive. Future work with SLA printers would involve having more effective ways in attaching the fabric to the bed [30].

Additive manufacturing can be used to create specially designed apparel for various applications. Multiple additive manufacturing methods can be used to create wearable parts from selective laser sintering, SLA, FDM, inkjet, as well as binder and micro-extrusion 3D printers. Specifically, FDM additive manufacturing is widely used to create textile and fashion pieces because of the availability of materials, simplicity, and low cost. Creation of complex and flexible structures is done with the use of computer added design for ease of customizability. The potential to create add-on parts with special functionality such as health monitoring or the ability to be better formed to a body is desired [31].

Additive manufacturing processes in the creation of shoe soles and accessories is already being done, but actual wearable garments are not something that is being sold currently. Fibrous materials embedded in a print were also previously researched where composites were made during additive manufacturing. Fully additive manufactured wearable clothing, with no fabric, was found to be feasible and as a possible application for the textile industry in the future. This would allow the skipping of multiple steps in a textiles production chain and limiting it to a

single additive manufacturing process. Figure 2.31 and Figure 2.32 shows the fully additive manufactured textiles made from PLA and assisted with soluble LAY-FOMM supports during creation. The glove specifically introduces the concept of additive manufacturing the fabric like material in parts as well as stiffening the parts in specific locations for the application [32].

Figure 2.31: Color modification of textile-like surfaces, (a) two color pattern, (b) pixel pattern, (c) UCF logo [32]

Figure 2.32: 3D printed glove, (a) additive manufactured parts created for sewing made of two materials, (b) surface design of parts, (c) flexible sewing pattern, (d) sewn together glove [32]

Using additive manufacturing to create specific products involves some of the following examples. Creation of integrated circuits, LEDs, and small electronic components on textiles was proven to be possible by additive manufacturing on fabrics with conductive materials. Inserted electronical components after manufacturing of framework on fabric is still required for functionality, however, which is not desired [33]. Combination of fabrics and additive manufactured parts allow the possibility for the combination of the mechanical strength of fabrics and the freedom of creating different 3D objects. Testing observed that the connection between fabric and additive manufactured parts is preferable for use on clothing to be worn. This would allow clothing to have aesthetic and functional designs created on them using additive manufacturing [4].

New customized shapes could be added to textiles as desired as well as potentially adding use for sportswear or protection clothes depending on the application. Previously different stiff materials like PLA and ABS have been tested for applications using additive manufacturing on fabric but some flexible materials are also being tested for this purpose. Ninjaflex polymer performed relatively well with the PLA counterparts, when created on fabrics, in terms of adhesion strength. The potential of allowing the creation of bendable applications given the polymers' high flexibility could lead to applications with wearable production that bend with the body [2].

Combining additive manufactured parts and textiles to customize garments as desired is of interest given the many potential applications it brings. Specifically individual or short run production of products could be done easily and effectively as well, given no additional joining processes would be needed. Applications have been found to apply snap fasteners or zip fasteners, as well as changing garment drape by patterns and the stiffening of materials for

orthopedic devices. Additions of conductive materials onto fabrics also could be used to create specific products, such as an integrated back protector and knee protector, as shown in Figure 2.30. A sound dampener could also be created given a specific shape as desired for the fabric and application specifications. TPS compounds were found to be better in terms of the wide ranges of hardness, providing better haptics as needed for these orthopedic applications. Future work involves ultraviolet stability and flame retardancy by specific TPU compounding [7]. Wearable electronics by integrating textiles with stiffer parts without changing the fit of the product to a person were created. Orthopedic braces for medical use could be created with additive manufacturing as well as smaller decorative features. Additionally, additive manufactured parts could be added to fabrics to maintain drape characteristics of the fabric which may be desired depending on the application [5].

After the creation of additive manufactured parts on top of textiles, copper fabric and phosphor blue paste could be applied to the composite to allow the paste to be luminescent given an applied alternating current. Adhesion strength between additive manufactured part and fabric was found to be sufficient for electroluminescent applications on textiles even after multiple washings. This would allow these textiles possible applications for interactive designs and creation of smart and wearable textiles. Specifically, in this case, for the use in entertainment or decoration [13].

The mixing of additive manufactured parts with fabrics interlaced between the layering of the part could be used for specific applications. Specifically, the interlacing of the fabric involves the additive manufacturing of a part, the pausing of the creation of the part, placing of fabric over the part, and the resume of the creation of the part. This effectively creates the additive manufactured part with a fabric layer in-between two of the layers, in some cases multiple fabric

pieces are interlaced between multiple layers depending on the application. A specific example of an application with an additive manufactured part created with a fabric in between two layers is shown in Figure 2.33 with a displacement sensor. Additive manufacturing parts on top and interlaced with fabrics can produce flexible products, like a band for a watch, as well [16].

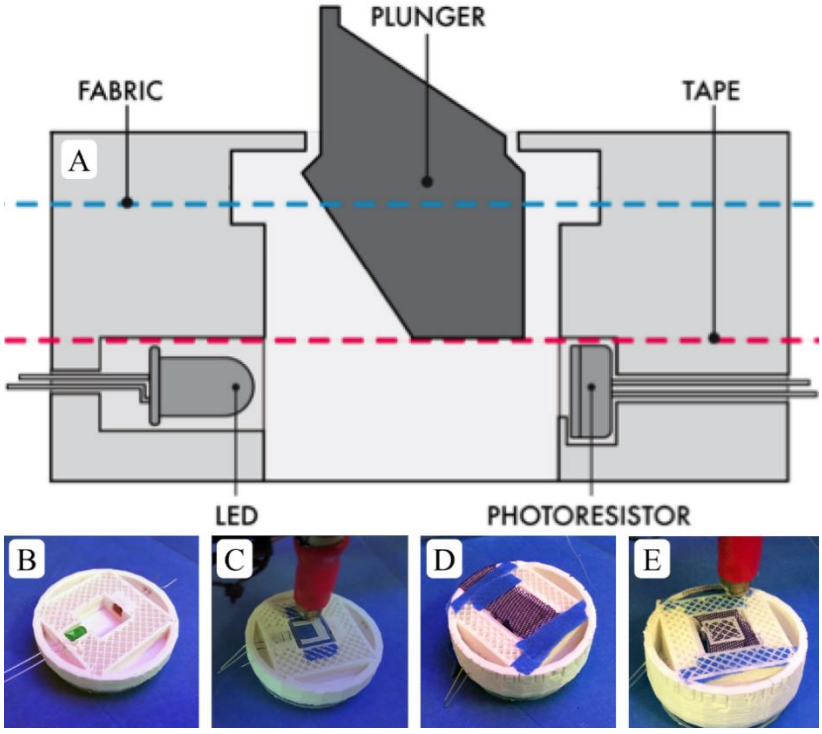

Figure 2.33: Displacement sensor created by additive manufacturing on fabrics (a) cross-section of textile-embedded displacement sensor, (b) electronics are inserted, (c) tape is placed to bridge gap to allow a space for the plunger to be created, (d) fabric is taped into place, (e) additive manufacturing resumes till part is complete with the fabric being sandwiched between two layers [16]

2.3 Material Properties of 3D Printed Parts

Ultimately the strength of the interface between the additive manufactured part and fabric is limited to the strength of the created part itself and the fabric. Meaning that the material strength of both additive manufactured parts and fabric should be determined. This is because if a force is put on the composite of fabric and 3D printed part and the fabric or 3D printed part fails before the interfacial forces then the maximum adhesion strength has been found a further improvement

is not needed. For our work given the differences between each fabric and how it is manufactured a fabric would have to be manually tested to compare to the interfacial strength properly. Testing methods such as ASTM D5034-21, DIN EN ISO 5084, DIN 53530, and ASTM D3776 are used for the testing of the tensile strength and mechanical properties of the fabric. In testing it has been observed that the samples' additive manufactured part was much more likely to fail before the fabrics' and so was given more effort in determining the strength of the part and comparing it to the interfacial strength.

Experimental testing of 3D printed parts was done to find the effects of shell thickness, layer height, infill density, the orientation of the fill angle, and print speed, with all other settings being at fixed values. A factorial design of 16 runs for these settings was tested using ASTM D638-10 type I standard tensile specimen testing. Black 1.75mm PLA filament was used. It was found that higher infill density affected part strength the greatest and improved it the higher it was. Higher shell thickness, fast printing speed, high layer height, and high orientation of the fill angle as well was found to improve material strength of a sample part [34] [35].

When creating dog bone or rectangular samples the fill angles the samples are created at three different angles. A 0 degree being along the length of the samples the 45 degrees at an angle between the length and width of the samples and the 90 degrees being along the width of the samples. A visualization of these fill angles is shown in Figure 2.34. The build orientation of how the sample is aligned in the 3D printer during creation has also been found to be a great factor. For build orientation a face-up XYZ version, edge-up XZY version, and upright ZXY version exist for potential orientations for sample creation [36] [37]. Specifically, the face up is the more commonly tested version attributable to the changes in fill angle being the most relevant in that orientation [38]. Figure 2.35shows a visualization of the three orientations where

FU stands for face up, EU is edge up, and SU is the upright samples. Visualizations of the print angles are shown in Figure 2.35 (b) – (d) where 30- and 60-degree angles are not required for our research. It was determined that the layers should be orientated with the tensile load to provide the greatest strength in the part. A finite element simulation could then be done to determine the correct orientation for an application [39].

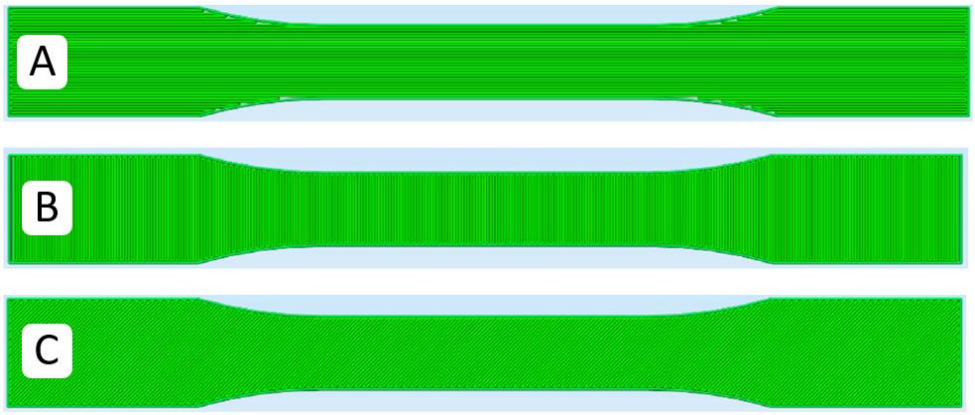

Figure 2.34: Fill orientation of dog bone samples in Simplify3D, (a) 0° layer sample, (b) 90° layer sample, (c) 45° layer sample [37]

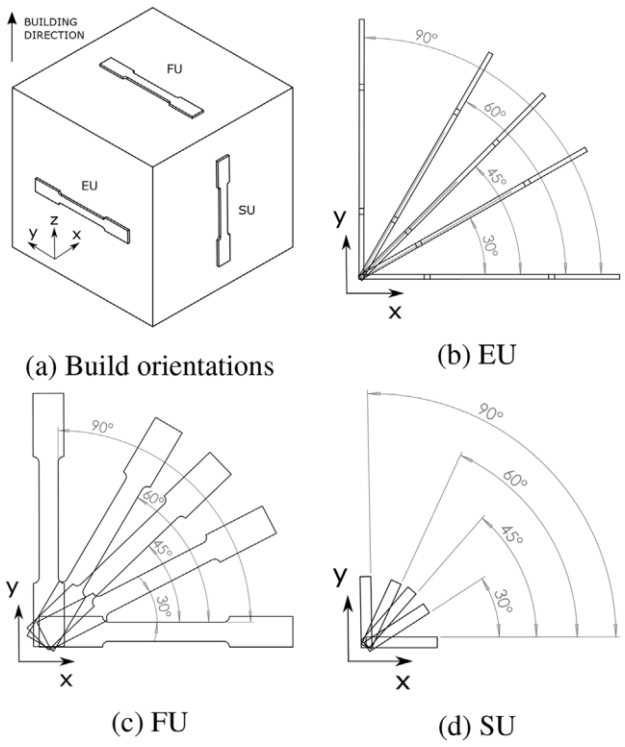

Figure 2.35: Visualizations of build orientation of dog bone samples, (a) Generalized orientations, (b) Edge up orientations (EU), (c) Face up orientations (FU), straight up or upright orientations (SU) [36]

Previous testing at the University of Maine's Advanced Structures and Composites Center involved the tensile testing of additive manufactured PLA dog bone samples. In this testing three PLA filaments were tested at various printing orientations using the ASTM D638-14 standard for tensile testing. It was observed that the upright (SU) XZ face manufactured transverse orientation had the worst mechanical properties. Where transverse refers to the print fill direction is along the width and the XZ face referring to orientation of the part to the front face of the printer being parallel to the face of the sample being created. The average maximum tensile stress was found to be 13.8 MPa for the three PLA filaments before failure of the samples. The PM brand filament was found to have the lowest tensile strength of the three PLA filaments tested at 4.70 MPa with a tensile modulus of 410 MPa.

For the in-plane shear strength of PLA an average of 18.0 MPa, with an in-plane shear modulus of 1092 MPa, was found in previous literature using the ASTM standard of D3518-13. This was with a fill direction of 45 degrees on an in-plane sample. The tensile strength, however, for a similar sample with a fill angle of 90 degrees, along the width of the sample, using the ASTM D638 standard was found to be an average of 37.1 MPa and an average tensile modulus of 3125 MPa [40]. Previous values of tensile strength were found in various previous research under a variety of different PLA filaments and printing orientations. Another range of PLA samples for tensile strength was found to be from 78.5 MPa to 40.9 MPa in previous research confirming that the strength of the samples is variable for PLA depending on the manufacturer [37] [41]. PLA molecular weight, melt flow index, and crystallinity are some of the material properties that affect mechanical properties and depend on how the manufacturer processes the material.

To combat the ranges of material properties of PLA, all samples created on the Ultimaker were created with either red or black Ultimaker PLA. The Ultimaker PLA has its properties defined by the manufacturer for an upright orientation in this case. These properties being a 33.1 ± 2.8 MPa tensile stress at break, 3071 ± 181 MPa for tensile modulus by using the ASTM standard D3039, as well as 52.0 MPa flexural strength at 4.4% strain, and 2740 ± 47 MPa for flexural modulus by using the ISO standard 178. These tensile and flexural strength results would be compared to the stresses and interfacial strengths found from both the pull and peel sample tests [42].

Issues with thin wall objects are that they often have printing difficulties from increased supports, trapped supports, and increased time of creation; the limited size of the printer allows only certain objects to be printed. Ahsan et al. proposes a segmentation suitable for curved free-form thin wall objects by generating grains and tessellating them with hexagonal cells. Parts are

then assembled with glue. Problems with other hollowing designs are that they introduce uncured trapped material inside the object like in powder bed fusion [19]. The bottom and top surfaces of these 3D printed parts, the flat surfaces both in contact and not in contact with the build plate, are generally considered of the best surface quality. However, when supports are added this can mess-up and damage the underside of parts as well as waste material and printing time [20]. Additionally, the bottom surface can suffer from elephant's foot where the bottom layer gets compressed, expanded horizontally, and made smoother than the top layer, which can cause issues with the mechanical properties. Anisotropy is a problem, when it comes to these additive manufactured parts, as material has to be laid down in a specific direction to get the strength you desire in a specific direction [43]. After the direction of intended forces on the additive manufactured part is determined it can be easy to tailor the best manufacturing orientations for the desired part.

The combination of additive manufacturing with textiles allows the creation of multi-material systems with special characteristics. The interplay between both materials was shown to affect the properties of the composite, given the modification of pore sizes and stiffness of locations. Changing the mechanical properties of both materials in these composites is required to get the desired properties of the entire composite. Specifically, auxetic structures would be additive manufactured on top of the fabric to get the desired properties in previous research [44].

Testing results showed that the mechanical properties of the dog bone samples created on jute fabric went down from the strength of PLA alone, finding that the jute hindered molecular motions during sample creation [14]. This finding of the strengths of the parts lowering when created on fabrics is concerning for applications going forward as it would have been expected that the combination of these materials as a composite would increase the total strengths. This

may be purely a problem with the jute fabrics and the flame-retardant materials applied to them. More research into the strengths of these composites would be desired to balance the interfacial strength of additive manufactured parts with fabrics with the mechanical strength of these composites.

2.4 Literature Review Conclusions

Of the fabrics used in previous literature adhesion testing the thicker and rougher fabrics promoted greater adhesion at the interface between additive-manufactured parts and fabrics. This makes the thin, artificially created, smooth fabrics have low adhesion strength at the interface. For filament polymers, given the wide amount of testing and availability, PLA appears to be the best polymer for adhesive testing. Flexible filaments such as Ninjaflex appear to have some potential but would need some more testing going forward. A limited amount of both fabrics and polymer filaments have been tested. Fabrics could potentially be tailored specifically for the additive manufacturing of parts on top of them to better understand how the properties of fabric effect the adhesion. Of the commercially available filaments many have yet to be tested for creation on top of fabrics. Preferable materials would include those with good mechanical properties and can easily be kept at a low viscosity for a long enough time to interweave with the fabrics.

Pre-treatments were done to fabrics, before having parts additive manufactured on them, as to observe how the changing material properties would affect the adhesion forces often at the interface. Polymer coatings were commonly used as treatments with the adhesion being observed as very low. However, for samples using filament polymers during additive manufacturing or fabric substrates with low thickness and roughness, the polymer coating could be used to improve the adhesion strength. Korger law was also found to be true in that

hydrophilic surfaces promote adhesion. Specifically, the wettability of fabrics appeared to be a factor with surface energy also being able to be controlled with washing or plasma treatment [2]. One case was found where the hydrophobic thin sample performed better than expected [30]. Moisture content was found to lower interfacial strength as well. Currently different pre-treatments do not appear to affect the combined strength of the fabric and additive manufactured part composite during tensile tests. Pre-treatments involving PLA filament found that PMMA and PLA coatings performed very well in promoting adhesion strength as well. Overall, pre-treatments appear to have potential in modifying the fabric substrates to have desired properties. Currently it appears that changing process parameters relating to bed temperature may lead to higher adhesion strength if that temperature is higher than the glass transition temperature of the applied coating. More testing on this would be desired but there is potential of thin coatings promoting both form-locking mechanical and chemical adhesion in adhesion samples. A combination of both adhesion mechanics, with improvements in chemical adhesion specifically, could find adhesion strengths higher than previously found.

The process parameters used by the 3D printer when additive manufacturing on top of fabric is the most important variable that determines interfacial strength at the fabric and additive manufacture parts interface. For woven fabrics having a fill orientation that is along the weft has been found to produce higher adhesion strength, for samples orientated along the warp of the fabric. Testing with samples fully orientated along the weft instead of the warp has yet to occur, however. Z-distance, the distance from the nozzle to the print bed, has been found to be a great factor in adhesion strength. Higher pressure tends to cause higher adhesion attributable to form interlocking with the fabrics and parts. This involves the nozzle being inside of the fabrics thickness to some degree. For thin fabrics, about 0.2 mm, the z-distance could remain

unchanged from the value normally used when not creating parts on fabric. Thicker fabrics often benefit from lower z-distances greatly given the higher surface area for form interlocking. However, too low of a z-distance into the fabric can cause the part to fail for thicker fabrics, so a balance must be found for each fabric. Generally, for 0.6 mm thick fabrics, going 0.2 mm inside the fabric is desired for the higher adhesion and low chance of sample failure.

Bed and nozzle temperature are two very important settings for a 3D printer with the longer the time for the placed filament material to cool the better. Where the time before the material goes below glass transition temperature the longer it flows deeper into the fabric increasing the strength of the interface. Ambient temperature and bed temperature keep the temperature up longer and are thought of as both being more important than the nozzle temperature. Having low viscosity for a long period of time is what matters in this case with the flow rate, layer height, small height versus width ratio, and higher print speed being the preferable to keep lower viscosity as well. For testing of adhesion with a specific parameter, fabric or filament, or pre-treatment having settings that produce average adhesion are preferable. This being 45-degree angle fill orientation, z-distances that do not have potential of failing the sample, and temperatures not exceeding the normal for the filament being used. This is so that results being found are applicable for all applications and are not accidentally overshadowed by other parameters that have more influence on adhesion at the interface.

Segmenting single large parts into multiple small parts can be useful as to create a part larger than the print volume of a printer. Parts could also be made by multiple printers to reduce time of manufacturing. However, the pre- and post-manufacturing of the object would require a lot of extra work, preparing and putting together all the parts. This is where additive manufacturing comes in, as parts could be created and kept together by the fabrics making for easy

transportation and assembly. Simplified 3D models from something like Insta-Meshes and unfolded models with Pepakura could be created for a desired object and then printed on fabric keeping all the parts uniform and together [29]. Unfolding would have to be curated, however, as the more parts additive manufactured on fabric adds potential that the previously created parts on the fabric interfere with the 3D printer during manufacturing. From this it could be determined that an unfolding where there is no self-overlap, is optimally one segment, and is unfolded as a single chain along the spanning tree with no branches would be optimal for additive manufacturing on fabric.

Applications for additive manufacturing on fabrics currently involve the embedding of sensors and other parts into fabrics for data collection or for aesthetic purposes. In some cases, fabrics were sandwiched between samples to allow the potential of more complex applications like the creation of a new displacement sensor [16]. Strength of adhesion and resistance to wear was found to be sufficient for the products to be worn. In the cases of the fabric creation, parts would be created into segments, stiffened in certain locations for strength, and sewn together [7] [32]. For this research, additive manufacturing on fabrics to stiffen the fabrics and create a pattern of connected parts on a fabric to use for their mechanical properties is desired. This would involve the use of the fabric to help the model fold as desired for transport, as well as have the curated strength for mechanical applications is desired. Currently there does not appear to be many previous applications of additive manufacturing on fabrics for mechanical purposes as desired. From these findings in previous literature, it could be assumed that there would have to be a balancing of properties between interfacial strength between additive manufactured part and fabric and the mechanical properties of the composite created. This is because certain manufacturing orientations and additive manufacturing process parameters, fill angle and bed

temperature, need to be set to specific values to greatly increase the interfacial strength between the fabric and the additive manufactured part. Then for the mechanical properties of the part they are desired to be tailored in a specific way depending on the application and can conflict with the process parameters for the interfacial strength. This could potentially lead to situations where you need to choose optimal interfacial strength to the fabric or optimal material properties. Additionally, from previous literature, it was found that additive manufacturing on fabrics to create a composite could lead to the additive manufactured part being weaker than if it was not created as a composite. This was an unexpected result and further testing in both the balancing of adhesive and material strength as well as the increasing of the mechanical properties of the composite would be desired.

CHAPTER 3

3D MODEL UNFOLDING

3.1 3D to 2D Unfolding Introduction

Three dimensional (3D) to two dimensional (2D) unfolding segmentation of desired object models allows 3D printers to create much larger objects than they would be able to normally. Depending on if the final object needs to be hollow or not, each face of the 3D model would be set as their own segmented part and could either be created as a plane or solid object. Large objects are created by having each face of the unfolded object as large as possible on the 3D printer and then by attaching all the faces together to create the object. Attaching the parts together is often done with adhesive or integrated connections.

Making multiple separated parts is not desired for most applications, as the amount of pre- and post-manufacturing requires having to join multiple separate parts. In this research, the unfolded faces are additively manufactured on top of fabrics to lower the amount of post-manufacturing. Each part would still be created as large as possible for the application, but now multiple parts would be created on the same fabric to keep them together. Additionally, this allows the object to be stored and transported, which is much easier than having many singular parts. In the case of the transportation and rapid deployment of singular objects or multiple patches of parts could be created, so to make transportation possible by personnel without equipment. The fabric and specific parts created on the fabric could all be customized for specific applications. This could involve fabrics with specific properties like flame retardancy and water proofing with additive manufactured parts with specific geometries.

However, when additive manufacturing all the faces of a segmented object onto a fabric, there are potential problems with the previously created parts hitting the 3D printer's frame. Fabric

would be folded around the print bed, but when the fabric has its parts created on it, it could become unreasonable to fold the parts to avoid the 3D printer's frame.

To solve this problem, the unfolding spanning tree would have to be done in a specific way to produce segmentation in a single chain, as a spanning tree with no branches. This is based on Graph theory which explains that when traveling between points on a spanning tree, for a chain unfolding, there are no branches. This would allow objects to be unfolded and additive manufactured all on one fabric if the object's geometry allows it. Orientation of specific parts during creation must be curated to allow the unfolded chain to not intersect with the printer. This is important, as it is possible to have the previous parts intersect with the printer, given that the chain will likely not be in a straight line.

For this research, a CR-10S 3D printer was used for additive manufacturing of parts where the supports on either side of the middle of the print bed were the interference parts. Printers like the Ultimaker S5 would have issues from interference with already created parts, given its enclosed nature. While other printers such as the Hangprinter would likely have no interference with the part given it is fully suspended from the ceiling [45].

3.2 Mimicking Origami Shelter Designs with Additive Manufacturing on Fabrics

An unfolded design, using additive manufacturing on fabrics, was created to build upon Verzoni's origami shelter work and the creation of hinges in an object's, or shelter's, design during initial manufacturing [46]. This specific model would require being created by a large 3D printer to keep all the parts together on one piece of fabric, while creating a full-size rectangular shelter. Otherwise, smaller scale or further segmented models would be required to create a full-scale shelter from a smaller printer. The integrated fabric parts also promote less post-manufacturing; however, the parts will still require segmentation to some degree.

Figure 3.1 shows a created model where four segmented patches of three triangular panels would be attached together and could then be folded into place and assembled into a cube shelter. This model includes various connections, where of the 18 edges between all triangular panels 8 edges are integrated with the model during manufacturing. The segmented design is meant to allow each segment to be carried by a small group of people instead of having a large singular piece. This limits the number of integrated hinges, in this case. For the edges between panels that are not integrated a hinge or latch must be added to the shelter, this is to assure the object remains fixed but could be easily taken apart afterward. Of the edges that don't have integrated hinges will have either fixed edges or flexible hinges added post manufacturing. Some of these for some of the hinges a latch or integrated hook and loop fastener could be integrated to the panels on initial manufacturing, otherwise mechanical hinges or fasteners would be required depending on if the edge needs to be able to bend or not.

The segmented nature of the design also allows it to be repaired and have replacements made easily, which in some cases the panels may need to be designed differently for specific applications. The fabric the panels are created on could also be chosen for specific properties the fabric may have, in some cases this would involve something similar to waterproofing. Otherwise, the main function of the fabric is to limit the post-manufacturing required to assemble the shelter, compared to where all the panels are created separately and connected afterwards.

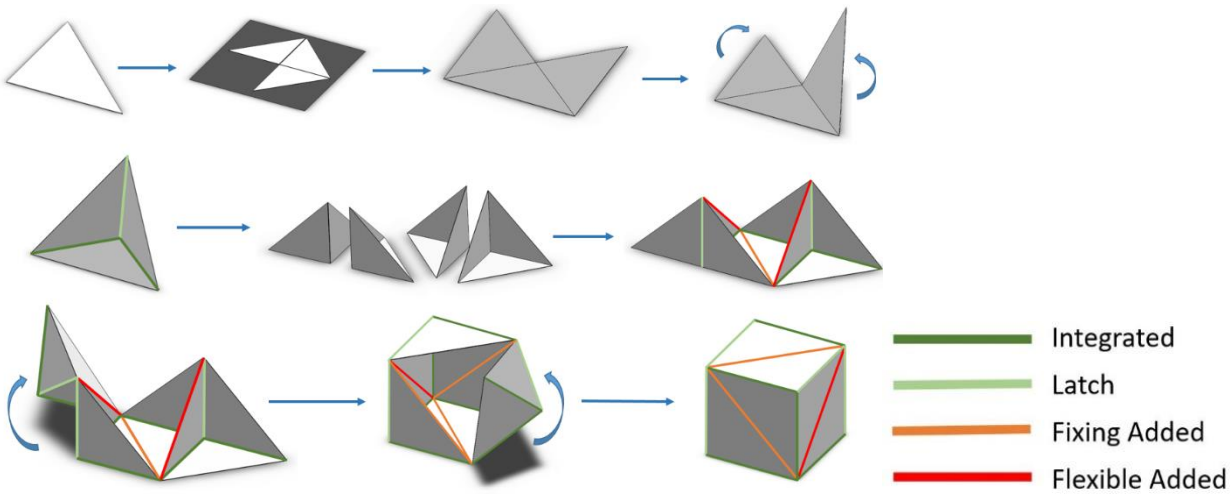

Figure 3.1: Foldable design for a cube shelter using additive manufacturing on fabrics; each patch of three parts could be carried and erected in the method shown by three personnel

On their own, a segment of three triangular panels could be folded in on themselves, to allow for easier transportation. With each segment weighing 600 N, each of the four segments could be carried into place by a group of three or four personnel without equipment. Assembly of the shelter would involve all four segments being erected and placed in the positions shown in Figure 3.1. The segments on the outside would then be connected by a hinge to the inside ones and flipped over the connected edges to the inside segments to create the roof. The fixed edges would then be created to prevent the shelter from falling apart. Assuring that the outer segments flip over and are fixed to the other panels would be the difficult part of assembling the shelter. This is because a group of people would have to flip the segment into place without putting too much force on the panels, which would be difficult with the inner segments being in the way. Forces required to raise the roof segments, the final four visuals in Figure 3.1, are shown in Figure 3.2. Equation 3.1 was used to find the force required on the outer corner of the segment as to rotate it into place (F), given the angle (A) the shelter is at from its starting position, while being rotated. The forces were found using an equivalent triangle panel of weight (W) of 1.16 kN and angle to the center of gravity (AC) of 16.6 degrees are also relevant. Future weight

optimization reasonably allows the models to be erected with three to four personnel. Initial strength testing of the interface between fabric and additive manufactured parts found that the strength of the interface could hold the weight of the additive manufactured parts on the fabric. This would mean the part could be held upside down in orientation from the fabric and not detach from the fabric, which is desired for use in real life applications. Later, adhesion strength discovered during testing confirmed this.

$$F = Sind(A + AC) * Cos(\frac{\pi}{4}) * \mathrm{W} \qquad \text{Equation 3.1}$$

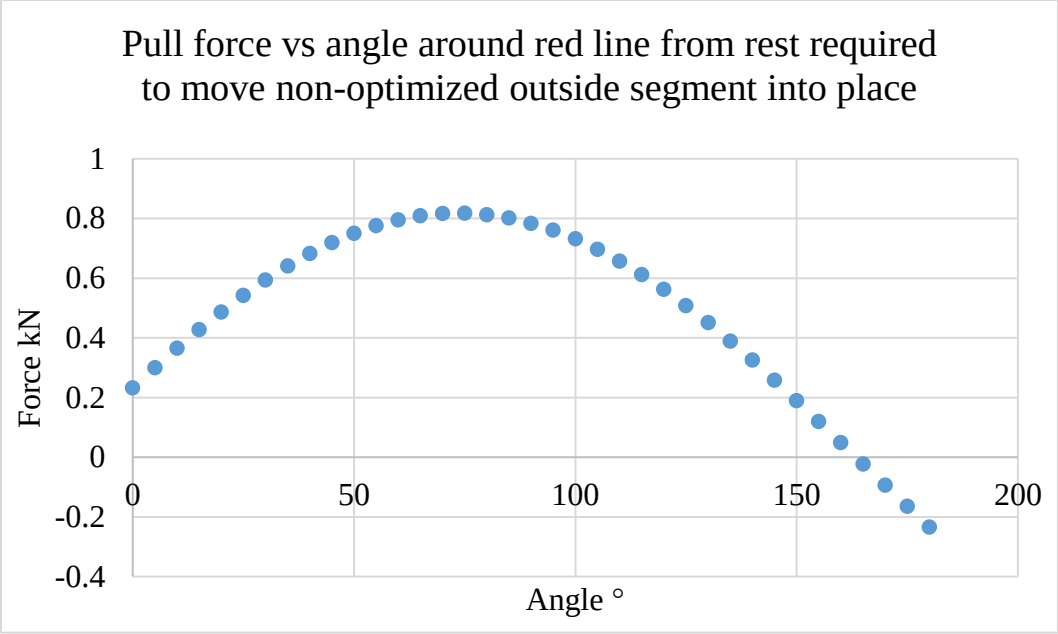

Figure 3.2: Erection forces required while providing force on the outer corner of roof segment pushing over the interface of floor segment

The created on-fabric cube shelter weighs a total of 2400 newtons. With the weight of the cube shelter being based off having unoptimized panels created by a fully solid, 25 mm thick PLA plastic panel with a side edge the length of 2.235 meters. From Verzoni's research it was determined that a weight optimization of at least 50% is feasible, allowing potential future improvements with lower weight in the future [46]. Otherwise for the on-fabric design

connectivity either involves free fabric hinges, fixed edges, or mechanical hinges. For the specific design the on-fabric shelter uses the segments allow the transportation of the shelter without heavy machinery, however. From these comparisons it could be determined that the on-fabric method of creating shelters could be used for the ease of transportation and creation. Designs for creating large shelters for specific applications would have to be created as needed and currently with the manually designed methods this would take a long time. There would be problems with quickly designing for an application because of this and so a more automatic approach that could work with any design would be desired. Specifically, UV unwrapping of 3D models for texturing, simplification of complex models, and the folding of paper models were researched. From this, the unfolding program, Pepakura was then used to unfold models. Each face from a model could be considered a panel and could be curated as desired to fit to an application.

3.3 Pepakura Unfolding

Pepakura Designer is a program that creates 2D unfolded patterns from 3D models. Normally used for papercraft, the 3D to 2D unfolding is created in Pepakura which makes the faces of the model flat to a plane with no overlaps. User input can be used to guide the unfolding; this allows models to be unfolded as desired in case the automatic unfolding in Pepakura didn't produce a preferable result. A model is generally created as lower quality with uniform face sizes, to not have too many faces and folds. Then a piece of paper would be able to be cut and folded into the shape; in our case each face of the unfolded pattern created is additive manufactured on fabric. A cut or a fold is chosen for each of the lines between the vertices of the model with the idea that the most important features should be kept and not split into parts. The unfolding often is split into multiple segments if the model is concave at any point in its geometry. This is because

when a model is concave, it is possible that the model must be split into multiple parts to fully fold out the model into a single 2D plane with no overlapping. In this case, for paper models' extra tabs must be created to allow the gluing of the multiple parts or panels of a segment together. Although for our application of the program, the tabs do not matter as we are using the unfolding to determine how a pattern of faces could be created together on fabric to create a 3D shape when folded. Alike programs such as the export paper model add-on for Blender could be used to produce similar results, but the ability to control the output by the user is very important in order to get desired unfolding patterns.

3.3.1 Manufacturability with Graph Theory

When translating the Pepakura 3D to 2D unfolding program to be used to unfold a model for 3D printing on fabric, each face will be an individual additive manufactured part. The additive manufactured parts would be created one at a time on the correct positions on the fabric decided, and preferably as a single segment or patch. This is done to create models as large as possible, given the provided 3D printers build volume. Problems can occur when creating multiple parts on the same fabric. The stiff, previously created parts interfere with the movement of the 3D printer by hitting the frame of the 3D printer.

To combat this, the model is unfolded in accordance with Graph theory and is specifically set up so that there are no branching paths between parts and no retracing between nodes in the spanning tree [47]. Effectively, the first part borders with the second part, the second part borders with the third part, and so on, for all the faces and parts of the unfolding; there is no circling back to previous parts, in an acyclic manner. The Pepakura unfolding would be manually curated to produce these single chains of unfolded models, if this was not possible, the models would be put into multiple segments. A more open concept Creality CR-10S printer was

used to allow the greatest amount of apace for previously created parts to not interfere with the 3D printer as easily, as shown in Figure 3.3. Orientation of each part needs to be set correctly in the slicer program to assure that previously created parts on the fabric do not interfere with the 3D printer as well.

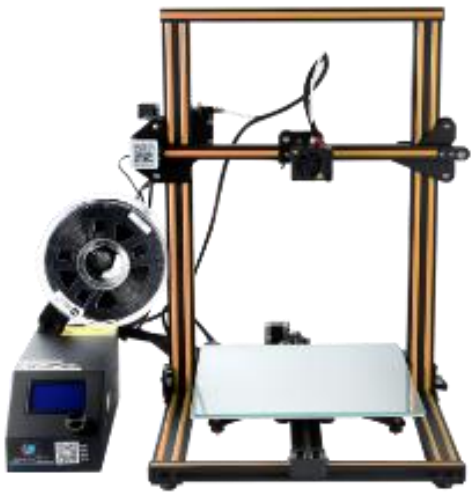

Figure 3.3: Visualization of a CR-10S 3D printer [48]

3.4 3D Printing Unfoldings

As an example of using Pepakura as a program to unfold models, Figure 3.4 shows a truncated octahedron created as a single object with a 3D printer. A thin layer of 3D printed material was made with the panels instead of fabric for this initial example. The truncated octahedron requires tape to stay in its erected 3D shape and has issues with folding on sharp corners created by the thin material layer, given how stiff the material is.

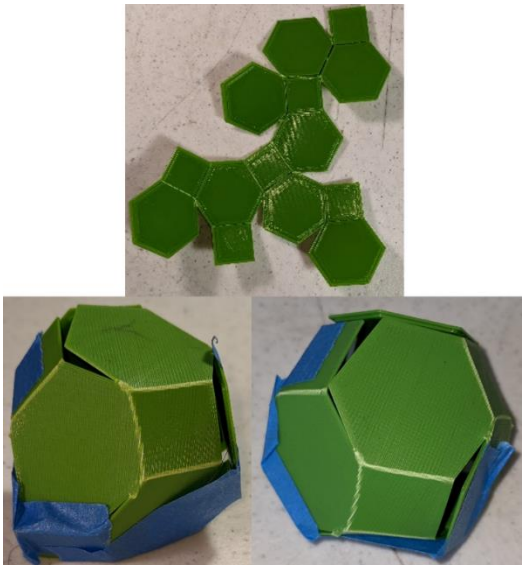

Figure 3.4: Created truncated octahedron with thin layer used for bending

3.4.1 Model Setup and Unfolding Method

The method for taking a 3D model and creating the applicable segmented parts will be explained here using the dodecahedron shown in Figure 3.5 as an example. To start, the dodecahedron, along with other basic shapes, the shapes were created using the Add Mesh: Extra Objects add-on in the 3D modeling program Blender to create regular solids by using the math function option. These models would then be exported as a .obj, or .stl, file and imported into Pepakura.

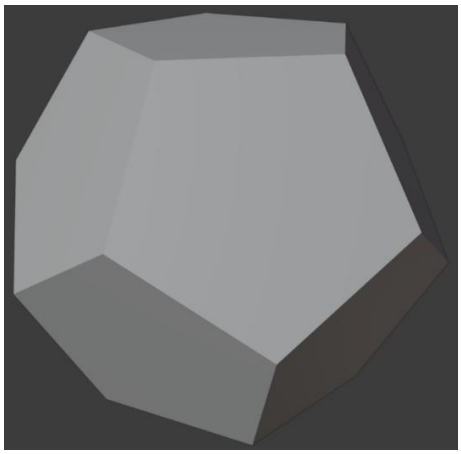

Figure 3.5: Example dodecahedron created in Blender

Once the desired model is imported into Pepakura, opening the file, selecting the direction for face normal, and which side is the front of the model will get the following shown in Figure 3.6. The size of the paper the 3D model is unfolded onto does not matter in this case, as all we care about currently is the pattern of the unfolding as we will set up the 3D models. At this point, we can unfold the model automatically using Pepakura's algorithm and then from there, tailoring the unfolding to be in the desired orientation according to Graph theory. This gets us a chain segment which can be seen on the right of Figure 3.6.

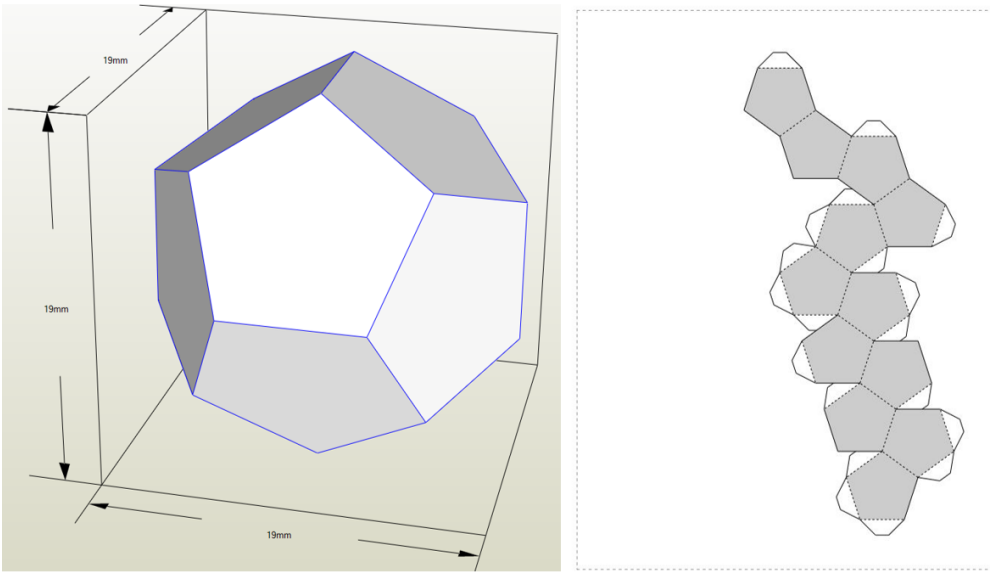

Figure 3.6: Unfolded dodecahedron in Pepakura, right side shows unfolded chain segment

Next, the unfolding pattern can be used in a 3D modeling program to create a 3D model for each of the specific parts of the unfolding. In this case, for the dodecahedron all parts are pentagon panels that are all the same so that only one model was needed to be created and sliced for the additive manufacturing of the dodecahedron on fabric. One thing to be aware of is that there were multiple orientations of this pentagonal panel. Creating multiple different slices of the pentagonal panel at different orientations helps to prevent the already created panels from interfering with the 3D printer.

3.3.1.1 Unfolding Method and Example

Pepakura allows quick unfolding of models from 3D to 2D; however, it requires input from the user and for more complex models. This could become a problem where no easily noticeable solution exists for creating unfolding patterns made of chain segments with no branches. To counteract this, pseudocode was written to represent an algorithm that unfolds simple models as chain segments. The pseudocode intends to create a method that makes chain segment unfoldings for 3D models, preferably making 2D unfoldings that are a single segment.

All faces for polyhedral shapes are given a normal vector from the middle of each face; a face is then chosen, typically one near the front and top of the model, and the closest face or randomly chosen face is then second on the string of faces for the pattern. If there are multiple faces the same distance from each other, a face is chosen at random. This goes on until all faces are in a string which creates a spanning tree [49]. This spanning tree includes a connection of normal vectors, or in this case the middle of each face, in order from face to face to show which faces connect in the 2D unfolded net and which do not. Once created, the spanning tree can be used to create a 2D unfolded net, which is the flat 2D version of the 3D model we desire. In this form, all normals are facing the same direction; however, depending on the polyhedral shape multiple segments may be required or branches may also be required. This is a not desired solution and would require the recreation of the spanning tree and the unfolding pattern again to create a different solution that limits segments and branches.

The unfolding methodology requires the edge unfolding of the models to have no branching in the spanning tree or overlapping in the unfolded net [50]. If there is no unfolding that can fit the methodology, then multiple unfolded nets would be required from the 3D model. It is believed that all convex shapes have a non-overlapping 2D unfolding, but no proof has been found yet

[27]. This means that convex shapes often require multiple segments to be created regardless of attempts to limit segmentations and branching; concave shapes, however, do not have this problem. Figure 3.7 shows an example of the unfolding of a concave polyhedron with two different solutions. Both solutions have no overlap as a single segmented group; however, Figure 3.7 (b) shows an unfolding pattern that is a chain segmentation with no branching while Figure 3.7 (c) shows a pattern with a very large amount of branching. Normally, either solution would be just as applicable in previous unfolding methodologies, but the chain unfolding is desired for additive manufacturing on fabrics to minimize interference with the 3D printer during creation.

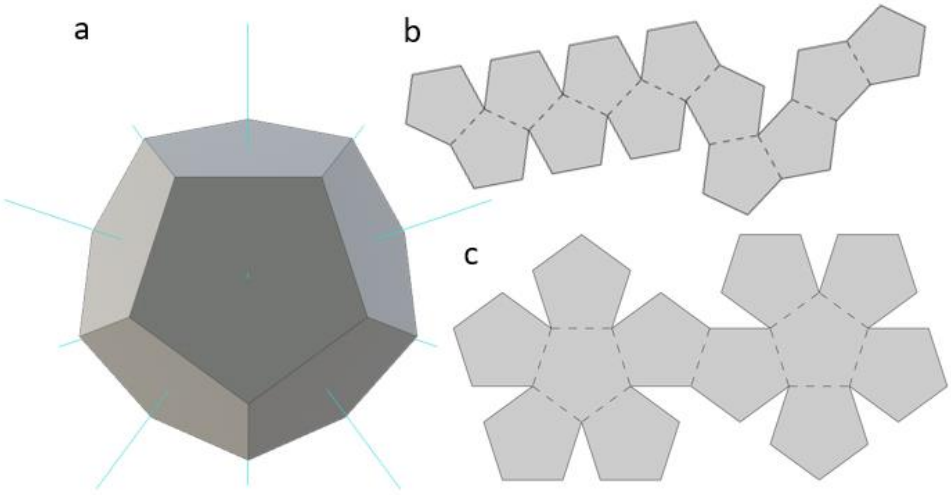

Figure 3.7: Unfolding of a dodecahedron using Pepakura, (a) dodecahedron with normals shown, (b) chain unfolding of dodecahedron, (c) common unfolding of dodecahedron

The pseudocode involves tracking all face normals of an object and choosing a face to be the base of the unfolding, with the end goal to have all face normals facing the same direction. The shortest distance from the base normal to the surrounding face normals is chosen. At this point, the face intersections with the base face are removed that don't involve intersections with the next chosen face, effectively separating the base face to all faces other than the chosen face. The

model, and all faces that don't have normals facing in the same direction as the base, is then rotated around the interface between the base face and the chosen face until the chosen face is coplanar with the base face. In the event multiple face normals have equally short paths then one is chosen at random. The chosen face is then considered to be the base face, and this goes on until the model is completely unfolded with all face normals in the same direction. Figure 3.8 shows a visualization of a cube being unfolded by the pseudocode. Specifically, the cube is being rotated 90 degrees at a time and each time a face is orientated to be coplanar with the base face until all faces are orientated properly.

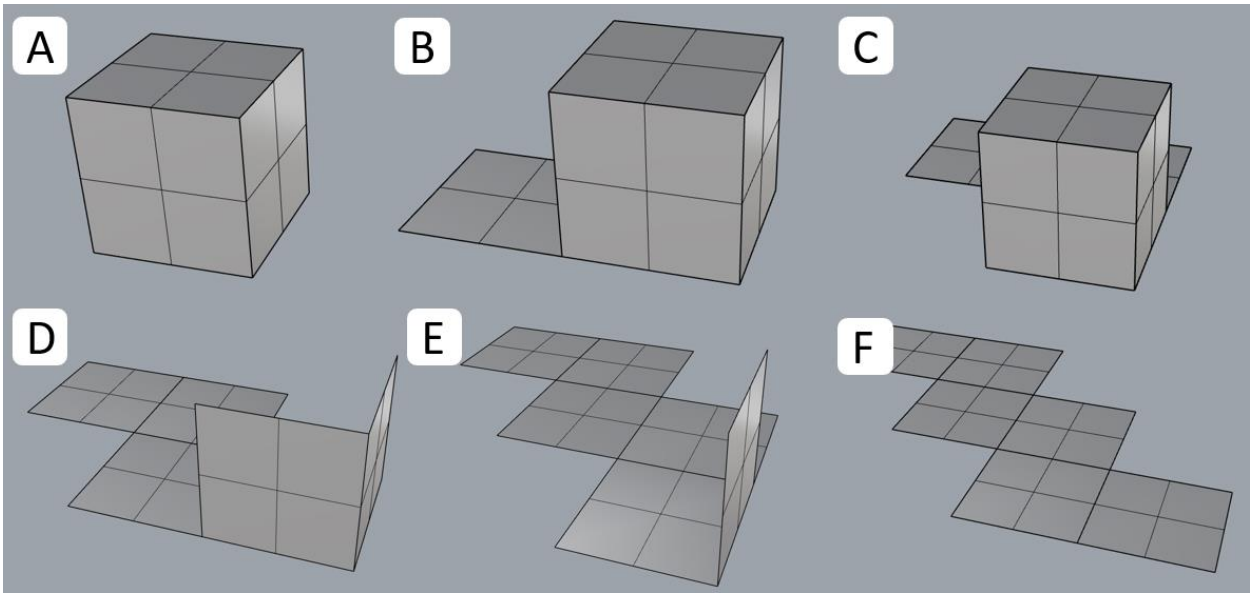

Figure 3.8: Theoretical example unfolding of a cube in Rhino using proposed pseudocode, the process (a-f) shows each time the model is reorientated as to have the next chosen plane's normal in line with the base plane's normal

The unfolding pattern for additive manufacturing large objcets on fabric ends up with a single chain spanning tree with no branches. If not the case, then at the most recent random choice a different path and face will be chosen for the unfolding. If all random choices are tested and still no single chain can be created, then at each point where a branch occurs, during the previous

iteration with the least number of branches, the longer branch will be removed from the chain and treated as its own chain. Figure 3.9 shows a visualization of the initial parts of the pseudocode, where the most important points is that the least number of segments are created and there are no branches in any of the segments. Pseudocode is by no means perfect and would need more revisions, as currently it exists to explain what kind of unfolding is desired for additive manufacturing on fabrics. Creation of an actual mathematical algorithm in a program like MATLAB would be desired going forward.

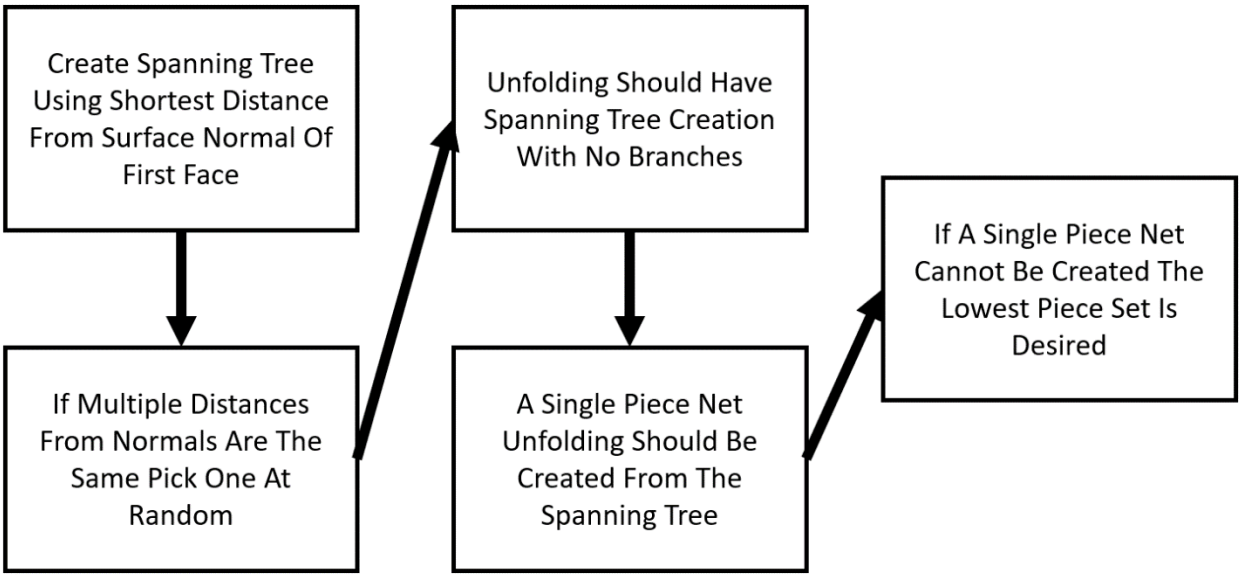

Figure 3.9: Process flow diagram for the proposed unfolding algorithm

3.4.2 Created Examples

The following are example creations of various 3D models by additive manufacturing on fabric. For these example models, most unfolding designs were created all at once to create flexible examples, and not with one panel at a time to create large objects. This would involve having the fabric cover the entire print bed and after manufacturing, the excess fabric would be cut away. To start off, the segmented foldable cube shelter parts based off the design in Figure 3.1, were created with 66 mm side lengths shown in Figure 3.10. A basic cube design was created to

compare to the segmented design, with the entire unfolding being created all at once in a single manufacturing cycle, shown in Figure 3.11. This cube design also shows the process of work from a 3D model, to unfolded design, to created product, and erected object.

Figure 3.10: Additive manufactured models of the cube shelter concept, the short edge is 66 mm

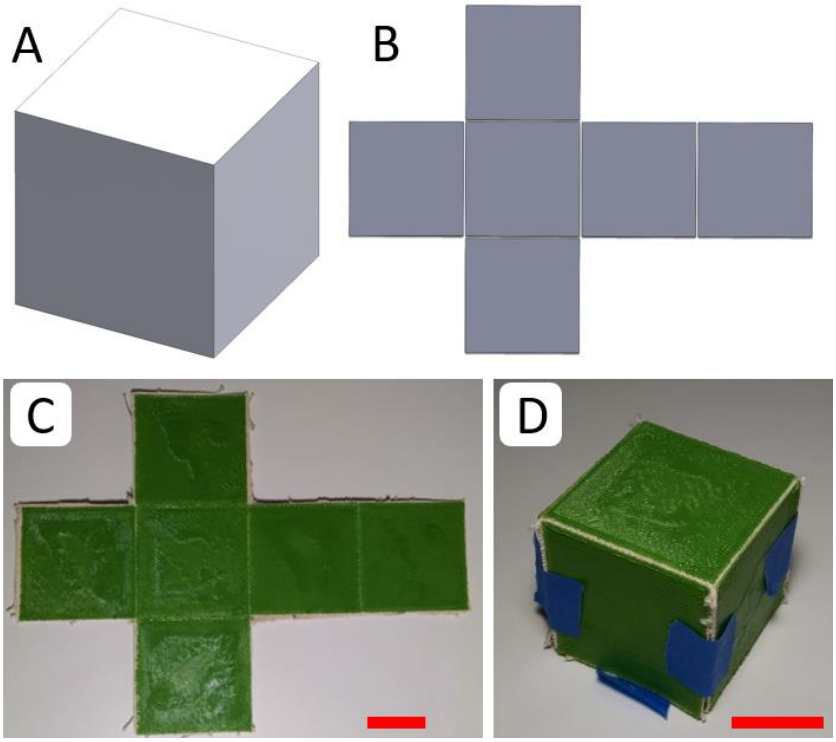

Figure 3.11: Cube unfolding concept and sample, (a) used 3D model, (b) unfolding design, (c) created product, (d) erected product with tape assists, red bar represents 25 mm, edge of squares is 52 mm

Multiple basic shapes were then created on one additive manufacturing cycle with the product being unfolded specifically to fit the size of the print bed of the 3D printer. Object's were manually set with unfolding patterns as suitable for the print bed at the time as to increase the objects size as much as possible. Doing this unfolded patterns with branches and single segments could be prioritized. Fabric would not have to be readjusted between each face creation, and there would be no risk of previously created faces interfering with the 3D printer structure. Figure 3.12 shows an initial creation of a dodecahedron with an unfolding design to match the 3D printers 300 by 300 mm print bed size. Manufacturing errors cause the surface of this model to be rough. Figure 3.13 shows a tetrakis hexahedron that was created to test slightly more complicated geometry. The creation of a simple tetrahedron was also done, as shown in Figure 3.14.

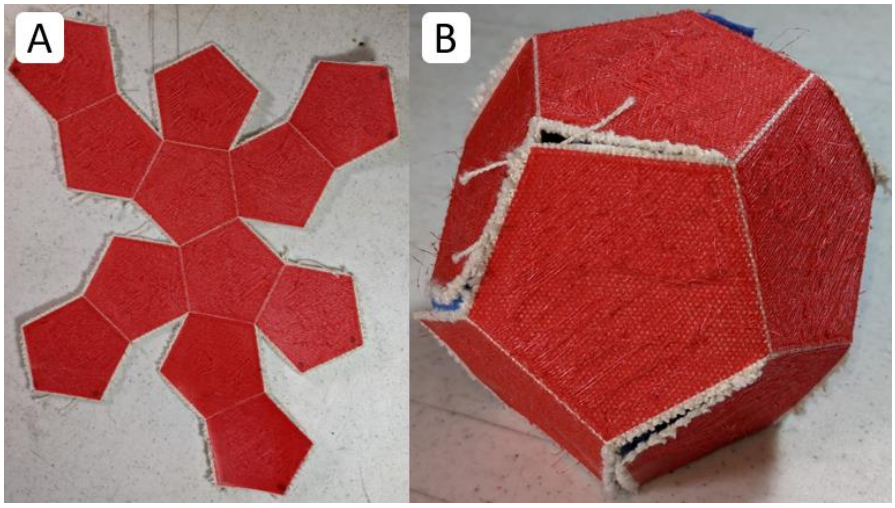

Figure 3.12: Created unfolding of a dodecahedron, (a) created unfolding pattern, (b) erected object, edge of pentagons is 37 mm

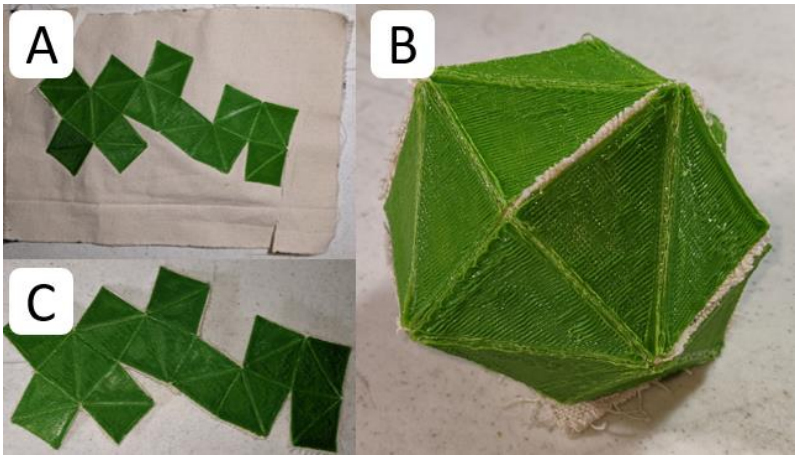

Figure 3.13: Created tetrakis hexahedron, (a) unfolded pattern with extra fabric still connected just after manufacturing, (b) faces cut away from the extra fabric, (c) erected object, short edge of triangles is 37 mm

Figure 3.14: Created tetrahedron, (a) created unfolded pattern, (b) erected design, edge of triangles is 45 mm

A large-scale dodecahedron model was then created with an unfolding pattern with branches, as shown with the small-scale model in Figure 3.15. This was done with single pentagon faces taking up most of the print bed of the CR-10S 3D printer. However, this required the folding of previously made panels, and after multiple faces had been created, it became too hard for the used fasteners to hold the part in place, caused the part to fail. After the initial dodecahedron failed the single chain segment unfolding pattern shown in Figure 3.7 was then used.

Parts were then created one at a time with the fabric being moved into the marked position on the fabric as needed when creating the next face, as shown in Figure 3.16. The final created dodecahedron is shown in Figure 3.17; problems would occur when trying to perfectly align the exact position where the next panel would be created on fabric. Often there would be a slight misalignment causing an issue with the panel's creation. The misalignment was often attributable to the difficulty in lining up marked locations on both the print bed and the fabric. Additionally, the previously created chain of panels had potential to get in the way of one of the corner fasteners making the fabric not as well fastened. This was an issue with how only one pentagon orientation was used on the 3D printer. Multiple different orientations of the same pentagon allow the fabric choices to be orientated better to previously created panels to avoid interfering with the fasteners.

As more and more panels were created the long chain of panels would be dragged around by the 3D printer as well. This drag would cause strain on the fastener clips and would result in the deformation of the second-to-last created panel, shown in Figure 3.17 (c). In the future, better fasteners and a flat space for the previously created chain to sit on would be desired to counteract this drag force. Once created, panels would need a flat space for holding, as the additional strain of the weight of these panels outside the 3D printer adds to the drag problem on the fasteners.

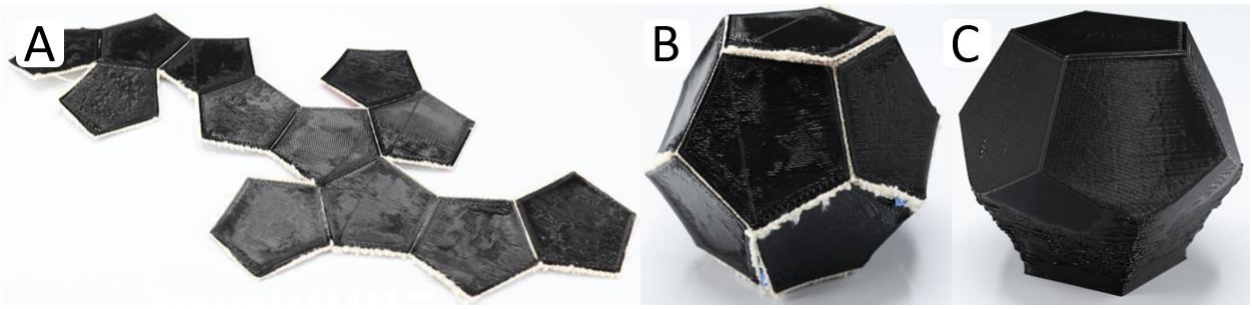

Figure 3.15: Small-scale dodecahedron sample model, (a) unfolded model, (b) folded model, (c) Solid model to compare

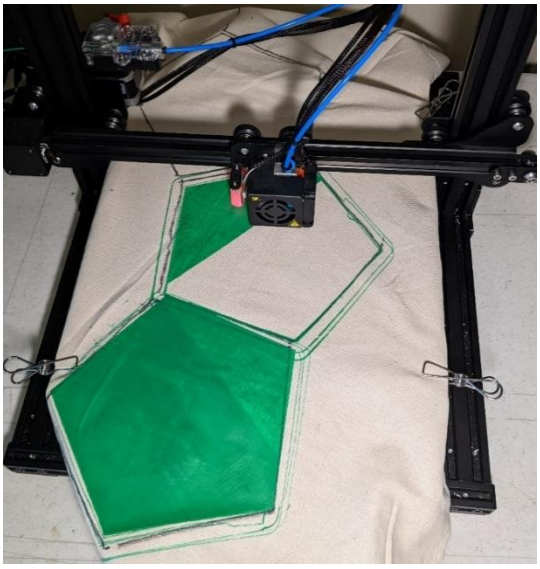

Figure 3.16: Creation of a large dodecahedron model, each panel is created one at a time where the fabric is adjusted to the marked positions for each panel's creation

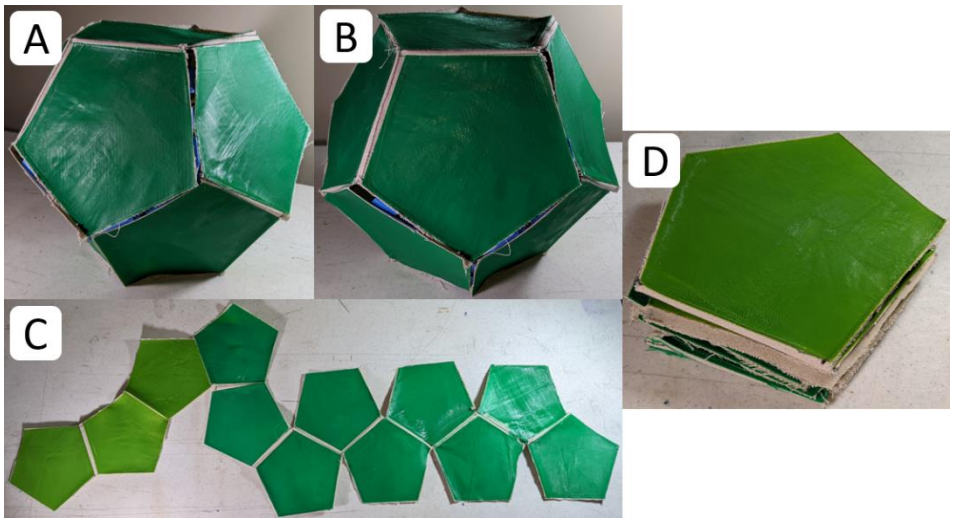

Figure 3.17: Large additive manufactured dodecahedron model, (a) and (b) show the erected dodecahedron model, (c) Unfolded pattern of model, (d) folded state for transportation, one edge of a pentagons face is 12 cm, second to last panel created in part (c) on the right had deformations due to the fasteners failing to drag the panel chain

3.5 Unfolding Conclusions

Unfolding of 3D shapes to 2D patterns for the additive manufacturing of objects for the use in mechanical applications has potential in the creation of large objects with small 3D printers. Specifically, optimized unfolding would allow 3D printers to create objects much larger than usual. Using pre-existing unfolding programs and algorithms the 2D unfolding patterns for 3D models can be found that limit segmentation and branching. This is desired when additive manufacturing large objects one panel at a time, where each panel can be created the size of the print bed. Fabric can be readjusted and set to accommodate the next fabric without chance of interference by the previously created panels. The use of correct fasteners and well orientated parts for creation can lead to properly created large objects with common, small 3D printers. In the future, hanging 3D printers would eliminate the chance of interference by parts hitting the 3D printers frame and could allow broader unfolding patterns to be created without issue. Limiting

the amount of user input required for the creation of the unfolding pattern and the monitoring of the parts being created would be desired.

Currently, the only parts created involved the unfolding of objects to 2D panels similar to paper unfolding. Going forward the unfolding of parts to 3D shapes to produce fully solid objects when erected would be desired. This would allow the potential for specific optimization of weight, storage, and transportation of parts as well as customization per part. The addition of specific features for a desired object could be tailored depending on the application as well as the fabric used. Loose edges could be joined either by the creation of parts on hook and loop fastener material as to allow connections between edges from manufacturing. Otherwise, the use of mechanical joints either incorporated in the additive manufactured parts or added in post manufacturing would be required. These joints would come in the form of mechanical interlocking shapes such as a dovetail joint or involve the post-manufacturing addition alike to a long piano hinge.

Going forward the specific spacing or beveling between parts should be created on fabric and how thick or how much extra geometry should be present will need to be researched. The accidental off-placement of panels when creating the large dodecahedron worked out well with the additional fabric to tuck inside of the part, but this will not always be the case. For objects only made of panels, the panels can be on the inside and outside of the object, with most samples preferring to have the panels shown on the outside for aesthetic purposes. However, for objects with specific geometry on them or intended for fully solid objects the fabric must be on the outside. This would require specific creation of parts on fabrics to limit having fabric flaps exposed or interfering with the interlocking of parts together. The potential of additive manufactured parts sandwiching the fabric in between two layers may help with this issue.

CHAPTER 4

INVESTIGATION OF PROCESS PARAMETERS

4.1 Introduction into Creating Objects using Additive Manufacturing on Fabrics

When initially working with and researching additive manufacturing on fabrics it was determined that the largest problem would be the strength of the interface between the fabric and the created part. From results in literature, it was determined what process parameters would be the most important to test when it came to increasing the strength of this interface. In this chapter, the specific parameters that were tested in this research will be detailed. Specifically, this includes which fabrics and filaments were used, which primer coatings or treatments were used on these fabrics, and process settings applied on the 3D printers. Process settings such as nozzle z-distance from level with the print bed, the bed temperature, the fill angle, as well as the settings that were set to be consistent through all testing will be stated. This consistent process settings involve the nozzle temperature, material used, and printer speed.

4.2 Fabric Preparation

4.2.1 Fabrics used and Tested

Before creating any parts on fabric, using additive manufacturing, the specific fabrics used and coatings to be tested must be prepared. Depending on the application, a finished object being created by additive manufacturing on fabric may use a different fabric than is optimal for getting the highest strength at the interface. However, for this work, acquiring the highest strength possible at the interface will be focused on. In previous research, it was described that the highest strength came from the melted plastic interweaving with the fabric creating a mechanical bond. There appeared to be potential in finding either a stronger mechanical or chemical bond than the strengths of the interface reported in previous literature. With this information, four

fabrics were chosen: two plane weave 100% cotton duck cloth fabrics, a plane weave 100% acrylic-dyed waterproof fabric, and a 200 denier 100% polyester ripstop fabric, from fabricwholesaledirect.com [51]. These four different fabrics were chosen because of their varying thicknesses and their deviation from each other with more natural fibers to synthetic fibers as well as different weaves

Three different house wraps were tested qualitatively. The finding was that the interfacial strength was very low and allowed the parts to easily be removed from the house wraps. The wraps were no longer tested, and it was clear that both the polyethylene and more paper derived wraps were not going to provide a high interfacial strength attributable to the lack of porosity. A Kevlar fabric was also tested. On initial attempts to create parts on it by additive manufacturing the created interface was not sufficiently different from the strength found from testing with the ripstop. No intensive mechanical testing was done to determine the specific strengths of the interface on the Kevlar fabric and instead only the duck cloth, acrylic, and ripstop fabrics would be tested initially. Results obtained that the cotton duck cloth had the highest interfacial strength during testing, and so going forward testing would only continue with the cotton duck cloth. However, when more cotton duck cloth needed to be ordered there were no more of the specific 0.93 mm thick, 15 oz. per square yard cotton duck cloth available. All future tests would use a 0.58 mm thick, 7 oz. per square yard, cotton duck cloth with a looser weave from then on. Additionally, all four fabrics used are shown in Figure 4.1. Pictures were taken at 50 times magnification with an E20:X50 microscope lens.

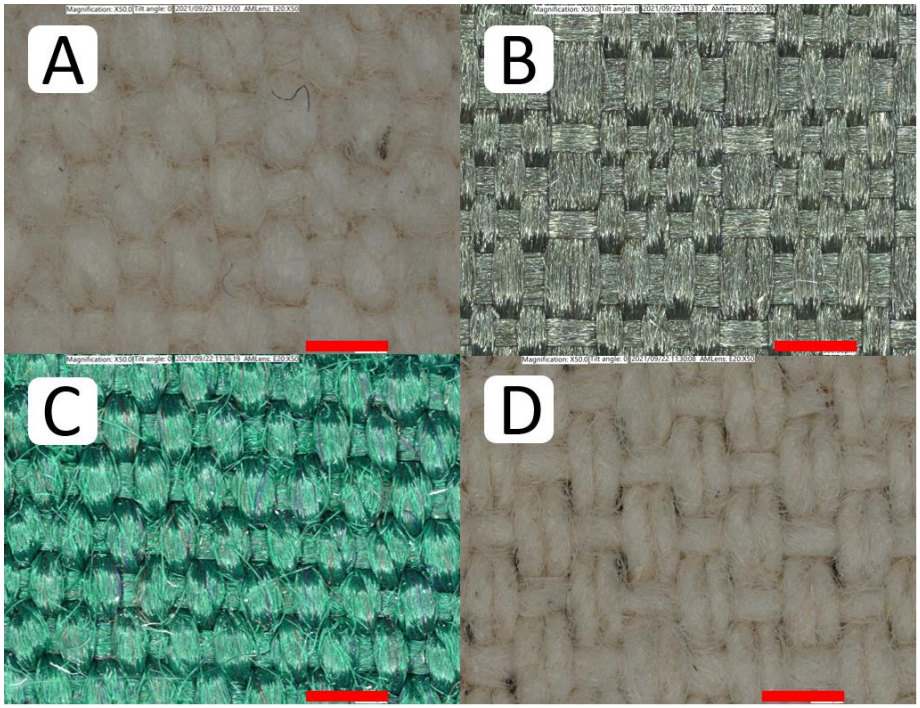

Figure 4.1:The four fabrics used during peel testing, (a) the initially used 0.93 mm thick cotton duck cloth, (b) polyester ripstop, (c) acrylic-dyed, (d) thinner 0.58 mm thick cotton duck cloth, the red bar is 1.0 mm

4.2.2 Coatings and Pre-treatments Tested on Fabrics

The polymer coatings and pre-treatments tested on fabrics, that were done exclusively on the cotton duck cloth, involved different plastics as well as different glues and washings of the fabrics. When it came to the polymer coatings, three candidate polymers were selected as: (i) poly-methyl methacrylate (PMMA) with 15k, 120k, and 350k molecular weights, (ii) poly vinyl alcohol (PVA) at a 90k molecular weight, and a pelletized (iii) nylon 6/6. The polymers were purchased from Sigma-Aldrich [52]. These initial tests involved the dissolving of the polymer into a solvent, the pouring of this solution onto the fabric and then using a film applicator to evenly spread the material out. For most polymers only one specific mixture for the solution is used, but for the 15k molecular weight PMMA two different solutions were tested. This was to determine if thinner coatings change the strength of the interface to a significant degree,

specifically if mechanical connections could be present with coatings. Fabrics would be left to dry in a ventilated hood at room temperature, after having solutions applied to them, to leave behind a smooth coating on them. PVA however was found to not be suitable for testing and the samples created were not tested, because of a powder being left behind after drying instead of a smooth coating. After creation of coatings on the fabrics, parts would be additive manufactured on them using the standard process parameters. Specifically, with the nozzle temperature of 220℃, bed temperature of 70℃, and fill angle of 45 degrees unless otherwise specified.

The initial testing of these polymers found that the surfaces of these polymers on the fabrics were greatly variable and would require the film applicator. The film applicator was included in the creation of the future pre-treated fabric samples to assure consistency throughout samples and was not used for the initial samples at the time. All covered samples created with the film applicator had their thickness measured at six locations along the fabric as shown in Figure 4.2. The thickness at these six locations is measured using calipers where the average of these thicknesses will be reported with the results of the testing. Additionally, initial fabric coating failed due to the fabric curling up when drying overnight because of the hardened polymers shrinking and enforcing a shape. To solve this, clips were used to fasten the fabrics to a flat pan while drying. For all the samples that involved a plastic coating pre-treatment over the fabric the 3D printed part would be created on top of the fabric the same as any sample without the coating. Some covered samples did however require a different Z-distance setting from the print bed as to compensate for the extra thickness of the sample. PMMA covered samples were tested with a bed temperature during additive manufacturing of the part at 70℃ and 120℃ as specified. Where 70℃ bed temperature was used due to it being a common bed temperature and 120℃ was used as it was closer to the glass transition temperature of PMMA.

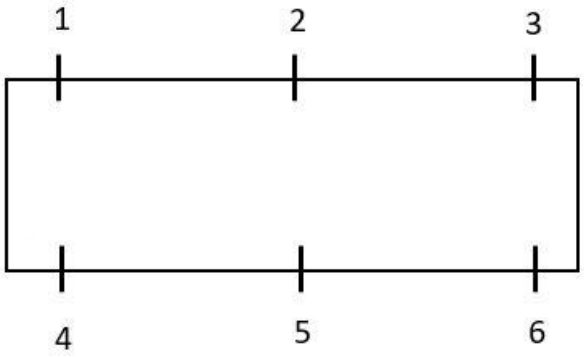

Figure 4.2: Locations 1-6 measured for thickness on a peel sample fabric

The primers applied to the fabrics that involved glue dealt with a starch adhesive glue stick, made by the UHU company, and a super glue made by Loctite, specifically Loctite 410. For the starch adhesive glue stick the adhesive was applied to a fabric sample right before the part was additive manufactured on it. Loctite, however, was applied to a control sample that was not manufactured on fabric as to determine if the Loctite adhesive could be used to adhere additive manufactured parts after creation.

After the results for samples created using the adhesive glue stick coating the results were compared to the results of similar tests without the adhesive coating. This was to determine if the addition of the adhesive affected resamples to a significant amount and was done with two different two-sample t-tests. The first using the MATLAB ttest2 equation, which uses Students t-test, compared multiple samples both with and without adhesive coating as a primer. The second test involved the use of RStudios t.test function, which uses the Welch t-test. Both would find a value of P and would be compared to an alpha value of 0.05. If the value of P was found to be below the alpha value, for both tests, then there was a significant change between sample sets with and without the adhesive. For the Loctite control, additive manufactured parts were created, and the Loctite was applied to one of the sides of these parts and adhered to the fabric samples.

The cotton duck cloth was also washed to determine if the removal of any sizing that was put on the fabric during manufacturing of the fabric, commonly referred to as scouring the fabric. The fabric was washed using two methods where both methods involved a relative solution of 1-liter deionized (DI) water, 10-milliliter Ecosurf EH-3 non-ionic surfactant, and 5-grams of sodium carbonate. The fabrics were put into the solution for 20 minutes at 70℃ and when the washing was done the fabrics were rinsed with DI water. Once rinsed the fabric are put into a second solution for another 20 minutes, with the same process, and then rinsed with DI water again. The first method would involve the washing of the fabric in a beaker on a magnetic hot plate with a stir bar stirring the solution as shown in Figure 4.3. The second involves the use of a 3510 Branson ultrasonic cleaner where the ultrasonics were turned on for two 20-minute treatments, as shown in Figure 4.5 with the washed fabrics drying. Because of issues with heating the actual temperature of washings for the beaker was around 60℃ both washings, and the ultrasonic washing solution temperature was around 46℃ for both washings. Once done it was determined that the washings made the fabrics wrinkle too much and could potentially cause the creation of additive manufactured parts on these fabrics to fail. To correct this the fabrics were smoothed out with a clothing iron and left to dry. Both solutions were found to have removed pigment from the fabric, beaker solutions had also changed color after testing. This was determined because the fabrics being much paler after washing, especially for the ultrasonic washed fabrics.

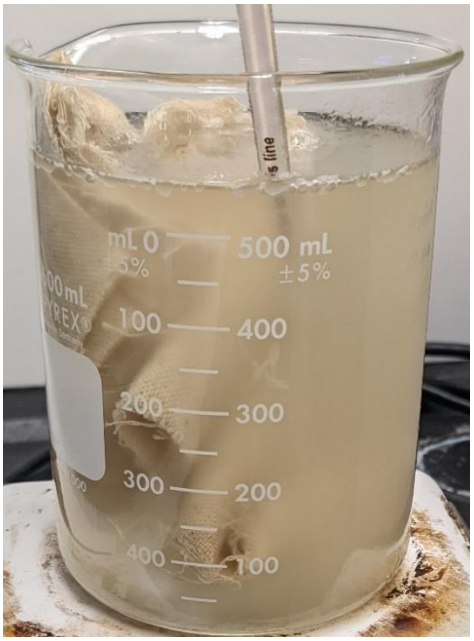

Figure 4.3: Visualization of the washing of fabrics in a beaker

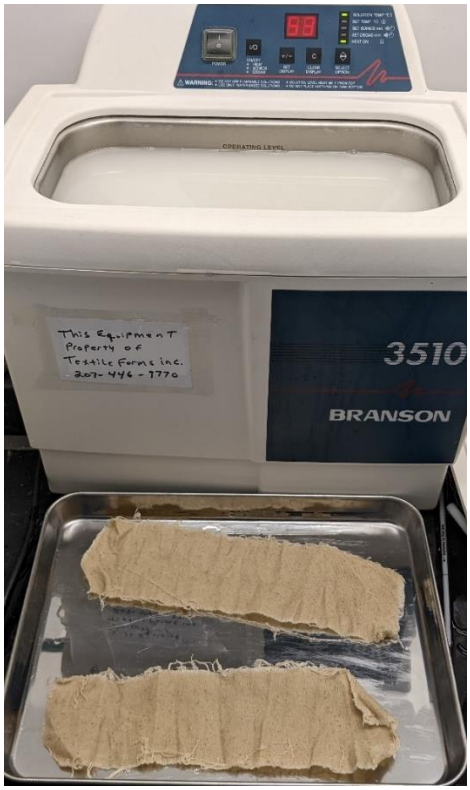

Figure 4.4: Visualization of the washing and drying of fabrics in the 3510 Branson ultrasonic washing machine

4.2.2.1 Solutions Used for the Creation of Coatings

When initially working on creating solvents and pouring solutions onto fabrics various solution mixtures were tested. In all situations a Corning model PC-220 magnetic stirrer with 120 VAC-283 Watts-60Hz was used to stir and heat the solutions. The following is the mixture amounts for all PMMA molecular weights and for the nylon 6/6 used for sample creation.

For the two nylon sample sets, formic acid was used as the solvent where 100 grams of formic acid would be used for every 12 grams of nylon. Materials would be put together in a beaker sealed with aluminum foil and rubber bands, to prevent evaporation, then mixed with magnetic stirrers overnight. Once mixed the solution would be poured onto the fabrics evenly and left to dry. The entire process would be done under a ventilated hood with personal protective equipment that is suitable for handling the dangerous formic acid.

For PMMA each molecular weight would be treated with different amounts of Omnisolve acetone to compensate for the high or low molecular weight of the PMMA. The 350k molecular weight 90 grams of acetone was used with 12 grams of PMMA. For 120k molecular weight 90 grams of acetone was used with 25 grams of PMMA. The 15k molecular weight had two mixtures tested: the first used 80 grams of acetone and 20 grams of PMMA, the second used 95 grams of acetone and 5 grams of PMMA. Once the solutions were created, they were poured onto fabric and left to dry on trays overnight in a ventilated hood. It was observed that a large amount of PMMA material would be left behind on the bottom of the fabric. To solve this problem, the samples were put at an angle to dry so that the excess solution would collect at one end instead of adhering to the bottom of the fabric. As shown in Figure 4.5, it is unknown if the use of this technique changes the adhesion strength, but it did help with acquiring even coatings on each of the fabrics. Microscope pictures of some of the coatings used on cotton fabrics can be

seen in Figure 4.6, all photos were taken at 20x and 50x magnification with a 0.5 mm lens. Both the 0.93 mm thick and the thinner 0.58 mm cotton fabrics are used for coatings, with the thinner fabric samples being the more recent and involving the use of the film applicator. Barely any PMMA can be seen on the samples for the thin coating.

Figure 4.5: Drying setup for samples, samples would be clipped into place on a pan after having the coating applied to them as to prevent them from curling, pan would be put at an angle to prevent solution creating a thick coating on the bottom

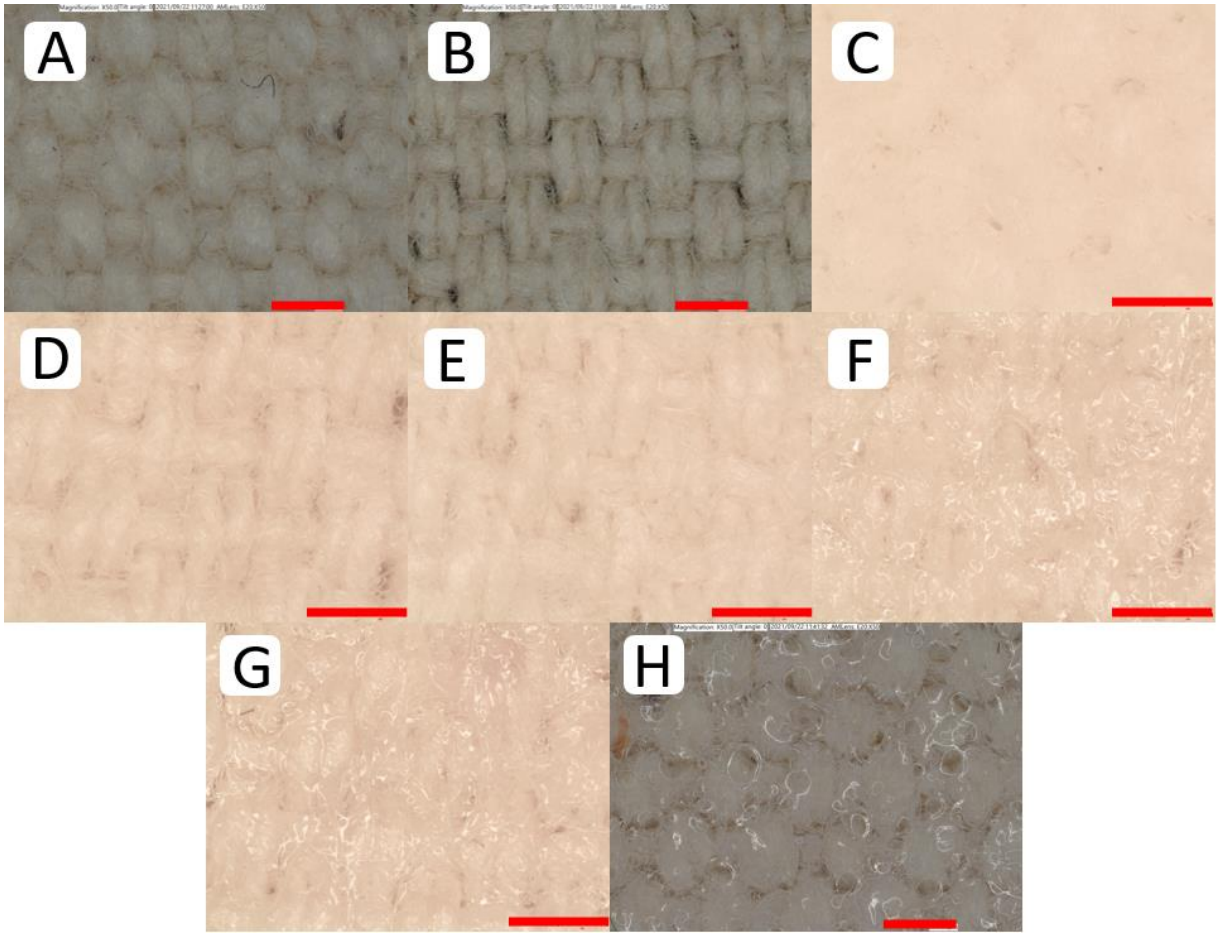

Figure 4.6: Polymer covered cotton fabrics (a) Original 0.93 mm thick fabric no coating, (b) 0.58 mm thick, thinner fabric no coating, (c) nylon covered thicker fabric, (d) 5-95 coating of 15k PMMA, thinner fabric, (e) 20-80 coating of 15k PMMA, thin fabric, (f) 120k PMMA, thick fabric, (g) 120k PMMA thin fabric, (h) 350k PMMA, thick fabric, the red line represents 1.0 mm

4.3 Process Parameters Tested and Their Selection Process

4.3.1 Consistent Parameters Throughout Testing

The following describes the process parameters used for the 3D printers that were consistent throughout all sample creations. A brim was created so that when setting a z-distance and leveling the bed both could be done as normal without the fabric interfering with the auto-leveling bed sequence the 3D printer had. Once the brim had started being created the print could be paused by the operator, the brim could then be used as a guide to place the fabric on the print bed. The material used for all samples would be PLA as PLA was found in previous

literature to have the higher interfacial strength than other tested common filaments. The nozzle temperature was set to 220℃, that being the highest nozzle temperature that is recommended for PLA. Printing speeds would also be kept at the default 70 $\frac{\text{mm}}{\text{s}}$. Z-distance would also be kept constant for each fabric sample but would be determined separately for each fabric used.

4.3.2 Z-Distance

The z-distance, or z-offset, is the distance from the first layer of material the 3D printer puts down to the print bed. When additive manufacturing parts on top of fabric the 3D printers are leveled when the fabric is not fastened on top of the print bed. When additive manufacturing on fabric the nozzle may be too far into the thickness of the fabric. This can result in the fabric being moved by the nozzle or material to start backing up into the nozzle causing the print of the part to fail. To prevent this the z-distance must be set properly as to not greatly interfere with the fabric during printing.

Results from the literature survey found that creating a part on fabric with the nozzle inside the thickness of the fabric, the strength of the interface between fabric and additive manufactured part would be stronger. From these results it could be determined that a different z-distance should be used for each fabric that involves the nozzle to be at least somewhat inside the fabric. This is because the further in the fabric the nozzle is the higher the interfacial strength, but if it is too far the fabric will move around during testing and the print will fail. Initial testing found that the ripstop and acrylic fabrics were so thin that no changes in the z-distance were required to prevent issues from the nozzle being inside the thickness of the fabric. This allowed the 3D printer to create parts as normal with no compensation for the thickness of ripstop or acrylic fabrics tested. Given both fabrics were thinner than 0.2 mm, not compensating for their thickness aligns with results found in literature [3].

Given how thick the cotton duck cloth was, multiple z-distances were tested, shown in Figure 4.7. These z-distances include the z-distance used when not creating parts on fabric for the printer, shown on the middle right of Figure 4.7 as -2.525 mm, and a difference of 0.1 mm for each sample going to the left except for 0.2 mm between the last two samples. After the samples were manually ripped off the fabric the surfaces of the additive manufactured part were inspected. This was to find the lowest height where there still was a uniform pattern of fabric left behind on the part, as for all samples some amount of fabric would be left behind on the additive manufactured part.

From this it was decided that a +0.2 mm z-distance would be used from normal bed leveling for parts created with the CR-10S. This would make it so that the nozzle is roughly 0.7 mm inside the fabric. After switching to the Ultimaker S5 the z-distance was set to +0.4 mm because of issues with manufacturing on the cotton duck cloth. These issues being that either the fabric would start being moved around by the nozzle and cause the part to be created improperly on the fabric, or the deposited material would back up in the nozzle. This makes the nozzle only 0.18 mm inside the fabric when manufacturing on top of the thinner duck cloth, and about 0.5 mm inside the thicker fabric. When creating samples on top of ripstop or acrylic fabrics they do not use any changes in z-distance for all samples. Additionally, different thickness of fabrics because of the coatings put on them would cause z-distance to change with variance from base fabric being added onto the z-distance. Thickness of the used fabrics are shown in Table 4.1 along with the z-distance adjustments used with them when the Ultimaker S5 printer was used to create the parts. Generally, this would mean the thickness would be set at 0.5 mm instead of 0.4 mm for all coatings on the thick duck cloth. Additional z-distance would not be added for the

covered thin cotton duck cloth samples, as it was determined the best z-distance would be 0.4 mm.

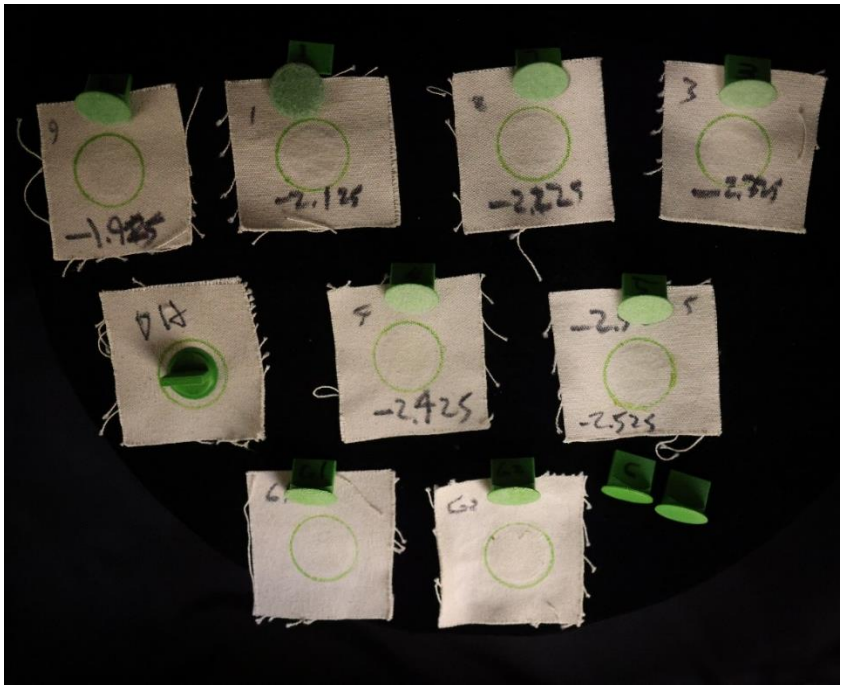

Figure 4.7: Various z-distances tested when additive manufacturing pull samples on top of cotton duck cloth. Samples are listed according to their z-distance used for the print, with -2.525mm being the one normally used for printing, and -2.325 being the desired z-distance for additive manufacturing on fabric

Table 4.1:Thicknesses of fabrics used with peel samples when using the Ultimaker S5 3D printer; polymer coatings included

Textile:	Structure, Material:	Thickness (mm):	Additional Z-Distance Added (mm):
Duck Cloth	Woven, Cotton	0.93	+0.4
Acrylic-Dyed	Woven, Acrylic Fibers with Cotton Fill	0.58	+0.0
Ripstop	Woven, Polyester with Polyurethane finish	0.2	+0.0
Duck Cloth	Woven, Cotton	0.58	+0.4
PMMA Mw 350,000 Coating on Duck Cloth	Woven, Cotton with PMMA Coating	0.98	+0.5
PMMA Mw 120,000 Coating on Duck Cloth	Woven, Cotton with PMMA Coating	1.00	+0.5
Nylon 6/6 Coating on Duck Cloth	Woven, Cotton with Nylon Coating	1.02	+0.5

4.3.3 Bed Temperature

The bed temperature used during the additive manufacturing of the samples on fabric was found in the literature survey to be a major factor in the interfacial strength. Bed temperature during sample creation is one of the major process parameters tested among sample sets. Bed temperature initially was set 60℃ during sample creation, but for specific bed temperature testing 70℃, 100℃, and 120℃ were the temperatures used. Temperature specifically was raised as to be closer the glass transition temperature of the PMMA used, this being roughly 120℃. Higher bed temperatures were not used because of keeping the bed temperature higher than 120℃ was unreasonable. This was done to keep the extruded material at a lower viscosity and facilitate the flow through the porosity of the fabric to acquire higher mechanical interlocking strength at the interface. The bed temperature will be specifically mentioned in reference to specific sample sets as applicable with most samples being set to 70℃ as to test process parameters separate from bed temperature.

4.3.4 Fill Angle

The fill angle of the samples created in reference to the warp of the fabric was also found in the literature survey to affect the strength of the interface. In Cura the setting that controls the fill angle, or fill orientation, is the Top/Bottom Line Directions setting. A visualization of the fill angle is shown in Figure 4.8 using a peel sample as an example. During testing, the fill angle was set to 45 degrees from the warp direction when testing parameters other than the fill angle itself. When testing the fill angle, the 0, 45, and 90 degree angles were tested to determine how this parameter affects the strength of the interface.

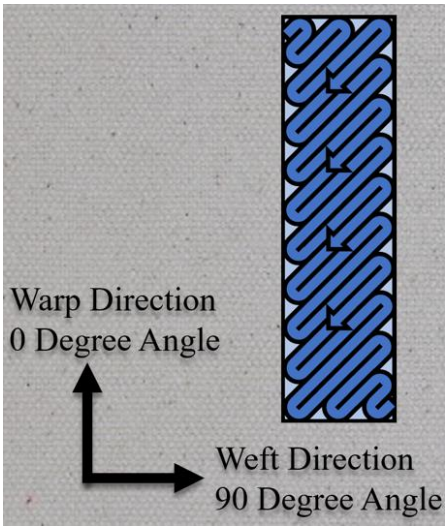

Figure 4.8: Visualization of fill angle with the warp and weft of a fabric

4.4. Manufacturing Protocol

The printing protocol involves the setup for the creation of samples, dependent on the sample being created, and involves certain process parameters to be consistent, a summary of process parameters is shown in Table 4.2. These consistent parameters for sample creation were that the nozzle temperature was set to 220°C, both on and off fabric, and the printing speed was the default 70 $\frac{\text{mm}}{\text{s}}$. The high nozzle temperature was set because it was the highest temperature

recommended for PLA plastic and the lower viscosity of the plastic caused by the extra heat was desired. PLA plastic was used for all samples created, with Ultimaker's brand specific PLA being used with the Ultimaker S5 printer. Generic PLA filament was used for sample creation from the CR-10S printer. Additionally, the Ultimaker was set in a sealed enclosure which better controls the environmental temperature and potential outside effects. For other settings not mentioned here the base settings for the CR-10S 3D printer were unchanged for a 0.4 mm nozzle to create a 0.20 mm layer height while using Simplify3D as the slicer. Specifically, three solid layers were used for top bottom and perimeter shells with 20% infill. The base settings for a 0.4 mm nozzle to create a 0.2 mm layer height when using the Ultimaker S5 3D printer were unchanged, while using Cura as the slicer. Every object to be additive manufactured on fabric first had the printer auto level and start printing a skirt around where the object would be created. During or after the creation of the skirt the 3D printer would be paused and the fabric would be put into position, using the location of the skirt as a guide, to have a part created on it. The fabric would then be fastened onto the print bed with tape as to prevent it from moving during creation of the part on it. The two sample types created for this research are the pull and peel sample tests which are detailed below. All samples were stored according to the ASTM standard D4933 as well.

Table 4.2: Process parameters used during creation of testing samples

Process Parameters Kept Constant:	**Parameter Values:**
Nozzle Temperature	220℃
Printing Speed	70 $\frac{\text{mm}}{\text{s}}$
Build Plate Adhesion	Brim
Layer Height	0.2 mm
Infill for Pull Samples	20%
Bed Temperature for Uncovered Samples	0℃-70℃-100℃
Bed Temperature for Covered Samples	70℃-120℃
Fill Angle to Weft Direction	0°-45°-90°

4.4.1 Pull Testing Protocol

Samples were created using a CR-10S 3D printer to make a plug on top of fabric referred to as pull testing samples. Samples were also created with 220℃ nozzle temperature and 60℃ bed temperature; three samples were created per sample set. This testing method was based on previous research by Rivera et al. and was created to test the interfacial bond strength between the fabric and the 3D printed plug created on it [16]. The pull sample is shown in Figure 4.9 (b) as 22.3 mm tall for the value of h, has a diameter of 25.4 mm on the bottom, and an area A = 510 mm^2.

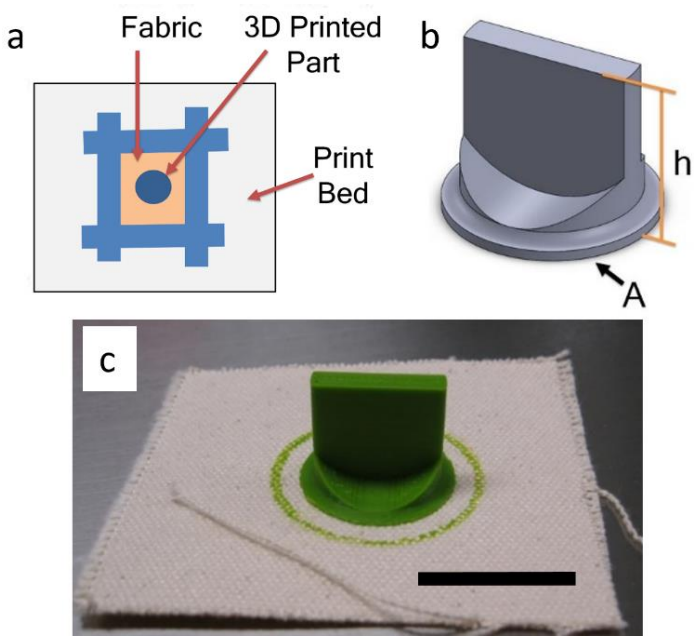

Figure 4.9: Visualization of pull samples (a) 3D printer setup for sample creation (b) Sample dimensions (c) Sample created on cotton duck cloth, black scale bar is 25 mm

Pull samples were tested, for interfacial strength, using an Instron 8801 tensile tester with a 2.5-kip load cell to remove the created part from the fabric, as shown in Figure 4.10. The fixture consisted of a lower grip holding onto a T-shaped platform that holds the pull sample in place by use of a plate with a circle cut out of it being clamped down onto the sample and platform. This fixture allows the sample to be removed from the fabric, in this case the part is removed at a rate of 3.175 mm for every 90 seconds for a maximum displacement of 25.4 mm. Once force and displacement were determined from testing the stress and strain were plotted using a MATLAB script shown in Appendix A.

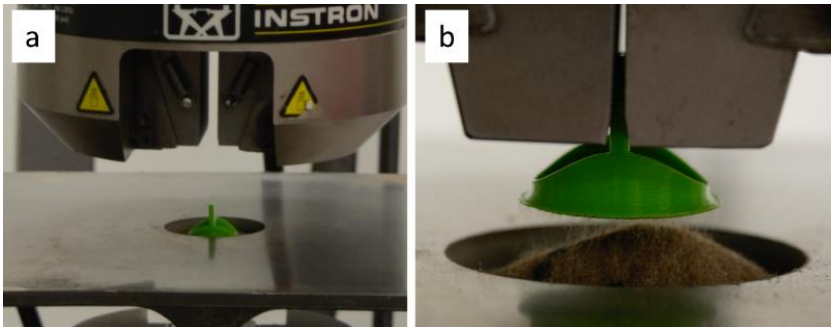

Figure 4.10: Pull testing of samples (a) Fabric is held down by clamped plate with hole for 3D printed part to stick through (b) 3D printed part is removed

4.4.2 Peel Testing Protocol

After pull testing for the base fabric samples was completed a different testing method, used in previous studies, was employed called peel testing. The peel testing is based off the standard DIN 53530 and used the use of standard ISO 6133:2015 to interpret the data into adhesive strength values $\frac{N}{mm}$. The standard DIN 53530 initially was for the determining the adhesive strength at the interface, as interfacial strength, between two fabrics and was modified to instead use an additive manufactured part as one of the fabrics. The additive manufactured part, created on top of the desired fabric, being a six-layer rectangle with a layer height of 0.2 mm for a total height of 1.2 mm when samples are created on the Ultimaker. When samples were created by the CR-10S the samples had an additive manufactured part with a three-layer rectangle with a total height of 0.6 mm. The layer height was changed because of the difficulty in removing the thin part from the fabric, so the additive manufactured part was made twice as thick for Ultimaker samples.

Three samples would be created for a sample set with the CR-10S and made with standard green PLA. The CR-10S was only used to create samples when testing the difference between the three fabrics to accurately compare to the relevant pull testing results. For the Ultimaker S5 3D

printer the brand specific Ultimaker PLA was then used for all samples with first red and then black colored PLA. Red was used for the thicker 0.93 mm thick duck cloth and black for the thinner 0.58 mm thick duck cloth. The Ultimaker is also inside an enclosure which assists with the control of the environment, specifically the temperature from being influenced from outside sources. Four samples would be used for all data sets with the Ultimaker. Nozzle temperature for all samples with both 3D printers was set at 220℃.

The additive manufactured peel sample part was a 25 x 152 mm flat long tab and the fabric was cut to a 76 x 305 mm rectangle to provide extra space for the created part. At least 100 mm of the sample must be peeled for a reliable testing sample, if samples break apart too much they would have to be thrown out. The additive manufactured part would either be created 25 mm away from one of the short edges of the fabric or in the middle of the fabric. Originally having samples created with the additive manufactured part 25 mm from an edge was to allow extra room during testing of samples. However, it became difficult to fasten the fabrics with tape when the sample was being created on one side so many later samples create the additive manufactured parts in the middle of the fabric for simplicity. All fabric samples have the warp of the fabrics in the long direction, and the fill angle of the additive manufactured part may be angled in relation to the warp of the fabric 0, 45, 90 degrees. After all peel samples were created, they were stored according to the ASTM standard D4933 and left to sit for at least 24-hours after initial creation. Pull samples were tested before this standard was adopted. Figure 4.11 shows the setup for the peel samples in reference to the warp direction, while Figure 4.12 shows the testing machine during peel testing. Once force and displacement data are found from sample testing the MATLAB script shown in Appendix B is used to create graphs for adhesion

strength. After these raw graphs are made, they are interpreted using the standard ISO 6133:2015 and graphed again in Excel.

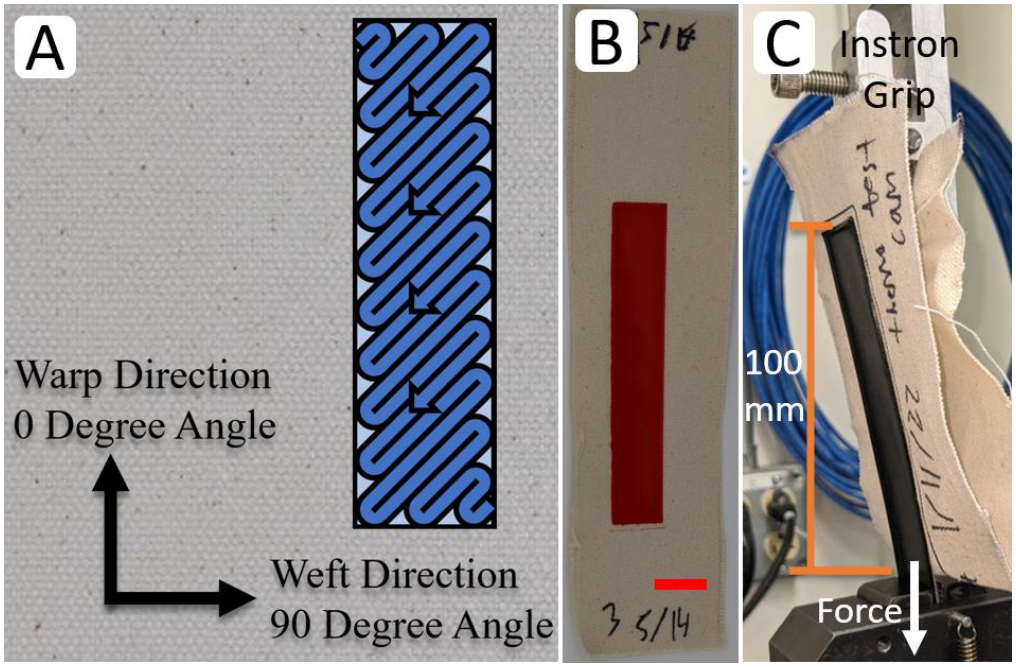

Figure 4.11: Peel sample setup (a) Peel sample infill orientation (b) Visual of created peel sample on cotton duck cloth (c) Peel test setup, black scale bar is 25 mm

Figure 4.12: Peel sample being tested on a 4466 electromagnetic Instron machine

Testing of the peel samples involved a 4466 electromagnetic Instron machine with a 10 kN load cell. This was to get higher accuracy in testing than with the mechanical tester used for pull tests. Of the 152 mm of the peel sample 52 mm is peeled back to allow the mechanical tester the ability to grip the additive manufactured part. Only 100 mm is needed to be peeled back by the mechanical tester to obtain an accurate result for interfacial strength. Testing setup of peel samples are shown in Figure 4.11 and Figure 4.12 where the sample is tested at a 180-degree angle of peeling compared to the 90-degree angle specified in the DIN 53530 standard. This is because of the stiffness and length of the additive manufactured part not allowing the part to be peeled at a 90-degree angle as shown in Figure 4.13.

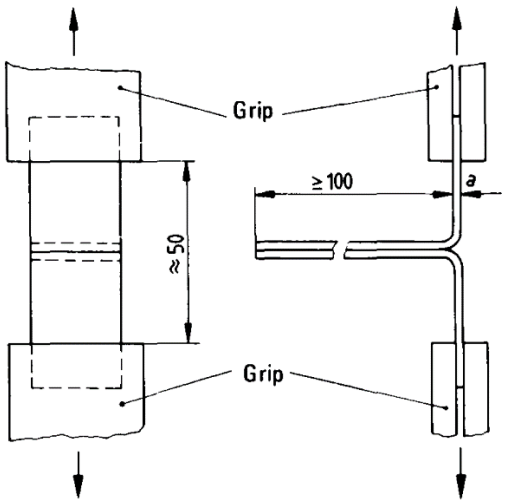

Figure 4.13: DIN 53530 testing standard diagram

4.4.3 Three Point Bending

Three-point bending testing of samples involves the creation of a 203 by 25 by 12.7 mm beam that is created on fabric and one that is not created on fabric to compare to. The beam sample that was created on fabric were tested with the fabric on the tension side. Both were tested according to three-point testing standard ASTM D790 with a given strain rate of 0.01 $\frac{1}{\text{min}}$. From

this standard it was determined the speed of the machine to test the sample would be 5.44 $\frac{\text{mm}}{\text{min}}$ given Equation 4.1. The purpose of this testing is to determine if having parts created on fabric and having the fabric on a side in tension will the part become stronger than if the sample was not created on fabric at all. Figure 4.14 shows the control sample during testing. Maximum force, displacement, and strain was calculated to be 1032 Newtons, 17 mm, and 0.031 as calculated from Figure 4.15 with values given by the manufacturer for Ultimaker PLA. Two sample sets of two were created: the first with a 0.6 mm nozzle to create a 0.6 mm layer height, the second a 0.4 mm nozzle to make a 0.2 mm layer height. The 0.6 mm layer height samples were also created with a 70℃ bed temperature and the 0.2 mm layer height with 100℃ bed temperature, both were created with a fill angle of 45 degrees. Once the force and displacement are found from sample testing the results are put into Excel to correctly graph the force versus displacement, stress versus strain, and find the tangent elastic modulus.

$$R = \frac{ZL^2}{6d} \qquad \text{Equation 4.1}$$

Z = Strain Rate, R = Rate of crosshead motion, L = Length of sample, d = Thickness of sample

Figure 4.14: Control beam during three-point testing

$$b := 25\ mm$$
$$d := 12.7\ mm$$
$$L := 203.2\ mm$$
$$S := 78\ MPa$$
$$E := 2.49\ GPa$$
$$I := b \cdot \frac{d^3}{12} = \left(4.267 \cdot 10^{-9}\right)\ m^4$$
$$F := \frac{2 \cdot b \cdot d^2 \cdot S}{3 \cdot L} = \left(1.032 \cdot 10^3\right)\ N$$
$$D := \frac{F \cdot L^3}{48 \cdot E \cdot I} = 0.017\ m$$
$$e := \frac{6 \cdot D \cdot d}{L^2} = 0.031$$

Figure 4.15: Calculations for finding the maximum force, displacement, and strain for the samples created for three-point bending samples

4.6 Process Parameters Summary

Samples are created either as pull or peel samples as to determine the strength of the interface between fabric and additive manufactured parts. The additive manufactured parts were created directly on top of the fabric during manufacturing to adhere the two. Different process parameters, materials, and primer coatings were used as an attempt to find the best setup for the highest interfacial forces between fabric and additive manufactured part. After peel samples were created, they were stored according to ASTM standard D4933 for at least 24 hours before testing. After a comparison between different sample sets using three different fabrics, it was decided that the peel testing would be more beneficial of a testing method compared to pull testing. This was due to peel samples having a tighter and more consistent range of resulting values, the testing method being based off a previously accepted standard, and the lower likelihood of samples failing during testing.

Once the interfacial strengths were found they could be compared the material strength of PLA, this was done to determine how close the strength of the interface is to the strength of the additive manufactured part. The tensile strength of PLA was compared to pull samples and the sheer strength of PLA is being compared to peel samples. The ideal is to find a set of parameters that get a strength at the interface higher than the strength of the fabric or the PLA plastic. If the interface is found to be stronger than the fabric or the PLA plastic than no additional strength is required as the fabric or PLA would fail before the interface, which is the desired result.

CHAPTER 5

CHARACTERIZATIONS OF ADDITIVE MANUFACTURED PARTS DEPOSITED ON FABRIC

5.1 Introduction

This chapter details the pull and peel interfacial strength test results as to determine the influence of 3D printer process parameters on the strength of the interface between fabric and part created on the fabric. Three-point bending test results are also detailed comparing the strength of the composite to the strength of the filament material. Results and conclusions are listed according to their relation to each other. Comparison of the interfacial strength found of 3D printed samples to previous literature with similar process parameters is also discussed.

5.1.1 Target Interfacial Strength for Comparison

Once interfacial strength was found for the pull and peel testing, they were compared to the material strength of PLA plastic. Pull testing was related to the tensile strength of the PLA as pull testing finds an equivalent to tensile stress. Peel testing was related to the shear strength of the PLA given the methods in which the additive manufactured parts are removed from the fabric. Adhesion strength from peel samples can be related to shear strength when converting adhesion strength by dividing it by the length of the sample, acquiring a stress. Previous testing observed tensile and shear strength results of additive manufactured PLA. Specifically, those created in the “upright” XZ transverse orientation were found to have the worst mechanical properties of all printing orientations for samples. The tests found that the average maximum tensile stress was 13.8 MPa, this tensile strength would be compared to the interfacial strength found during pull testing. Peel testing results for interfacial strengths was compared to previous literature from Ferreira et al. finding the maximum shear strength of PLA to be 18.0 MPa when

using the ASTM standard D3518 [40]. Comparisons were done to determine if the maximum strength of the interface found was close to the material properties of the PLA. The goal of these comparisons is to determine either the PLA or the fabric fail before the interface between them fails. If that happens it means that no additional strength at the interface would be necessary.

5.2 Pull Testing

5.2.1 Pull Testing Results

Pull testing of fabric samples involves the testing of the interfacial strength by separating an additive manufactured plug from the fabric it was created on, strength is found in Stress. The samples done during this testing involved the additive manufacturing of sample sets on three fabrics this being duck cloth, ripstop, and acrylic fabrics. Each of these fabrics would additionally have sample sets created where the fabrics have a starch glue stick applied to them just before the part is created on them. Pull testing had multiple samples fail during testing because of the additive manufactured part breaking and other testing complications. Going forward it is desired that a different sample testing method be used with this being peel testing. From the pull testing, however, it was determined that the cotton fabric is desired to be used in testing going forward, because of its high promotion of interfacial strength, and that the application of the glue is producing lower interfacial strength.

5.2.1.1 Pull Testing of Fabrics as a Control

Table 5.1 shows the test results for pull samples using thick cotton duck cloth, ripstop, and acrylic fabrics. Maximum stress of sample sets was also compared to the PLA material tensile strength and a percentage difference was found. All percentage differences were found to be substantial, and that the interfacial strength is not near the material strength of PLA currently. The duck cloth sample that failed was getting a maximum force of 310 N before the additive

manufactured part snapped in two. Given the interface had not actually failed, the strength was much different than the other two samples and was much higher. However, the sample was not considered part of the sample set because of the part itself failing instead of the interface. Otherwise, the results from the sample sets showed what was consistent from previous literature that being the thicker, rougher, and more porous duck cloth had the highest interfacial strength. This was followed by acrylic and then the ripstop fabric samples who had lower adhesion strength to the cotton duck cloth.

Table 5.1: Results for pull samples without adhesive pre-treatment, cotton duck cloth, polyester ripstop, waterproof acrylic-dyed

Fabrics without Adhesive Pre-treatment:	**Duck Cloth**	**Ripstop**	**Acrylic-Dyed**
Number of Samples	2	3	3
Average Maximum Force (N)	220	69.2	142
Average Maximum Displacement (mm)	10.1	5.59	8.5
Average Maximum Stress (MPa) + (Standard Deviation)	0.435 (0.005)	0.137 (0.005)	0.28 (0.028)
Percentage Difference from PLA Tensile Strength	188%	196%	192%

5.2.1.2 Pull Testing with Adhesive Primer

Table 5.2 shows the test results from pull samples involving the application of a starch glue stick on thick cotton duck cloth, ripstop, and acrylic fabrics. Results from the starch glue primer applied samples are relatively the same as the unprimed samples, but with a higher failure rate. The primed samples often would behave very differently from each other in unexpected ways,

these samples were thrown out for the final data sets. This either leads to samples being improperly tested resulting in their failure or having force versus displacement curves that were unexpected from samples of its set. These failures were likely due to the lack of consistent application of the adhesive to the fabric. Of the adhesive prime samples that were tested all of them had the interface fail between the adhesive and the fabric as little to no glue would be left behind on the fabric where the part used to be. Visualizations of the duck cloth samples that had glue applied to them are shown in Figure 5.1, where a discoloration and lack of glue left behind on the fabric can be seen as well as a small amount of fabric on the additive manufactured part. All adhesive primed samples appeared to have a lower interfacial strength from the unprimed ones for all fabrics, so two sample T-Test calculations were done to determine if there was a significant difference.

Table 5.2: Results for pull samples with adhesive pre-treatment, cotton duck cloth, polyester ripstop, waterproof acrylic-dyed

Fabrics with Adhesive Pre-treatment:	**Duck Cloth with Adhesive**	**Ripstop with Adhesive**	**Acrylic-Dyed with Adhesive**
Number of Samples	1	2	3
Average Maximum Force (N)	152	17.8	100
Average Maximum Displacement (mm)	6.71	4.31	7.72
Average Maximum Stress (MPa) + (Standard Deviation)	0.3 (N/A)	0.035 (0.005)	0.2 (0.008)

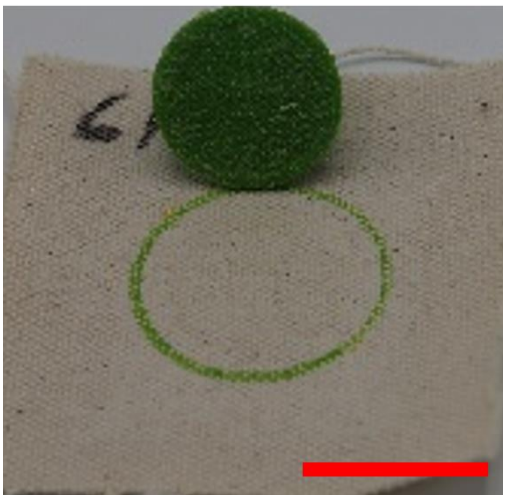

Figure 5.1: Adhesive primed pull sample with additive manufactured part removed from sample, there is no fabric left on the part as normally seen in control, and the glue is removed where the part was, red bar is 25 mm

5.2.1.3 Pull Testing Results Comparison and T-Test Calculations

Comparison of the pull sample set averages for both the applied load versus actuator displacement are shown in Figure 5.2 and Figure 5.3. Standard deviation from both primed and unprimed sample sets was low which was desired. Each averaged set shows the applicable values till the maximum applied load is reached as the maximum strength is what we care about the most. From these graphs it can be determined that the adhesive application lowers the interfacial strength of the samples before interfacial failure.

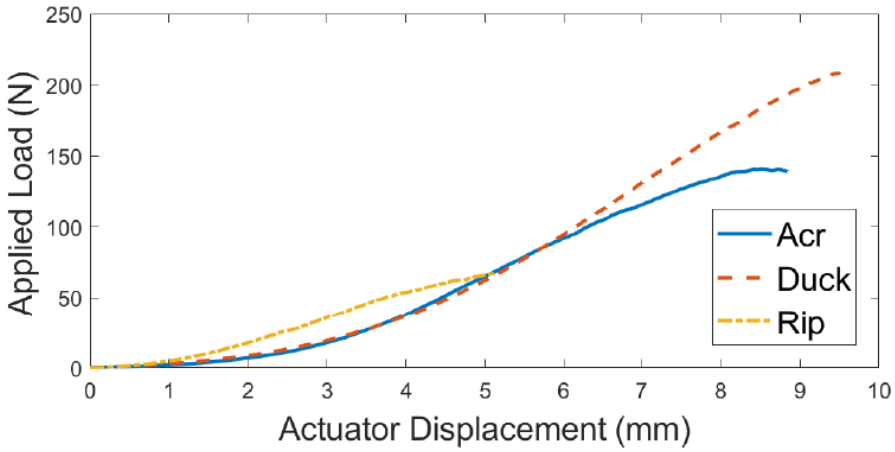

Figure 5.2: Adhesion strength of pull samples without adhesion during testing

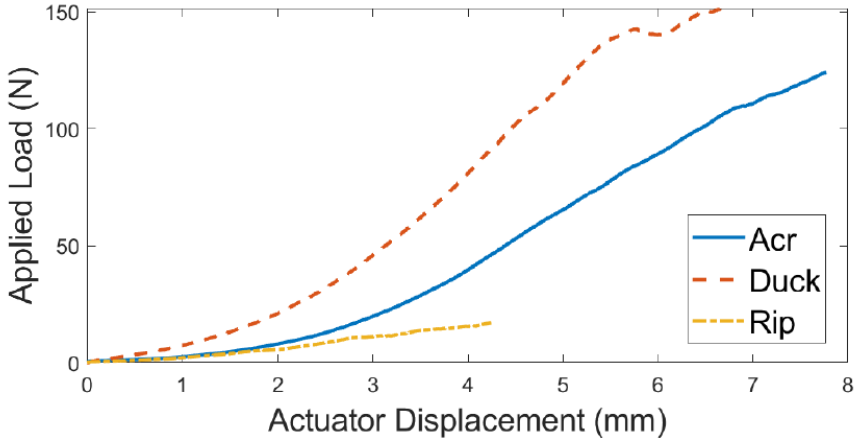

Figure 5.3: Adhesion strength of pull samples with adhesive during testing

After it appeared that the starch glue stick adhesive reduced the strength of the interface for all samples two sample T-Tests were performed between each of the fabric sample sets with and without the adhesive primer. There were two T-Tests used on the average maximum force the Student's T-Test by using the ttest2 function in MATLAB, and the Welch T-Test by using the two-sample t.test function in RStudio. Table 5.3 shows the values of P found from the two tests and compares them to the standard alpha value of 0.05. All values of P were found to be under the alpha value meaning that the strength of the interface was significantly impacted by the

application of the starch adhesive primer. Average P value was found to be 0.027 between the adhesive primed and non-adhesive primed sample sets with a common standard deviation of 0.05. Also observed is that there is an average loss of 31% and 28% of average max tolerable force for duck cloth and acrylic sample sets. Ripstop, as an outlier, had a 74% drop in average max tolerable force at the interface. This is likely because ripstop already had the lowest interfacial strength and the application of adhesive compounded lowering the strength exponentially.

Table 5.3: P-Value Results for the Three Fabrics Found using Students T-Test and the Welch T-Test

	Duck Cloth	**Polyester Ripstop**	**Acrylic-Dyed**
P Value (MATLAB, Students T-Test)	0.0408	0.0004	0.0184
P Value (R-Studio, Welch T-Test)	0.0236	0.0043	0.0479

5.2.2 Pull Testing Failure Mode Analysis and Conclusions

In reference to the non-primed thick duck cloth sample that had the additive manufactured part fail there was no specific reason the sample could have had such a large maximum force compared to the others of the same set. Since it was the only sample that failed due to the part breaking that did not involve the adhesive primer it is possible that the interlayer strength of the additive manufactured part had been attained for this sample. From the cross-sectional area of the pull tab being 85.5 mm^2 and the maximum force found during pull testing being 310 N gets a stress of 3.63 MPa on the pull tab. The 3.63 MPa on the tab only being equivalent to 0.608 MPa on the fabric to part interface. With interlayer tensile strength was found to be 3.63 MPa

and was much lower than the expected 13.8 MPa found in previous research. This shows that the interface between PLA and fabric is weaker than the PLA to PLA and that there is room for improvement of the interfacial strength between PLA and fabric. However, given a sample failed during testing attributable to the additive manufactured part breaking it is possible either the sample was created improperly, or the testing method is too rough on parts. Future pull testing would need fully solid additive manufactured parts to prevent future sample failures, otherwise a new testing method would be needed. Since parts did not achieve the desired strength, it can also be concluded that going forward much higher interfacial strengths can be found.

All pull samples created without the adhesive showed that there was fabric left behind on the additive manufactured part after it was removed, as shown in Figure 5.4. At no point was any of the additive manufactured parts were left behind on the fabrics. From these observations it could be determined that the fabric fibers the additive manufactured part has formed around are first to fail allowing the part to be removed. For samples with the adhesive primer applied, the interface between the glue and fabric was found to be the weakest part as very little fabric was left behind on the part and little to no glue is left behind on the fabric with no fabric on the removed part. From this it could be determined that the lower strength of the samples with the adhesive primer because of to the lack of adhesion to the fabric by the glue. The blocking of the additive manufactured part to solidify around and interweave with the fabric also contributes to the lower interfacial strength. When the samples fail there is a period after the maximum strength is reached where the fabric is still attached to the part providing resistance and additional displacement from the part. The period after maximum strength is present in all samples tested. Samples removed from primed sample sets in testing were attributable to the force versus

displacement curve being uncharacteristic of the other samples, likely because of the lack of consistent application of adhesive to the samples. In the future, a more consistent method of applying the adhesive should be created.

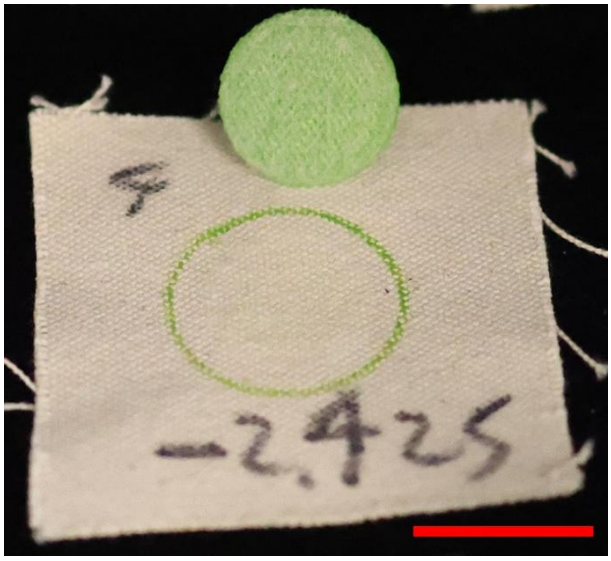

Figure 5.4: Tested plug sample with fabric left behind on the removed part, but no polymer is left behind on the fabric, ring shown on fabric is the brim and not part of the plug sample, red bar is 25 mm

Of all sample sets it was clear that the cotton duck cloth would be used for future testing of process parameters given the highest amount of interfacial strength that was found. Because of the failure of samples in previous tests it was clear that if testing was to go on a different testing method would be desired. Specifically, a testing method that would not potentially have failures attributable to the sample part breaking, or sample testing errors due to varying samples. Pull testing mostly had problems with one sample that broke and the improper testing and application of adhesive for specific samples. Comparing pull testing to a peel sample testing, commonly used in other literature for sample consistency and wider range of interfacial strengths, is desired at this stage. The method of the two that could limit the sample failures, prevent early sample failure, and have more consistent results would be preferred. Peel testing from this point on was

decided as the testing method going forward attributable to its larger range of strength and lower potential of sample failure, compared to pull testing. Peel testing also having more literature to directly compare the interfacial interfacial strength to was also a deciding factor. It is possible that if pull testing became more refined in its sample creation and had better primer application methods it could become the preferable option.

Initial strength testing of the interface between fabric and additive manufactured part found that the strength of the interface could hold the weight of the additive manufactured part on the fabric. This was from given a cube shelter with side lengths of 2235.2 mm and triangular panels made of PLA with a density of 1.24 $\frac{g}{cm^3}$ and a thickness of 25.4 mm, gets a 2.5 m^2 surface area to the fabric. With the mass of the panel being 39339 grams, or 385.8 N, the stress on the interface if the panel was held upside down would be 154.44 Pa. This would mean the panel could be held upside down, in orientation from the fabric, and not detach from the fabric, given the adhesion strength from later pull testing being 0.436 MPa. This is desired for use in real life applications as to prevent delamination of parts from the fabric from normal use.

5.3 Peel Testing

5.3.1 Peel Testing Results

Peel testing of samples with an interface between additive manufactured part and fabric find the adhesion strength in $\frac{N}{mm}$ compared to the strength in Newtons from the pull tests. Rectangular 25 x 152 mm parts are additive manufactured on 76 x 305 mm as to be tested according to the DIN 53530 and then used standard ISO 6133:2015 to interpret the data. Initial testing involves comparing peel testing to the pull testing by using the same three fabrics to make samples that

being the cotton duck cloth, acrylic, and ripstop fabrics. Fill angle for samples was 45 degrees unless otherwise stated.

After determining that peel testing would be the desired testing method going forward different coatings on the cotton duck cloth fabric were tested. This involved the testing of both the 120k and 350k molecular weight PMMA, nylon 6/6, as well as the use of Loctite 410 to adhere a control sample to fabric. These initial samples were created with a bed temperature of 60℃ on the Ultimaker S5 3D printer with the thicker 0.93 mm thick cotton duck cloth. Process parameters were changed to determine how they affect the adhesion strength. Specifically, bed temperature changes to 70℃ and 100℃ from 60℃ and the fill angle of the infill of layers to the warp of a fabric. The thinner 0.58 mm cotton duck cloth was used from this point on as well along with the use of the Ultimaker S5 as the 3D printer. To better understand the bed temperature changes sample sets were tested with different fill angles and with both 100℃ and no bed temperature.

More coatings were tested with 120k and 15k molecular weight PMMA on the thinner cotton duck cloth. Specifically, the 15k molecular weight PMMA was used to create two different solutions to test how the thickness of coatings would affect sample performance. These coatings would also be created on fabric with both bed temperatures of 70℃ and 120℃. This was to determine if the strength of the interface would greatly increase if the bed temperature were set above the glass transition temperature of the PMMA. Fabrics were then washed using two different methods using non-ionic surfactant, soda ash, and DI water. A beaker washing method and an ultrasonic machine-washing method were used, in this case, for the washing of the fabrics to remove the sizing on them from the manufacturer. It was decided that the washed fabric samples would also be created with 100℃ bed temperature.

5.3.1.1 Testing Among Three Fabrics

Results from the initial tests using the three base fabrics were compared to pull testing results. Samples were found to be less likely to fail during testing and had a larger range of values between each of the fabrics. The CR-10S 3D printer was used to create these samples. Deviation between samples was low and the cotton duck cloth still performed the best as expected. From the results in Figure 5.5, it was decided that the cotton duck cloth would be used going forward in future tests because of its high interfacial strength. Additionally, Figure 5.6 shows one of the cotton duck cloth samples tested; fabric can be seen on the removed part. This sample was made with the Ultimaker and was not part of the sample sets tested here, but has similar fabric left behind on the part. No amount of the additive manufactured part is left behind on the fabric

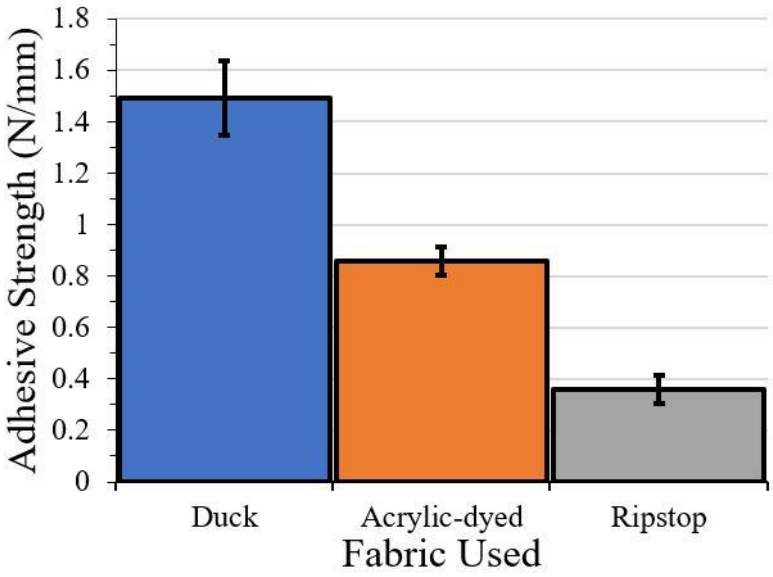

Figure 5.5: Adhesion strength at the interface for the three base fabrics

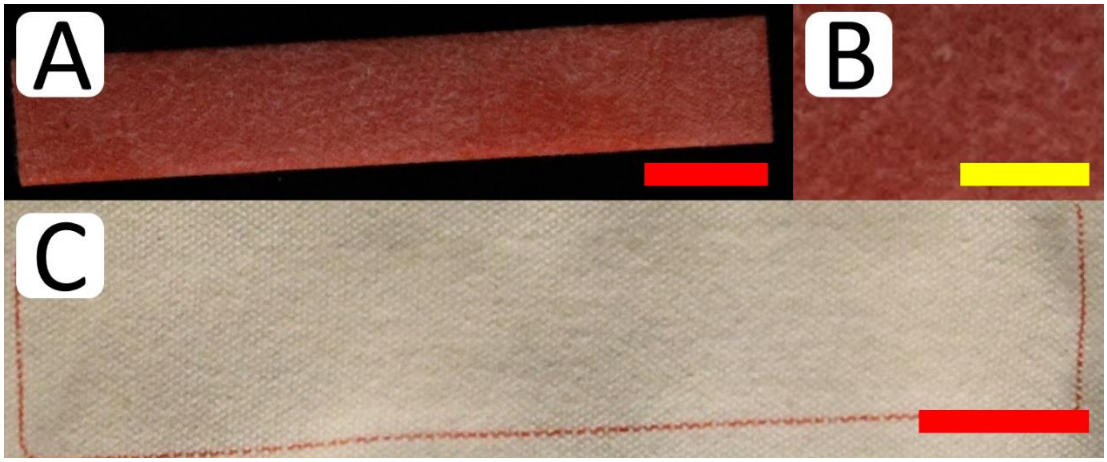

Figure 5.6: Peel samples after testing, 0.93 mm thick cotton fabric testing sample, (a) removed part with fabric left behind on it, (b) close up of roughly even coating of fabric on part, (c) fabric appears undisturbed with no part left behind, red scale bar is 25 mm, yellow scale bar is 10 mm

5.3.1.2 Initial Tests of Coatings as Primers

The initial round of testing is shown in Figure 5.7 with polymer coatings which involved the use of the nylon 6/6 coating as well as 120k and 350k molecular weight PMMA. The use of Loctite 410 to attach a control part to fabric was also done. Results found that the Loctite performed poorly, likely owing to the uneven application of the adhesive making adhesion variable throughout the sample. Additionally, going forward, testing with a more specialized adhesive for fabric and plastic would be desired. An Ultimaker S5, in a sealed enclosure, was used to create all samples in this section as well as all future sections.

The nylon coatings were found to perform extremely poorly for promoting interfacial strength as the nylon would barely be attached to the fabric and cause a weak boundary layer. It was expected that the nylon would bond well with the deposited PLA however the bonding of the nylon and the fabric was very low. This is likely because of a low amount of nylon interweaving with the fabric. If nylon was to be revisited a new method of applying the material to fabric would be desired. The PMMA coatings, however, performed much better than expected with

values higher than initial fabric testing proving that the use of coatings can improve interfacial strength. All PMMA samples had fabric on the removed parts after being tested, but not in the same amounts as when there were no coatings. Adhesion strength did have a large standard deviation at the time, this is likely due to the uneven application of the coatings due to the film applicator not being used for these samples. Figure 5.8 shows one of the 350k molecular weight PMMA samples after testing where fabric can still be observed on the removed sample but in spots instead of an even coating. This is likely because of the adhesion of the PMMA to the fabric not being evenly distributed.

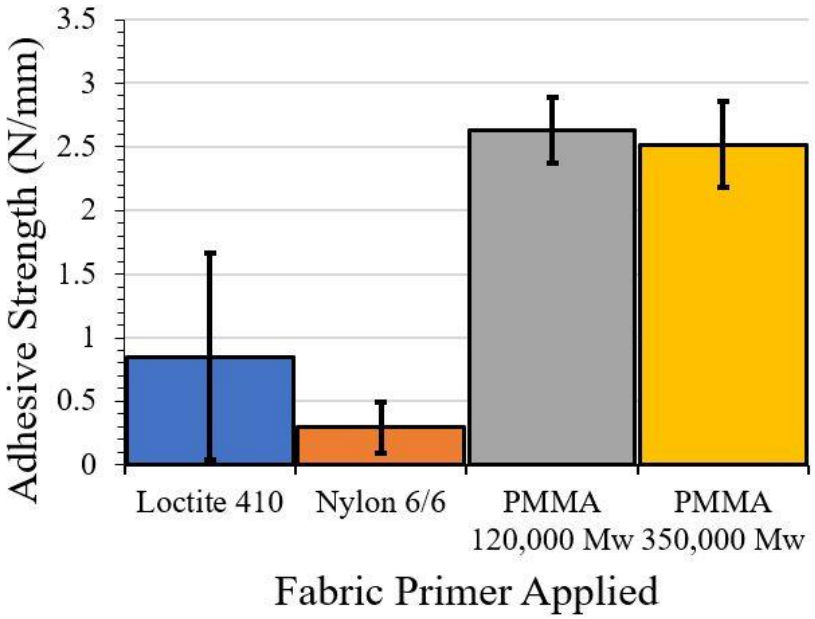

Figure 5.7: Adhesion strength at the interface for the initial coatings, nylon 6/6, 120k molecular weight PMMA, 350k molecular weight PMMA, and adhesive Loctite 410 control

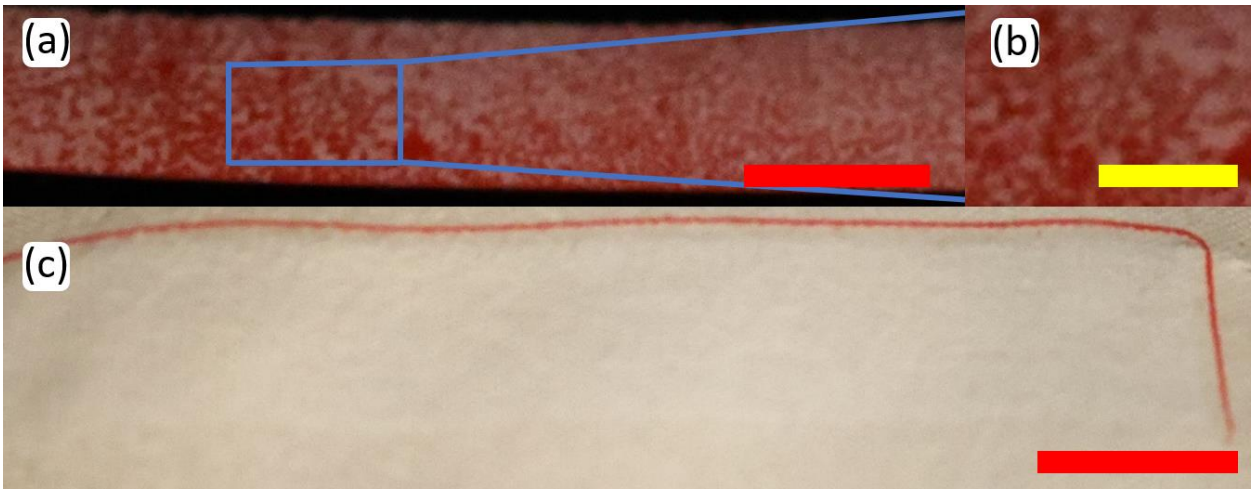

Figure 5.8: 350k PMMA covered peel sample after testing, (a) removed part, (b) zoom in on uneven amount of fabric left behind on part, (c) no PMMA left behind on fabric, red scale bars are 25 mm, yellow scale bars are 10 mm

5.3.1.3 High Bed Temperature and Fill Angles

After adhesion testing the initial set of PMMA coatings, the process parameters were tested, specifically the fill angle and bed temperature were changed, as shown in Figure 5.9. This was to determine how much these changes would compare to each other and the coatings. To start, the first sample set's fill angle and bed temperature was set to 45 degrees and 70℃, as a standard to be compared to the future tests. The other two sample sets had a fill angle of 90 degrees, along the weft, and a bed temperature of 100℃. Both the sample sets were found to increase the adhesion strength greatly, with the bed temperature being a larger factor for interfacial strength than the fill angle. Adhesion strength differences between similar peel samples with the Ultimaker compared to the CR-10S found that the strength was a little greater when using the Ultimaker. This was likely due to the enclosure the 3D printer is in and the 70℃ bed temperature used instead of the 60℃ the CR-10S used.

Samples created with 100℃ bed temperature were found to have PLA material on the other side of the fabric that had flowed through the fabric during manufacturing. This was likely the factor

explaining why the bed temperature was more influential as this has not been previously. The 100℃ samples also had a failed sample attributable to the fabric ripping during testing, as seen in Figure 5.10. The ripping of the failed sample, however, was because of improper testing as manually peeling the additive manufactured part from the fabric became very difficult. The sample was then tested with an improper grab on the additive manufactured part and the fabric ripped. In the cases of other samples parts had broken off attributable to the difficulty of peeling a place for the machine to grab onto so this sample was not peeled as far to avoid that. Because of the difficulty in manually peeling back the part from the fabric, in the future, a different method of peel sample creation would be desired, so the manual peeling was not necessary. The sample that failed can be seen in Figure 5.10, along with a successful sample that shows the fabric had been greatly roughed up, after part removal, and some of the part had been left on the fabric making it appear slightly pink. The fabric left behind on the removed part is also an even coating with a specific pattern. A microscope picture of both the front part, where the samples were, and the back of the successful peel sample's fabric that were tested with 100℃ bed temperature is shown in Figure 5.11. These samples mark the first time that some of the additive manufactured part was left behind in the fabric. Additionally, when it was determined that high bed temperatures could increase adhesion strength greatly, samples were created using the acrylic and ripstop fabrics using 100℃. Both samples were manually tested to determine if the strength was significantly larger than before. It was determined that the strength was far lower than the strength observed from the duck cloth, so no quantitative testing was done with them.

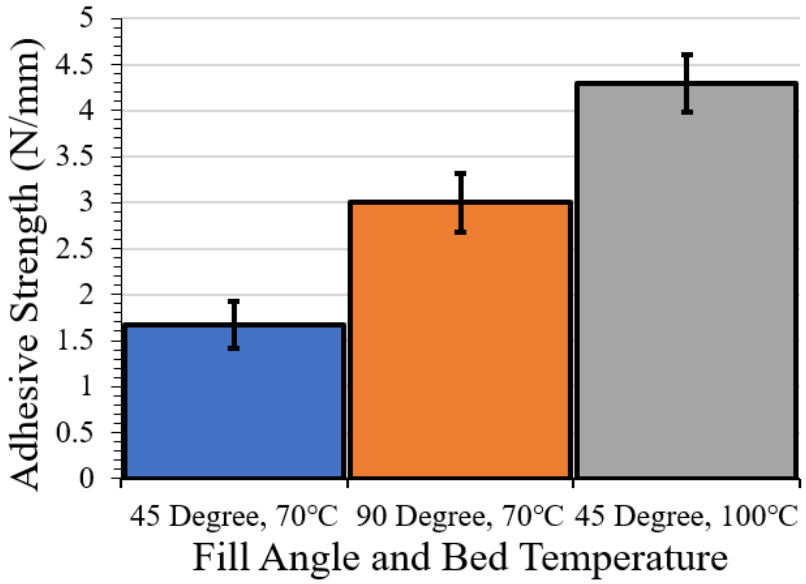

Figure 5.9: Adhesion strength at the interface for samples comparing adhesion fill angle and bed temperature

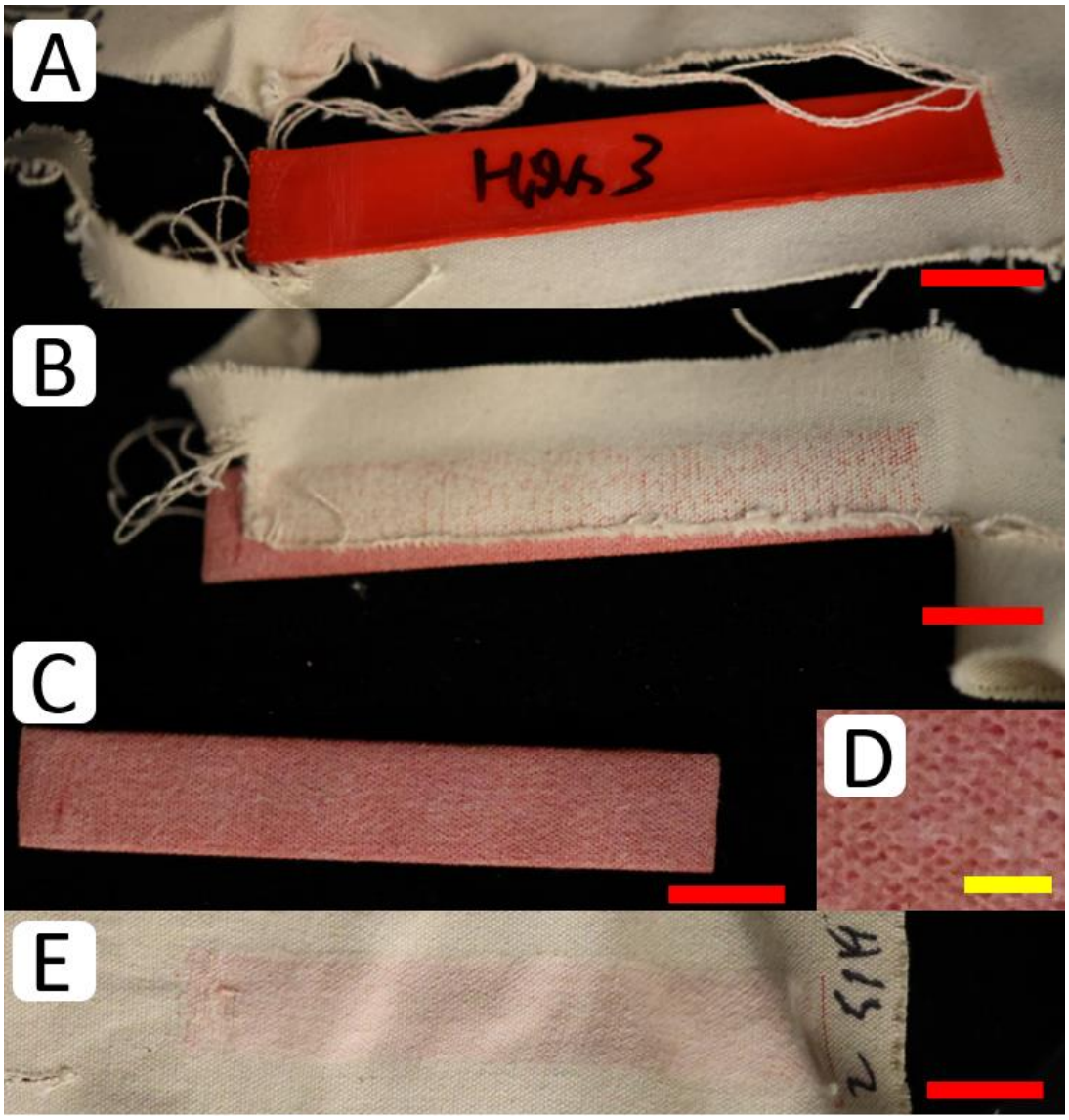

Figure 5.10: Peel samples created at 100°C on fabric, (a) front of failed sample, (b) back of failed sample showing that the PLA had gone through the fabric, (c) successful sample removed from fabric, (d) close up of removed part with fabric on it, (e) some material is left behind in the fabric making the fabric appear slightly pink, red scale bar is 25 mm, yellow scale bar is 5 mm

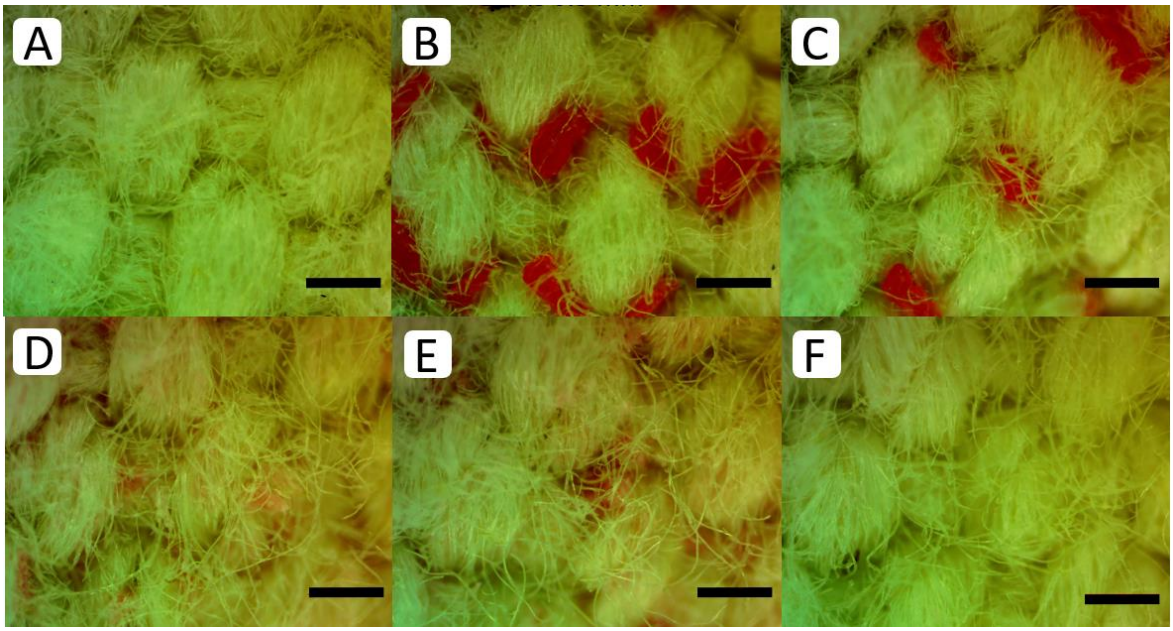

Figure 5.11: Close up of 0.93 mm thick cotton fabrics used in peel testing of samples using a 100℃ bed, (a) base fabric, (b) back of a sample, (c) back of a sample, (d) front of a sample, (e) front of a sample, (f) front of a sample, black bar is 0.5 mm

After determining that both fill angle and bed temperature greatly increased interfacial strength, samples were created with 0-, 45-, and 90-degree fill angle along with 100℃ bed temperature, as shown in Figure 5.12. Sample sets were created using an Ultimaker S5 as well as using the thinner 0.58 mm cotton duck cloth going forward for all future sample sets. Results from this testing found that the thin duck samples created on the Ultimaker had a 16% increase in interfacial strength when comparing the fill angle samples of 45 degrees. This was likely attributable to the changes in the thickness of the fabric and the looser weave of the fabric allowing easier flowing of material through it. Sample results have found that far more material was found on the other side of the fabric when using the thinner fabric, as shown in Figure 5.13. Otherwise, the more the fill angle is along the weft direction of the fabric, the higher the adhesion strength, but increases with diminishing returns. It is observed that the high bed temperature and assistance from the enclosure is greatly overpowering the influence from the fill

angle in this situation. This is because of the low difference between 45- and 90-degree fill angle for 100°C bed temperature but is a much greater variance for the 70°C bed temperature samples.

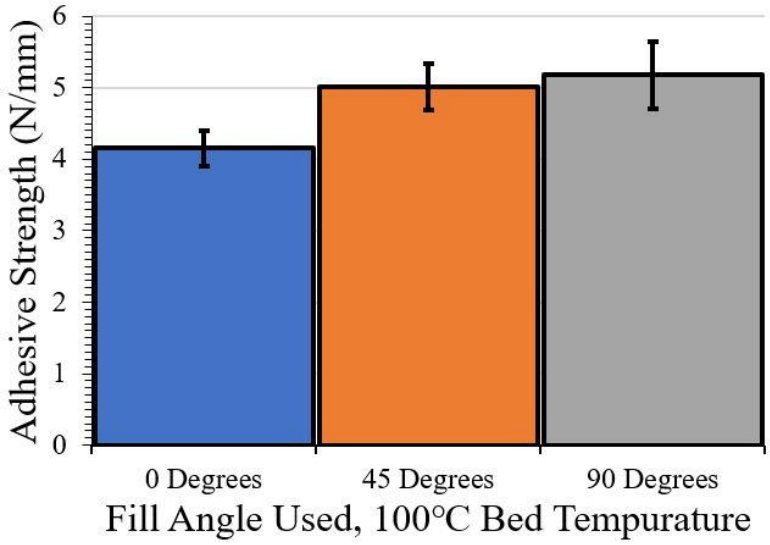

Figure 5.12: Adhesion strength at the interface for with different fill angles at 100°C

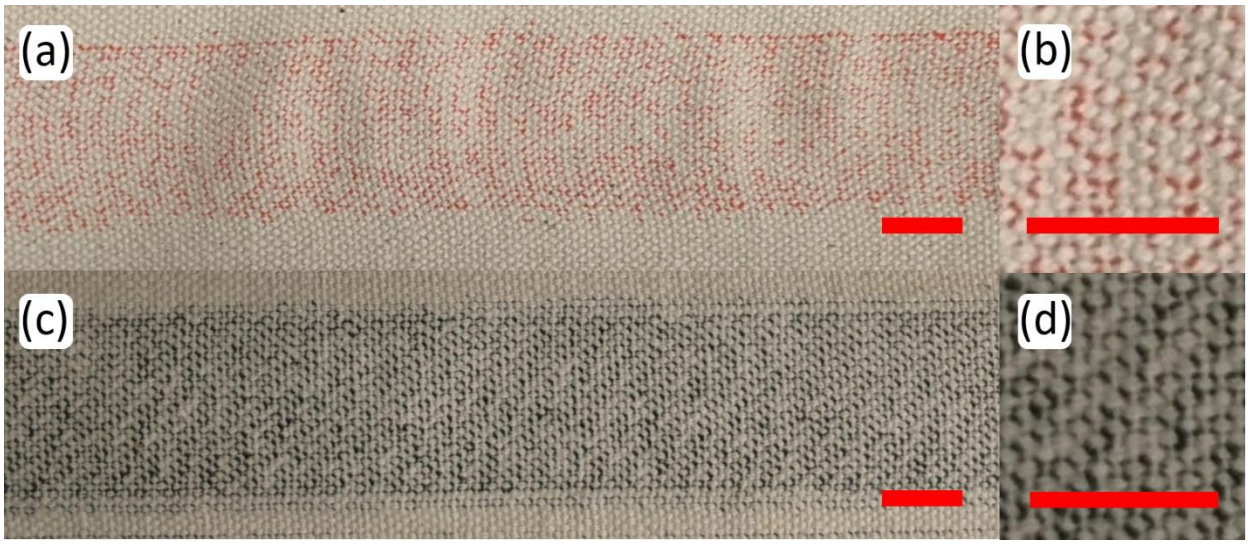

Figure 5.13: Back of both 0.93 mm thick and 0.58 mm thick cotton duck cloth samples after having parts additive manufactured on them at 100°C bed temperature, (a) back of thicker fabric sample, (b) close up of thicker fabric sample, (c) back of thinner fabric sample, (d) close up of thinner fabric sample, red scale bar is 25 mm, yellow scale bar is 5 mm

5.3.1.4 No Bed Temperature and Fill Angles

After determining that the high bed and environmental temperature is a big factor in interfacial strength a baseline of samples with no bed temperature were done. The thinner 0.58 mm cotton duck cloth was used with the Ultimaker S5 3D printer. Results from the testing can be seen in Figure 5.14 with three sample sets with 0-, 45-, and 90-degree fill angles. All 100°C bed temperature samples were somewhere between three to four times higher depending on the fill angle. This proves the great value of the bed temperature for interfacial strength. It could be considered that the longer the polymer is kept above the glass transition temperature and the closer it is to the melting temperature that the viscosity will remain lower for longer. This would allow the filament polymer to flow between the weaves of the fabric and create a stronger mechanical interlocking bond with the fabric. This means that bed temperature should always help with adhesion but help much more if it is keeping the polymer at a higher temperature than its glass transition temperature. However, given it needs to heat the polymer through the fabric it may need higher heat to keep it above glass transition temperature.

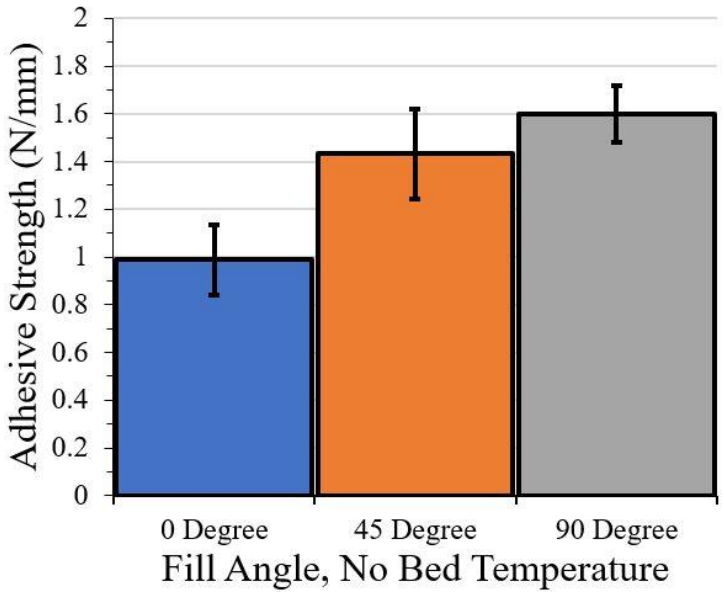

Figure 5.14: Adhesion strength at the interface for with different fill angles with no bed temperature

5.3.1.5 PMMA Coatings and Bed Temperature

After observing the changes to the interfacial strength that the bed and environmental temperature did for the untreated fabrics it was decided that the same could potentially be done for polymer covered fabrics. To test this, with the thin 0.58 mm thick cotton duck cloth, multiple sample sets were created with PMMA coatings with one group created with 70℃ and one with 120℃. Because the glass transition temperature of PMMA is around 110℃, we expect to find the adhesion strength to increase significantly between sets. Additionally, three different PMMA coatings were used where 120k molecular weight, and two different amounts of 15k molecular weight PMMA were used. The two 15k PMMA coatings were labeled as 20-80 and 5-95 in relation to the amount of PMMA and acetone respectively used to create the solutions for the creation of the coatings. Specifically, the 5-95 thin coating of 15k molecular weight PMMA is used to determine if mechanical interlocking could be promoted if coatings are thin enough to allow filament through the coating layer. All PMMA coating samples had their thicknesses

measured as shown in Table 5.4. The film applicator setting per sample is also listed. Each sample set consisted of four samples and the thickness is the average of six locations on the fabric; a control with no coatings is also measured. It was attempted to keep the coverings of the two 15k sample sets around the same thickness.

Table 5.4: Thickness of fabrics with PMMA coatings applied, both 70℃ and 120℃ bed temperature samples

Fabric Coating and Bed Temperature used – Film Applicator Setting:	**Thicknesses of the Set (mm):**
No Coating - None	0.662, 0.658, 0.65
120k 70℃ – 0.55 mm	0.792, 0.787, 0.787, 0.798
15k 20-80 70℃ – 0.55 mm	0.715, 0.700, 0.697, 0.699
15k 5-95 70℃ – 0.55 mm	0.650, 0.652, 0.653, 0.652
120k 120℃ – 0.55 mm	0.750, 0.812, 0.808, 0.857
15k 20-80 120℃ – 0.60 mm	0.702, 0.688, 0.698, 0.707
15k 5-95 120℃ – 0.65 mm	0.698, 0.703, 0.703, 0.713

Results of the testing are shown in Figure 5.15 and Figure 5.16 for the 70℃ and 120℃ bed temperature sample sets respectively. From these results it could be considered that the strength of the interface greatly increases attributable to the higher bed temperature. This is likely due to the PMMA and manufactured PLA both being kept at temperatures above their glass transition temperatures for longer. The higher bed temperatures resulted in a significant increase in interfacial strength for the 15k 5-95 PMMA covered sample sets than the 15k 20-80 PMMA samples. This is likely because of the solution producing a more porous coating with the 5-95 allowing the higher temperature to help the PMMA and PLA bond together and with the fabric better. However, there is still no additive manufacturing part left behind on the fabric like the

high temperature no coatings samples had. This would mean that higher adhesion strengths would be possible and that it is the PMMA and fabric interface that is failing, as no PMMA is left on the fabric. Thinner and lighter coatings appeared to have some potential but currently the thicker 120k molecular weight had the highest adhesion of all sample sets with both 70℃ to 120℃ bed temperatures.

The increases in strength from 70℃ to 120℃ for the PMMA coated samples are not nearly as great as the jump from 70℃ to 100℃ when no coating is used, and this is true for all covered samples. This is likely because of the bonding of the PMMA to the fabric not being strong enough as no PMMA is left behind on the fabrics. This is shown in Figure 5.17 with one of the 15k 5-95 PMMA samples at 120℃ bed temperature after the additive manufactured part had been removed. Some fabric is attached to the removed part much better than with the previously shown 350k PMMA sample in Figure 5.8, but no PMMA is left behind on the fabric.

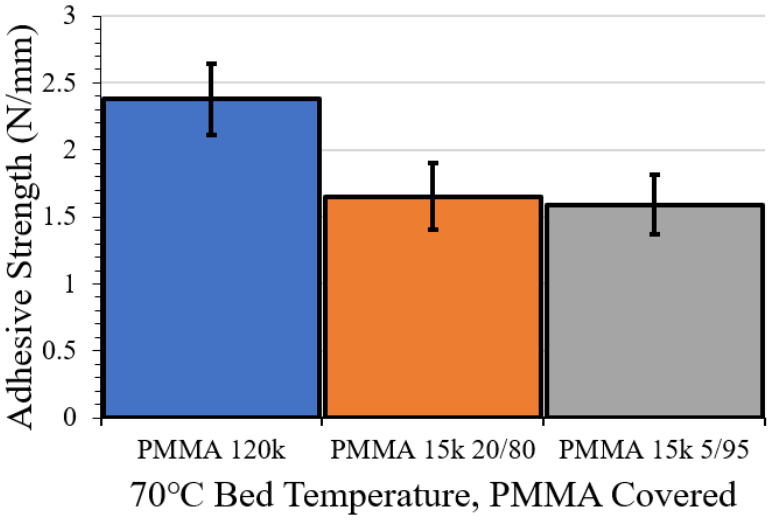

Figure 5.15: PMMA covered peel samples at 70℃

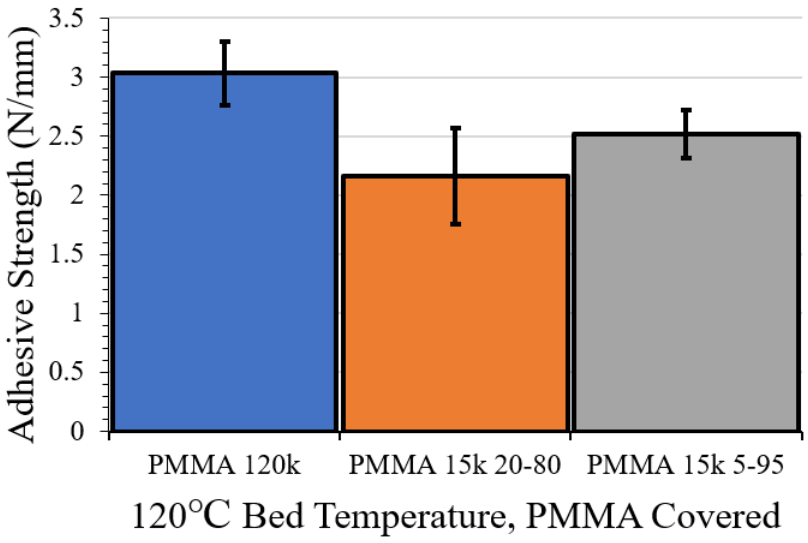

Figure 5.16: PMMA covered peel samples at 120°C

Figure 5.17: 15k 5-95 PMMA coating sample created at 120°C bed temperature, shows an even amount of fabric left behind on the sample compared to previous covered samples (a) Fabric on removed peel testing part, (b) fabric part is removed from, the red line is 25 mm

5.3.1.6 Washed Fabric Samples

The washed samples were found to have their additive manufactured parts created with a waviness to them, making the samples unreasonable to use for qualitative results. This waviness is likely due to the shrinking of the fabric from the ironing and not letting the fabric sit for long enough before creating the part on them. The fabric peices had their parts created on them the same day they were ironed for example. Because of this the results found from testing were unreliable and had a few parts fail entirely. Due to the 100°C bed temperature used it would be

reasonable to think that the additive manufactured part could visibly be seen to have formed on the other side of the fabric, but this was not the case for some samples. For one of the ultrasonic samples, however, it was found to be too difficult to peel the part from the fabric manually to give the machine space to grab onto it. This would lead to the potential that the ultrasonic washing did help create high adhesion, but the failure of the creation of the samples could not confirm this result quantitatively. Maximum forces achieved during peel testing for the beaker washed samples were found to be around 140 N or 5.6 $\frac{N}{mm}$, with the ultrasonic washed samples getting around 146 N or 5.86 $\frac{N}{mm}$. These were rough estimates from unreliable data but showed good potential for future tests that take the fabric shrinkage into account. Figure 5.18 shows the washed samples and their waviness, the ultrasonic washed fabric was found to have lost much more of its color than the beaker washed.

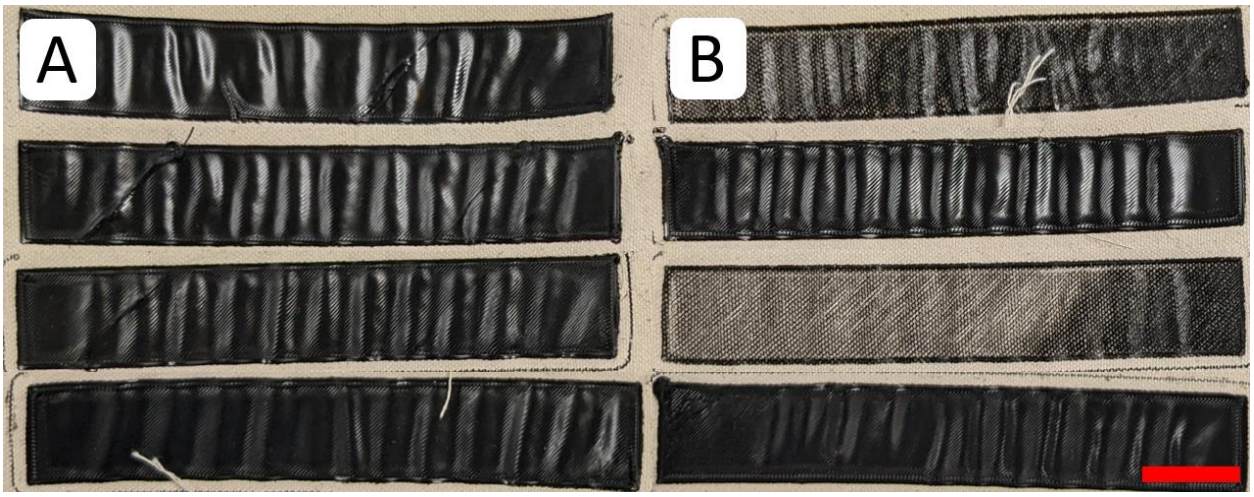

Figure 5.18: Washed samples and their visible waviness (a) beaker washed, (b) ultrasonic washed

5.3.2 Peel Testing Failure Mode and Conclusions

Results from peel testing have found that the adhesion strength for duck cloth samples was the highest of all the fabrics tested alike to pull testing. The cotton duck cloth was decided to be

used for all future process parameters and pre-treatment testing; a thinner duck cloth would be used for later tests. Peel samples were much less likely to fail as no samples had failed during testing, additionally there was a wider range of adhesion strengths between the three fabrics tested. Peel testing was then chosen as the ideal testing method going forward. When creating similar samples on both the CR-10S and the Ultimaker S5 3D printers the results were very close. The Ultimakers adhesion was slightly higher likely because of the enclosure that it was in as well as the 70℃ bed temperature used compared to the 60℃ used with the CR-10S. The Ultimaker also had a higher range of potential bed temperatures going forward which was desired for future testing.

Coatings and primers to fabrics were then tested with the nylon coating not performing well attributable to its low adhesion to the fabric; this was proven by how no nylon was left on the fabric. The Loctite 410 samples created by adhering a control part to the fabric had extremely variable adhesion strength due to how it was applied. Future testing of adhesives would have to involve specialized adhesives for fabrics and polymers as well as better application of them. The initial PMMA coatings worked very well and had achieved higher strengths than the initial testing with no coatings. This shows the potential that coatings have going forward. No PMMA was left behind on the fabric, where the part was removed, meaning the interface between PMMA and fabric had failed. Fabric was however found on the removed part in an irregular pattern compared to the fabric left behind for samples that had no coatings added. There was higher standard deviation for the PMMA covered samples and this was likely due to the irregular bonding the PMMA had with the fabric. Increasing this bond would be desired going forward.

Fill angle and bed temperature were then found to result in higher adhesion at the interface if the fill angle was along the weft and the bed temperature was higher. Currently the peel sample has

only been tested with its rectangle orientated in the direction of the warp; having the part orientated along the weft or otherwise may lead to greater adhesion strength. The higher strength is likely because of the higher roughness encountered and potential for additive manufactured material to interlock with the fabric. Higher bed and environmental temperature raise the adhesion strength the longer the material can be kept at low viscosity. Specifically, if the material its kept above is glass transition temperature the goal is to keep the bed and by extension the fabric above that threshold.

Bed temperatures of 100℃ used to create samples on untreated fabrics were found to have the additive manufactured material to flow through to the other side of the fabric. Strength also increased greatly for samples with this effect compared to those that do not have material going through the fabric. The additive manufactured parts of samples became so difficult to remove from the fabric that in one case the sample failed due to low grip on a small amount of the part and the fabric ripped instead. This means the interfacial strength is reaching the limits of what manual removal of parts from the fabric can reach, without breaking the part that is. Future testing would desire peel samples to have a tab created that could be easily grabbed and doesn't have to be manually peeled back to remove any potential of error. From testing between the thicker and thinner versions of the cotton duck cloth used for sample creation it was determined that the thinner fabric performed much better. This is likely because of the fabric still being fairly thin, at 0.58 mm from the manufacturer, as well as being much more porous and looser. Additionally, with it being thinner it is much easier to heat the filament being laid down on it so that is goes through it than with the denser thicker fabric. More material was found to have flowed through the fabric as well. Increased strength going forward would likely be to further promote interlacing with the fabric and additive manufactured material until the fabric fails first

or the part cannot be removed without being broken. Future testing would involve better environmental control, different orientations for the peel sample on fabric, and higher bed temperatures.

From the results showing that bed temperature above the glass transition temperature of the additive manufactured part increases the adhesion strength it was decided to do the same with coatings. Specifically, the glass transition temperature of PMMA is around 110℃ and so a comparison of samples created with a bed temperature of 70℃ and 120℃ was done. Results found that the strength of the interface increased greatly between the lower and higher temperatures with the thicker coating performing the greatest. This seems to suggest that the thicker the coating the better for interfacial strength, but it was observed thinnest coating used increased in interfacial strength much more than the other coated samples when being exposed to higher bed temperatures. This leaves potential for the thinner coatings to help much more in adhesion; in the future even thinner coatings with high bed temperature should be tested. All samples had no PMMA left on the fabric where the part was removed proving that the PMMA and fabric interface is the weak point still and not the connection between PMMA and the part. The thick coating has potential to be used for thin and smooth fabrics to help their adhesion as they cannot benefit greatly from the additive manufactured part interlocking with them.

For the washed samples initial testing failed to create suitable samples. Because of this samples with wavy additive manufactured parts were created. The samples were wavy due to the fabric shrinking after the fabrics were ironed out and not left to sit for long enough. The parts were adhered irregularly, with some having failed during manufacturing, and so after being tested no graph was created and only a basic idea of their potential strength was found. Results appear to show that adhesion strength is great, but this is likely because of the samples being created at

100℃. Future work will consider that the fabrics will shrink and will wait before creating parts on them after ironing.

5.3.2.1 Comparative Peel Testing Strength to Literature Conclusions

After determining the adhesion strength for multiple different setups with coatings and process parameters some of the best results are compared to other results found in literature. Table 5.5 shows the adhesion strengths at the interface observed. Specifically, those using cotton fabrics and PLA filament for the creation of additive manufactured parts are compared to each other [3], [12], [15]. Additionally, the highest adhesion strength results found in literature are listed, these being a half cotton half polyester knitwear fabric and an aramid knitwear fabric with a polyester based TPU being used as the filament [7]. From our results it was observed that we had the highest adhesion strengths when compared to the thin cotton duck cloth; it is likely that this is the greatest cotton duck cloth and PLA can be promoted at this time. Interestingly the knitwear and TPU combination had the greatest interfacial strength of all samples found in literature, only slightly lower than our observed highest. The combination of a rough knitwear fabric with an elastomer filament was unexpected to have worked as well as it did given the difficulty in creation of elastomers with 3D printers. Going forward changing filaments from PLA to an elastomer would be desired to determine how viable elastic materials are for promoting interfacial adhesion. Otherwise the samples were created much alike to ours with the nozzle greatly into the fabric, a 45 degree fill angle, and then specifically tailored the temperatures to work the best for the elastomer [7].

Table 5.5: Comparing interfacial adhesion results to literature

Peel Test Results:	Peel Adhesive Strength (N/mm):
Duck Cloth 100% Cotton Woven 0.9mm Thick with 70℃ Bed Temperature	1.45
Duck Cloth 100% Cotton 0.9mm Thick with 100℃ Bed Temperature	4.20
Duck Cloth 100% Cotton 0.58 mm Thick with 100℃ Bed Temperature	5.18
Peel Test Results from Literature:	
Cotton Woven 0.21 mm Thick (Grimmelsmann et al. [3])	0.70
Cotton Woven 0.39 mm Thick (Spahiu et al. [15])	2.20
Cotton Twill 3:1 Woven 0.9 mm Thick (Kozior et al. [12])	0.70
Cotton Polyester Knitwear 0.44 mm Thick with Polyester Based TPU as Filament (Korger et al. [7])	5.0
Aramid Knitwear 0.42 mm Thick with Polyester Based TPU as Filament (Korger et al. [7])	5.0

Comparing the shear strength of PLA found in previous literature, which was 18.0 MPa, to our highest adhesion strength observed finds that a much higher adhesion strength is possible [40]. The highest adhesion strength was found to be 5.18 N/mm from our research. These samples were tested over a length of 101.6 mm of a given sample which gets an equivalent shear strength of the interface to be roughly 0.051 MPa. This means there is still a great deal of adhesion strength before the PLA breaks apart before the interface between additive manufactured part and fabric does. This comparison, however, may not be fair given it is adhesion strength that is found not shear strength and a different method of finding strength may be desired to compare to material strengths. In the future, more pull samples may give a better idea of how strong the interface is to the material strength of PLA.

5.4 Three Point Bending Testing

Three-point bending involves the testing of a solid beam of additive manufactured material created on top of fabric to determine if the fabric increases the strength of the composite. Specifically, the fabric was placed on the side in tension during the three-point testing to see if it helps the beam in tension. The sample was created along with a control sample not created on fabric to compare to. Two sets of two were tested for this in which the first was created using a 0.6 mm nozzle with a 0.6 mm layer height that ended up having manufacturing errors. The second being created with a 0.4 mmm nozzle and 0.2 mm height and no manufacturing errors.

5.4.1 Three Point Bending Results

Initial three-point bending tests were done with parts being created with a 0.6 mm nozzle diameter and a 0.6 mm layer height, with one sample created on fabric and one not. This was unusual compared to the normal 0.4 mm nozzle size and 0.2 mm layer height, this was done to complete the part much faster but led to issues. Samples were also created with a 70℃ bed temperature. The samples created are visibly porous on the sides due to an additive manufacturing error as shown with the fabric sample in Figure 5.19.

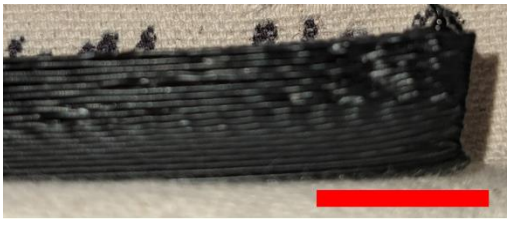

Figure 5.19: Three-point testing sample with manufacturing errors, scale bar is 15 mm

Figure 5.20 and Figure 5.21 show the results of the testing with the samples in force over displacement and stress over strain. The maximum force, displacement, and strain expected of the PLA calculated to be 1032 Newtons, 17 mm, and 0.031, from the equations in Figure 4.15,

can be compared to with these results. The sample not created on fabric was found to have broken when it reached its ultimate strength while the one created on fabric did not and the sample testing had to be stopped. From these results it was observed that the modulus of toughness for the sample created on with fabric was twice as large as the sample without fabric and still had the same ultimate strength. However, the tangent modulus of elasticity for the sample created with fabric was found to be 17% lower than the modulus found for the sample not created on fabric. The tangent elastic modulus found for the with fabric and no fabric samples were 2303 MPa and 2738 MPa. This is compared to the expected modulus of 2490 MPa supplied from the manufacturer. This appears to imply that the fabric is lowering the elastic modulus of the sample and is assisting in keeping the part together when the PLA starts to fail. This was not expected as it was initially expected that combining materials together would raise the with fabric beam composite strength higher than the material strength of the without fabric beam. Because of the unexpected results and the manufacturing errors, it was decided to remake the samples with the standard 0.2 mm layer height.

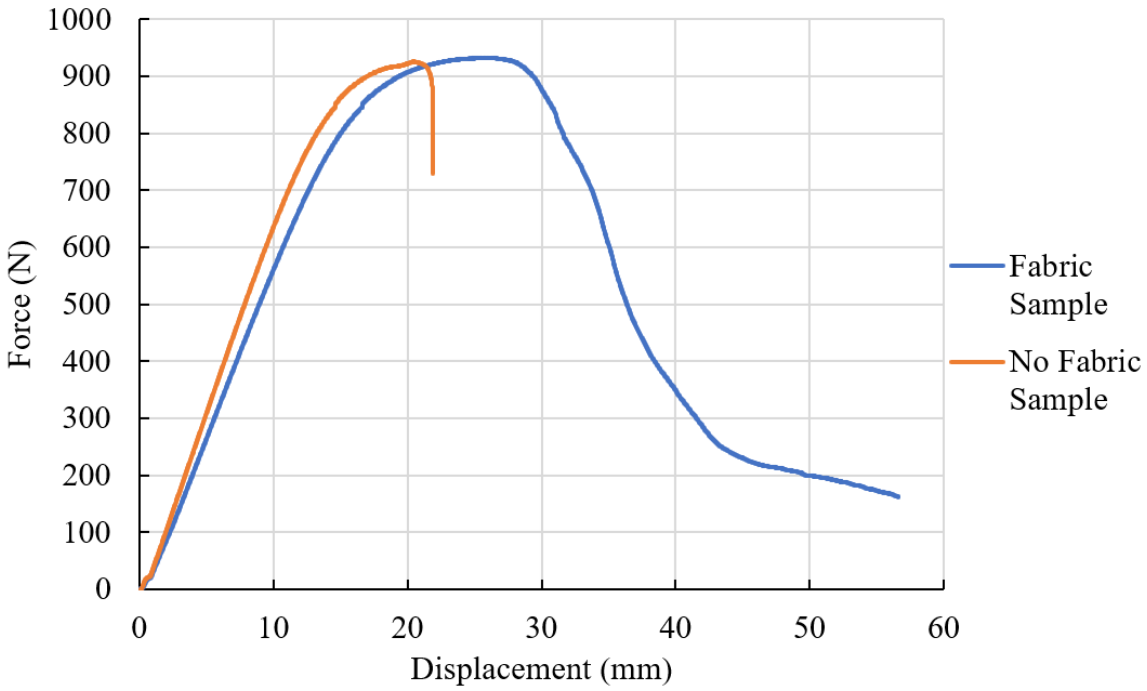

Figure 5.20: Three-point testing force versus displacement results from the 0.6 mm layer height samples

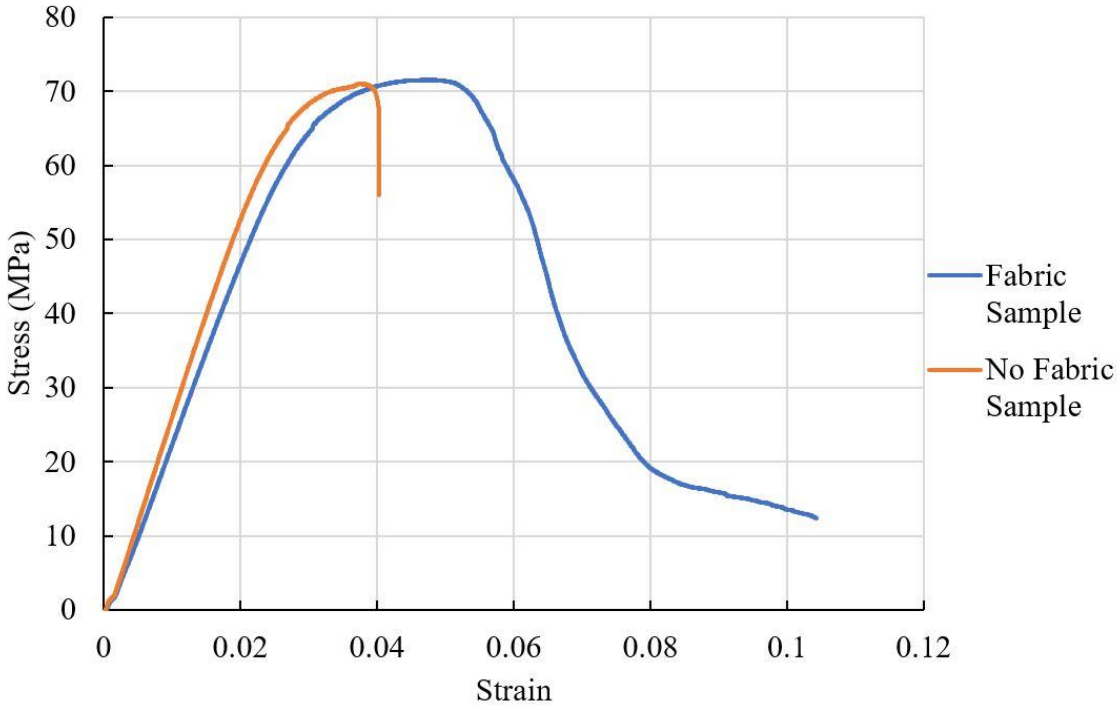

Figure 5.21: Three-point testing stress versus strain results from the 0.6 mm layer height samples

Figure 5.22 and Figure 5.23 show the force over displacement and the stress over strain for the three-point bending samples that were created with a 0.4 mm nozzle, a 0.2 mm layer height, and a 100℃ bed temperature. Because of the 100℃ bed temperature some of the additive manufactured part can be seen on the other side of the with fabric sample. The results found that both samples broke at their ultimate strength, the with fabric sample was not able to hold for longer as with the previous test. In this case, both the ultimate strength and the elastic modulus were found to be lower for the with fabric sample than the without fabric sample. The tangent elastic modulus was found as 2265 MPa for the with fabric sample and 3107 MPa for the without fabric sample. Additionally, Table 5.6 compares the elastic modulus, modulus of toughness, and maximum stress from all three-point testing samples. From this it could be determined that the parts created on the fabric lower the material strength of the PLA making the composite weaker than PLA on its own. This is likely because of the first layers of PLA interweaving with the fabric instead of forming a solid block with the rest of the PLA, and that the fabric adds thickness to the part without adding a great amount of strength. When the bed temperature was set to 100℃ this only increased the amount of material interweaving causing the elastic modulus and ultimate strength to go down. The break line of the samples was straight down the middle of both samples, instead of being slightly along the fill angle like before, is shown in Figure 5.24. This straight brake line is likely because of the much more solid creation of the 0.2 mm layer height sample compared to the 0.6 mm layer height.

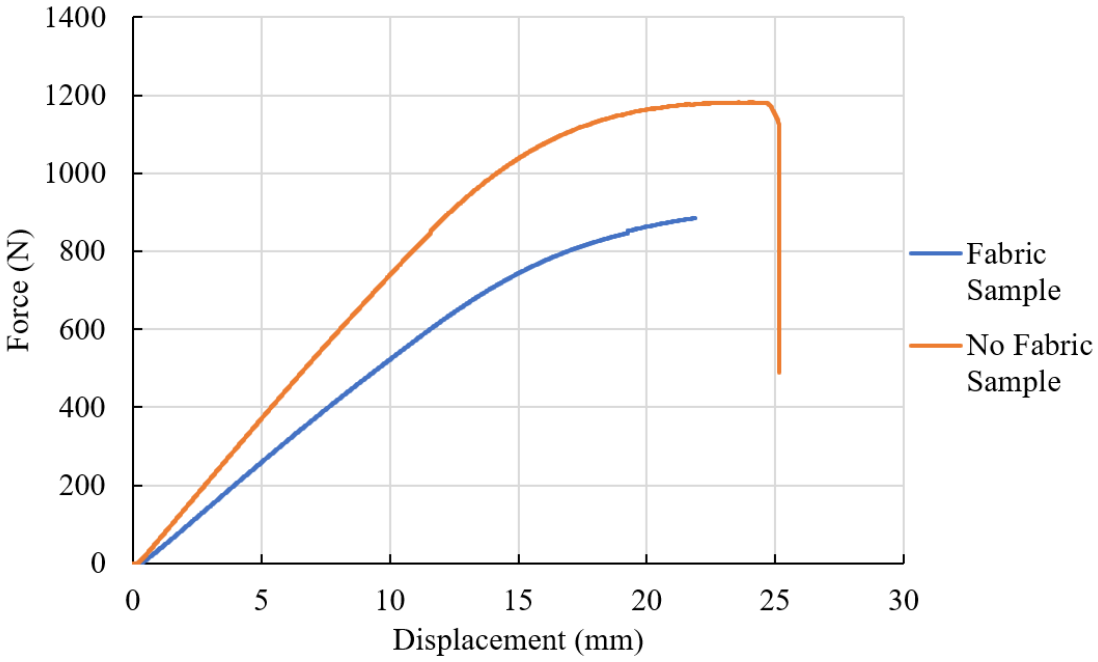

Figure 5.22: Three-point testing force versus displacement results from the 0.2 mm layer height samples

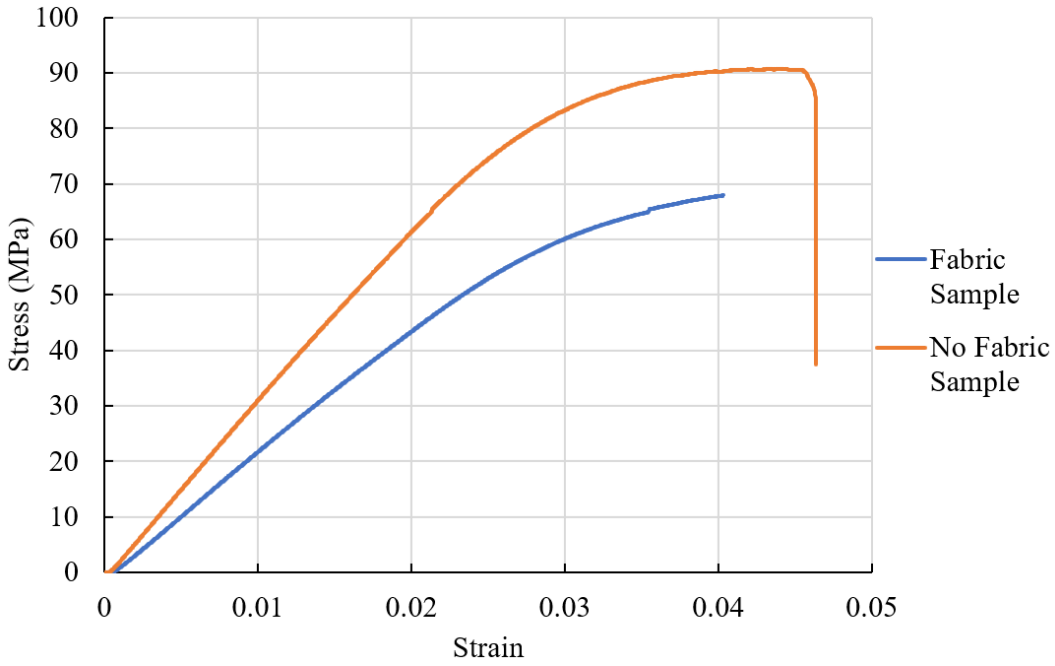

Figure 5.23: Three-point testing stress versus strain results from the 0.2 mm layer height samples

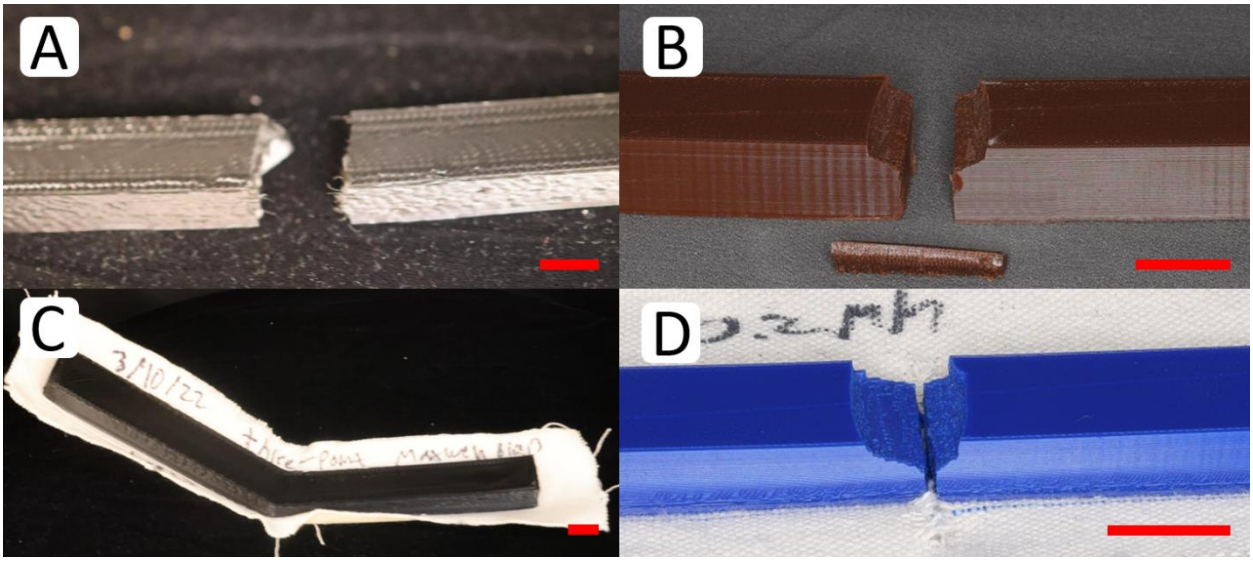

Figure 5.24: Visualization of three-point bending samples after testing, (a) jagged break of 0.6 mm layer height sample not with fabric, (b) straight break of 0.2 mm layer height sample no with fabric, (c) lack of braking of 0.6 mm layer height sample with fabric, (d) straight break of 0.2 mm layer height sample with fabric, red scale bar is 15 mm

Table 5.6: Elastic Modulus, Modulus of Toughness and Maximum Stress Results from Three Point Testing

	Tangent Elastic Modulus (MPa):	**Modulus of Toughness (MPa)**	**Maximum Stress (MPa)**
0.6 mm Layer Hight Samples with Fabric	2303	4.15	71.6
0.6 mm Layer Hight Samples No Fabric	2738	1.86	71.1
0.2 mm Layer Hight Samples with Fabric	2265	1.62	68.8
0.2 mm Layer Hight Samples No Fabric	3107	2.80	90.7
Properties from Manufacturer	2490	N/A	91.6

5.4.2 Three Point Bending Conclusions

From the results it could be concluded that additive manufacturing on top of fabric as to create a composite makes a composite weaker than the additive manufactured part by itself. This is likely because of the interweaving of the additive manufactured material into the fabric causing

the created part to not be solid and have a lower strength. As well as the added thickness the fabric adds to the sample without the substantial gain to mechanical strength. It appears that with higher interweaving the lower the strength of the composite, so a balance between interfacial strength between additive manufactured part and material strength of the composite must be made. However, it is possible that if adhesion at the interface is increased without the interweaving of the deposited material, like with polymer coatings, then the strength of the composite stronger than the additive manufactured part on its own. Future testing would involve creating samples that don't promote interfacial adhesion through interweaving greatly as to confirm this conclusion. This would involve different smooth and thin fabrics as well as different coatings and pre-treatments. Beam testing with fabric on top of and in-between layers of deposited material would be desired if the compressed fabric would still lower composite strength, or if the added thickness to the beam alone lowers composite strength.

5.5 Interfacial Strength Results

When additive manufacturing on fabrics so to determine the strength of the interface and the strength of the composite, three testing methods were used. These three were pull testing, peel testing, and three-point beam testing. For pull testing, the maximum strength it takes to remove a sample was found for samples. From this testing it was determined that between thick cotton duck cloth, acrylic, and polyester ripstop fabrics, the cotton duck cloth had the greatest interfacial strength of the three. This was likely due to the high thickness and roughness of the fabric. Sample sets were then created with glue applied to the fabric before the additive manufactured part was created on it. From the results, it was found that the interface between the glue and the fabric failed, given that there was no glue in the area where the part was removed. The interfacial strength significantly lowered when the glue was applied. This lower

strength was due to the blocking of the interweaving of the additive manufactured part during creation with the fabric causing a weak boundary layer. The glue samples also had variable applications of glue on them, causing some samples to fail early due to their poor interfacial strength, so their data was discarded at the time. For all samples, fabric would be left behind on the removed part, but less so for the glue applied parts. The thicker and rougher duck cloth would also promote the interweaving due to its porosity and is why the strength of the interface with the duck cloth is higher than other fabrics. One duck cloth sample had an unusually high adhesion strength, and the sample broke during testing before the interface failed; it is unknown why one sample had a much higher interfacial strength. However, this would mean that the pull testing method is flawed, and going forward if higher interfacial strengths were found, the samples would also break. There is potential that a better pull testing method could be possible.

Initial peel testing work was copying samples used in pull testing to compare to pull testing and determine if peel testing would be more suitable going forward. For this testing method, adhesion strength would be found instead of the force required to remove the parts. Results for samples similar to the pull samples found that the cotton duck cloth performed better again and that there was a larger range between strengths of each fabric. Additionally, the results were much more consistent with lower standard deviation as well as less likely to have failed samples. From this, and the ease of comparison to previous literature, peel testing was chosen going forward as the testing method for the interface.

It was determined different pre-treatments, coatings, and process parameters such as higher bed temperature would be desired to be tested to find the highest interfacial strength. From this point, it was decided that the cotton duck cloth would be used for all samples, and the Ultimaker S5 3D printer in an enclosure with a bed temperature of 70°C, z-distance of +0.4 mm and twice

as thick peel samples. This would be used instead of the CR-10S at 60℃ and a z-distance of +0.2 mm. Nylon was not found to be suitable as a coating, as it greatly reduced the adhesion strength; the interface between nylon and fabric was the one to fail. The two PMMA coatings were tested with different molecular weights, and both found adhesion strength greater than testing without the coating. This proves that coatings have potential to increase adhesion strength as fabric is still found on the removed part, but in uneven spots. This means that adhesion could potentially be increased later, and that the failure is at the interface between PMMA and the fabric and not the PMMA and the deposited PLA. This would mean that the PMMA is causing a weak boundary layer between the PLA and the fabric. PMMA covered samples had a higher standard deviation to other samples, likely because of the uneven coating on the fabric; a film applicator would be desired going forward to smooth the coating out. An additive manufactured part not created on fabric was then adhered to some fabric using Loctite 410. Results were unreliable due to the uneven application of the adhesive, in the future an adhesive that works well with fabrics and polymers would be desired, along with a better application of the material.

Different process parameters of the 3D printers were then used to determine how the adhesion strength would change at the interface. Specifically, a control sample set, a sample set with a fill angle along the weft instead of at a 45-degree angle between the warp and weft, and a sample set with a bed temperature of 100℃ instead of 70℃ were used. From these tests, it was determined that both had a great effect on the adhesion strength of the interface with the higher temperature being a much larger factor. After this, a thinner cotton duck cloth of 0.58 mm thickness was used for all samples going forward. Next, three sample sets of fill orientation of 0-, 45-, and 90-degrees using a bed temperature of 100℃ were then created and tested. From these results it

was confirmed that the temperature affects the adhesion strength much more than the fill angle. Additionally, the fill angle would be desired to be along the weft of the fabric and not the warp, for highest adhesion strength with the strength getting greater with diminishing returns till along the weft. This is likely due to the weft being much rougher given the rectangular nature of the weave allowing, more material to interweave with the fabric.

The higher bed temperature also greatly affects the strength by promoting the interweaving of the additive manufactured material into the fabric. It does this by keeping the viscosity of the material as low as possible for a longer period of time, after it leaves the nozzle of the 3D printer by keeping the material above its glass transition temperature. The enclosure that the Ultimaker 3D printer is in also could be potentially assisting this by controlling the environment temperature as well. From this test it was also observed that the difference between adhesion strengths for fill angle was much lower than expected. This is likely due to either the thinner fabric influencing the adhesion despite being the same weave, or that the higher bed temperature is overpowering the influence of the extra roughness from the fill angle. All samples created found that some of the additive manufactured PLA material of the samples had gone through to the other side of the fabric, because of high bed temperatures. This was true for both the thick and thin cotton duck cloth used and likely is the cause for the great increase in adhesion strength when using the higher bed temperature.

All samples also had a thick coating of fabric left behind on the removed part; the fabric was also very abused and ripped where the part was removed. For the first time, additively manufactured parts had also been found left behind in the fabric. This would mean that both the fabric and additively manufactured parts were starting to interweave fully with each other. The deposited material weaved into the fabric was being broken off from the main part and left behind in the

fabric. The fabric weave and interweaved material of the additive manufactured parts were then both contributing greatly to the interfacial strength, which isn't normally seen. This was seen when a sample was being set up for testing where the samples became very difficult to manually peel a small amount to be grabbed for testing. The sample was then improperly tested with the small area for the gripper to hold onto and instead of the interface between fabric and part failing the fabric instead ripped due to the uneven loading. Although this isn't good for results it does prove that the strength of the interface is getting too hard for manually peeling back a section for testing and that the interface is approaching the strength of the fabrics. Future samples are desired to be created so no manual peeling is required.

After determining that the high bed temperature greatly increases adhesion strength, and more so when above the glass transition temperature, it was decided to test high bed temperatures with coatings. Specifically, with a sample set with PMMA coatings with a 70℃ bed temperature set to compare to and a sample set at 120℃ which is above the glass transition temperature of the PMMA. Coatings were applied with a film applicator to keep the coatings smooth as well as three different thicknesses of PMMA used. Results found that the thickest coating of PMMA had the highest adhesion strength and that all coatings greatly increase in strength with the higher temperature. However, the adhesion strength was still lower than the samples created with no coating and 100℃ bed temperature, due to a weak boundary layer being created between the PLA and the fabric. The thinner coatings did not perform as well as the thicker fabric, which was not expected; however, the thinnest coating did greatly gain in interfacial strength with the higher temperature. This means that even thinner coatings have the potential to increase the adhesion strength. This is likely due to the higher adhesion to the PMMA and either a minor amount of interlocking with the fabric or the porous, thin coating. All samples had no PMMA

left behind on the fabric after the part was removed and fabric was found left behind on the part meaning the PMMA and fabric interface had failed.

To start testing more with pre-treatments to change the properties of fabric the cotton duck cloth was washed using a non-ionic surfactant and soda ash solution. Two washing methods were used, the first using a beaker to wash the fabrics in, the second using an ultrasonic washer. The larger amount of solution and constant stirring by the ultrasonic machine was used to remove the sizing left on the fabric by the manufacturer much more than the beaker washing. Given the beaker solution was left with a color close to the cloth fabric after washing, it is likely that it didn't have as much chance to remove as much as the ultrasonic machine. Both fabric's sets were found to be much paler than before and were found to be very wrinkly and so they were ironed just before they had their additive manufactured parts created on them. However, because of the ironing and washing the fabric appears to have shrunk while the parts were being created on them leading all samples to be wavy. This made the samples unusable for quantitative results; however, the samples were still tested to get a general idea of their strength. Samples were very irregularly adhered leading to a great amount of deviation, but high adhesion was found for both sample sets.

The highest adhesion strengths observed from testing were then compared to previous literature and the strength of PLA. It was determined that the interfacial strength is still much lower than the material properties of the PLA although currently it is difficult to say for certain. More pull tests may be desired in the future as they can be better related to material strengths. Of all other previous studies using thick cotton fabrics we have found the highest adhesion strength with the bed temperature of 100℃. However, two sample sets using a polyester-based elastomer instead of PLA on rough cotton-polyester knitwear and on rough aramid knitwear fabrics performed

very well. It was unexpected to see the elastomer perform so well at the time. Going forward knitwear as a fabric with different materials as well as different elastic filaments should be tested.

CHAPTER 6

CONCLUSIONS AND FUTURE WORK

6.1 Conclusions

In order to create flexible, and potentially large, objects by additive manufacturing on fabrics an unfolding pattern must be created. The unfolding pattern involves the creation of a 2D pattern of panels from 3D models in a chain unfolding. This unfolding allowed the creation of objects with integrated flexibility using a desktop 3D printer with minimal post-manufacturing attributable to the panels being connected by fabric. Paper unfolding programs was useful in creating these large, unfolded patterns, but needed some assistance to make desired chain unfolding patterns. The chain unfolding patterns of models were found to be desired because of their ability to be created without interfering with the 3D printers frame during manufacturing. Specifically, the use of an open concept Creality CR-10S 3D printer allowed the ease of creation of these chain unfolding patterns compared to enclosed 3D printers. Each panel of a model would be created one at a time on fabric in the unfolding pattern. The fabric would be fastened, moved, and refastened to the print bed of the 3D printer for each part. A dodecahedron was created using this technique and printer with an edge length of 12 cm making the object much larger then could have been created as a single part.

The testing of parameters, pre-treatments, and materials to achieve the highest adhesion strength obtainable at the interface between additive manufactured part and fabric was also done. High strength at the interface would allow the potential for uses in different applications that would require created products to be under great stress. Pull sample testing was initially used to measure the strength of the interface but this was changed to peel testing after finding that peel testing could be more consistent. Of the initial fabrics tested the highest adhesion found was

with the cotton duck cloth, at 1.49 $\frac{\mathrm{N}}{\mathrm{mm}}$, and so all properties and testing going forward was done using the cotton duck cloth with either one of two different thicknesses. When glue was applied to the fabric before sample creation on top of it was determined that the glue lowered the adhesion strength of the interface. This was due to the glue blocking the interlacing of the additive manufactured material into the fabric, in this case due to a weak boundary layer being created.

Polymer coatings and adhesives were then tested on the samples. PMMA was found to be a great coating as the adhesion strength greatly increased the adhesion strength of the interface, given standard process parameters. However, when compared to adhesion strength obtained by changing the process parameters without adding a covering the interfacial strengths found by PMMA coverings were found to be much lower. Alike to the previous samples the removed part would have fabric on them showing the interface to the fabric had failed, however, there also was no PMMA left on the fabric. The interface between the PMMA and the fabric is what was found to fail showing a weak boundary layer being created again, although much stronger than for the adhesive covered samples.

After initial coating tests, 3D printing process parameter testing was done, with both fill angle and bed temperature. It was found that both higher bed temperature and a fill angle along the weft of the fabric increased the adhesion strength. The longer the additive manufactured material is kept at a low viscosity and above its glass transition temperature the more the material can interlace with the fabric greatly increasing its adhesion strength. All samples created with the higher 100°C had the additive manufactured material go through the fabric and be visible on the other side which is assumed to be the cause of the great adhesion strength. For the fill angle the strength was greater in the weft direction because of the rectangular nature of the weave.

This made the weft direction rougher allowing more material the chance to interweave in the fabric. Diminishing returns on the increase of adhesion strength were also observed the closer the fill angle was to the weft direction. The thicker cotton duck cloth was much more influenced by the fill angle than the thinner duck cloth tested. Fill angle also was greatly overshadowed by the influenced by higher bed temperature when testing, making fill angle matter much more when low bed temperatures are used with smoother fabrics. Highest interfacial strength observed was with an uncovered sample set at 100℃ with a fill angle along the weft direction at $5.18\ \frac{\mathrm{N}}{\mathrm{mm}}$.

More PMMA coating tests were done with higher bed temperatures at 120℃, which is above the glass transition temperature of the PMMA. Multiple thicknesses of PMMA coatings were tested. Results found that the higher temperature increased adhesion but less than the adhesion strength of the untreated fabric samples with a bed temperature of 100℃. The thickest coating of PMMA was found to have the highest adhesion strength. The thinnest coating had the greatest amount of adhesion increase when going from a bed temperature of 70℃ to 120℃ likely because of the coating being more porous. All coated samples had fabric on the removed part and no PMMA left behind, meaning the PMMA fabric interface is failing. Washed fabrics had issues during manufacturing where the fabric shrunk during part creation on them leading to wavy parts. This led to unreliable data but showed the potential for washed fabrics. From three-point testing it was determined that the strength of the composite was lower than the strength of the PLA part was. This is assumed to be because the part is interwoven into the fabric and not kept as a solid part, while adding additional thickness to the part in total. The added thickness by the fabric also likely contributed to lower composite strengths as the fabric does not add a great amount of material strength to the composite either. This means that with the more interweaving of the

additive manufactured part and fabric for interfacial strength the lower the strength of the composite. A balance must be made, depending on the application, between interfacial strength and strength of the composite.

The results of the adhesion strength were compared to the strength of PLA and to previous literature results for adhesion strength. Pull testing results determined that the interface fails before the material strength of PLA does and that there is still a large gap before the interface is stronger than the material strength of PLA. However, pull sample testing was not optimized and could potentially show better results. Peel testing does not currently appear to be a useful way to relate to material strength. However, when relating to previous research it was found that the $5.18\ \frac{\mathrm{N}}{\mathrm{mm}}$ result for the duck cloth sample created with a bed temperature of 100℃ and fill angle along the weft was the highest recorded. A result from previous research, however, was very close that being a polyester-based elastomer on rough knitwear got $5.0\ \frac{\mathrm{N}}{\mathrm{mm}}$. This shows that there is potential in testing different filaments and polymers to be used by the 3D printer

6.2 Future Work and Recommendations

In the current research we used simplistic graph theory based Hamiltonian path method for unfolding simple shapes and creating flat panels and solid geometry. For complex geometry and shapes advanced unfolding techniques will be necessary. For the proof-of-concept PLA was used which can be extended to other polymers in the future. For fabrics only one type of weave at two different thicknesses was tested extensively, coverings as well only extensively tested PMMA coverings and only had one method of fabric covering. In the future, a comprehensive standard characterization protocol for testing the proposed novel systems, the parts, the segmentation, the fabric, and the assembled object will be developed.

Unfolding and segmentation methods for additive manufacturing large objects currently requires an unfolding pattern that is difficult to make and for some shapes impossible. Creation of irregular shapes and would be desired going forward as to determine how well objects can be unfolded and created. Pushing the boundaries of how large a singular object could be created using this method would also be desired. Additionally, user input of models is required to edit the base unfolding pattern to a chain pattern in Pepakura. Going forward, the creation of an algorithm that could automatically make the unfolding designs that are in a single chain, would be desired. Use of better clamps and well orientated parts to be created on the 3D printer to reduce chances of error during manufacturing would also be desired. The use of ceiling hanging printers in the future would remove the necessity in chain unfolding as there would be no chance for impedance from 3D printer frames. Currently with segmentation being based around paper unfolding the final product created is hollow which may not be desired. Future segmentation would be desired to create solid or semi solid objects that would have fabric on the outside instead of the created parts. The parts created would be able to be tailored for specific mechanical strengths and with specific features for applications. Parts would have to be beveled or spaced from each other correctly as to assure correct interlocking of parts. Additive manufacturing with fabric in between layers also has potential to create much more complex parts for applications.

The use of different filaments other than PLA and different fabrics would be desired to increase interfacial strength going forward. Specifically, the use of flexible filaments and fabrics either with high roughness and thickness or with special properties like waterproofing etc. Testing of fabric properties would be desired going forward specifically the material strength, wettability, surface energy, amount of hydrophilicity, type of weave used, and roughness. Better

environmental control for sample creation would be desired specifically to promote higher temperatures and better interweaving of the polymers with the fabrics. The enclosure the 3D Ultimaker S5 3D printer was in helped keep the samples unaffected by outside influence and temperature during sample creation, this assisted in consistent sample creation, as an example. Different adhesives should also be tested, specifically adhesives used for fabrics and polymers. These adhesives should also be applied evenly over the sample. Washing the fabrics should also be attempted again as to remove the manufacturers sizing, specifically preventing the shrinking of fabrics affecting sample creation.

Use of different pre-treatments to change the properties of fabrics as desired could be done to either change the properties of the fabric to increase interfacial adhesion or add properties like waterproofing etc. Testing appeared to show that the application of coatings would lead to lower adhesion strength when fabrics that can promote adhesion strength through interlocking are used. This means that these coatings could be used to improve the interfacial strength when using thin or smooth fabrics that do not promote interfacial strength well. However, when using thin coatings at high temperature, close to and above the glass transition temperature of both the coating and filament, it was observed that the strength of the interface would increase higher than expected. It is assumed that coatings above the glass transition temperature of the coating and filament used could promote an interfacial bonding greater than with the mechanical interlocking with rough and thick fabrics. Future work would be desired to increase the interfacial strength between the coating and fabric with higher environmental temperatures and compare both thick and thin coatings of polymers on fabrics. Testing involving the conditioning of created samples left under certain environmental conditions is desired as well. This is to determine the viability

of additive manufactured on fabric objects and their ability to keep their form under various conditions, such as in water or in the snow.

When comparing the interfacial strengths of similar PMMA covered samples on two different weaves of cotton duck cloth it was determined that fabric used does not greatly affect the interfacial strength. The ability to add a covering as to acquire a specific interfacial strength would be useful with fabrics that do not promote interfacial strength as much as the cotton duck cloths tested. This would have to be tested with much different fabrics than cotton to be confirmed, however.

Future testing of peel samples would have to involve the creation of samples that do not have to be manually peeled enough to be machine tested. This is to allow the potential for higher adhesion strengths outside of the range of human strength to be tested as well as lowering the chance of sample failure from user input. Force balance will have to be done for samples using interweaving with fabrics as to determine if the part has the desired material strength going forward. Strength of the interface would have to be tested either with a new kind of pull testing or some other testing method as to compare to the strength of PLA and other polymers. This would help get a better idea of how strong the interface can get before the created part starts failing before the interface does, this as well as fabric strength. Seamless automation of the proposed additive manufactured on fabric system will be our future research direction.

REFERENCES

[1] J. Shah, B. Snider, T. Clarke, S. Kozutsky, M. Lacki, and A. Hosseini, "Large-scale 3D printers for additive manufacturing: design considerations and challenges," *Int. J. Adv. Manuf. Technol.*, vol. 104, no. 9–12, pp. 3679–3693, Oct. 2019, doi: 10.1007/s00170-019-04074-6.

[2] M. Korger, J. Bergschneider, M. Lutz, B. Mahltig, K. Finsterbusch, and M. Rabe, "Possible Applications of 3D Printing Technology on Textile Substrates," *IOP Conf. Ser. Mater. Sci. Eng.*, vol. 141, p. 012011, Jul. 2016, doi: 10.1088/1757-899X/141/1/012011.

[3] N. Grimmelsmann, M. Kreuziger, M. Korger, H. Meissner, and A. Ehrmann, "Adhesion of 3D printed material on textile substrates," *Rapid Prototyp. J.*, vol. 24, no. 1, pp. 166–170, Jan. 2018, doi: 10.1108/RPJ-05-2016-0086.

[4] L. Sabantina, F. Kinzel, A. Ehrmann, and K. Finsterbusch, "Combining 3D printed forms with textile structures - mechanical and geometrical properties of multi-material systems," *IOP Conf. Ser. Mater. Sci. Eng.*, vol. 87, p. 012005, Jul. 2015, doi: 10.1088/1757-899X/87/1/012005.

[5] E. Pei, J. Shen, and J. Watling, "Direct 3D printing of polymers onto textiles: experimental studies and applications," *Rapid Prototyp. J.*, vol. 21, no. 5, pp. 556–571, Aug. 2015, doi: 10.1108/RPJ-09-2014-0126.

[6] M. Ayvali, L. Bussieweke, G. Druzinin, M. Korkmaz, and A. Ehrmann, "3D printing on warp-knitted fabrics," *IOP Conf. Ser. Mater. Sci. Eng.*, vol. 1031, no. 1, p. 012019, Jan. 2021, doi: 10.1088/1757-899X/1031/1/012019.

[7] M. Korger *et al.*, "Testing thermoplastic elastomers selected as flexible three-dimensional printing materials for functional garment and technical textile applications," *J. Eng. Fibers Fabr.*, vol. 15, p. 155892502092459, Jan. 2020, doi: 10.1177/1558925020924599.

[8] T. Kozior, T. Blachowicz, and A. Ehrmann, "Adhesion of three-dimensional printing on textile fabrics: Inspiration from and for other research areas," *J. Eng. Fibers Fabr.*, vol. 15, p. 155892502091087, Jan. 2020, doi: 10.1177/1558925020910875.

[9] R. Hashemi Sanatgar, C. Campagne, and V. Nierstrasz, "Investigation of the adhesion properties of direct 3D printing of polymers and nanocomposites on textiles: Effect of FDM printing process parameters," *Appl. Surf. Sci.*, vol. 403, pp. 551–563, May 2017, doi: 10.1016/j.apsusc.2017.01.112.

[10] P. A. Eutionnat-Diffo *et al.*, "Stress, strain and deformation of poly-lactic acid filament deposited onto polyethylene terephthalate woven fabric through 3D printing process," *Sci. Rep.*, vol. 9, no. 1, Dec. 2019, doi: 10.1038/s41598-019-50832-7.

[11] Bielefeld University of Applied Sciences, Faculty of Engineering and Mathematics, Interaktion 1, 33619 Bielefeld, Germany *et al.*, "Increasing adhesion of 3D printing on

textile fabrics by polymer coating," *TEKSTILEC*, vol. 61, no. 4, pp. 265–271, Dec. 2018, doi: 10.14502/Tekstilec2018.61.265-271.

[12] T. Kozior, C. Döpke, N. Grimmelsmann, I. Juhász Junger, and A. Ehrmann, "Influence of fabric pretreatment on adhesion of three-dimensional printed material on textile substrates," *Adv. Mech. Eng.*, vol. 10, no. 8, p. 168781401879231, Aug. 2018, doi: 10.1177/1687814018792316.

[13] M. G. Tadesse, D. Dumitrescu, C. Loghin, Y. Chen, L. Wang, and V. Nierstrasz, "3D Printing of NinjaFlex Filament onto PEDOT:PSS-Coated Textile Fabrics for Electroluminescence Applications," *J. Electron. Mater.*, vol. 47, no. 3, pp. 2082–2092, Mar. 2018, doi: 10.1007/s11664-017-6015-6.

[14] E. A. Franco-Urquiza, Y. R. Escamilla, and P. I. Alcántara Llanas, "Characterization of 3D Printing on Jute Fabrics," *Polymers*, vol. 13, no. 19, p. 3202, Sep. 2021, doi: 10.3390/polym13193202.

[15] T. Spahiu, M. Al-Arabiyat, Y. Martens, A. Ehrmann, E. Piperi, and E. Shehi, "Adhesion of 3D printing polymers on textile fabrics for garment production," *IOP Conf. Ser. Mater. Sci. Eng.*, vol. 459, p. 012065, Dec. 2018, doi: 10.1088/1757-899X/459/1/012065.

[16] M. L. Rivera, M. Moukperian, D. Ashbrook, J. Mankoff, and S. E. Hudson, "Stretching the Bounds of 3D Printing with Embedded Textiles," in *Proceedings of the 2017 CHI Conference on Human Factors in Computing Systems*, Denver Colorado USA, May 2017, pp. 497–508. doi: 10.1145/3025453.3025460.

[17] Y. Yan, R. Zhang, G. Hong, and X. Yuan, "Research on the bonding of material paths in melted extrusion modeling," *Mater. Des.*, vol. 21, no. 2, pp. 93–99, Apr. 2000, doi: 10.1016/S0261-3069(99)00058-8.

[18] J. Yin, C. Lu, J. Fu, Y. Huang, and Y. Zheng, "Interfacial bonding during multi-material fused deposition modeling (FDM) process due to inter-molecular diffusion," *Mater. Des.*, vol. 150, pp. 104–112, Jul. 2018, doi: 10.1016/j.matdes.2018.04.029.

[19] A. N. Ahsan and B. Khoda, "Honeycomb pattern on thin wall object with grain based 3d printing," *Procedia Manuf.*, vol. 26, pp. 900–911, 2018, doi: 10.1016/j.promfg.2018.07.117.

[20] R. Li and Q. Peng, "Surface quality improvement and support material reduction in 3D printed shell products based on efficient spectral clustering," *Int. J. Adv. Manuf. Technol.*, vol. 107, no. 9–10, pp. 4273–4286, Apr. 2020, doi: 10.1007/s00170-020-05299-6.

[21] H.-K. Chen and M.-W. Li, "A novel mesh saliency approximation for polygonal mesh segmentation," *Multimed. Tools Appl.*, vol. 77, no. 13, pp. 17223–17246, Jul. 2018, doi: 10.1007/s11042-017-5287-4.

[22] X. Chen *et al.*, "Dapper: decompose-and-pack for 3D printing," *ACM Trans. Graph.*, vol. 34, no. 6, pp. 1–12, Nov. 2015, doi: 10.1145/2816795.2818087.

[23] L. Luo, I. Baran, S. Rusinkiewicz, and W. Matusik, "Chopper: partitioning models into 3D-printable parts," *ACM Trans. Graph.*, vol. 31, no. 6, pp. 1–9, Nov. 2012, doi: 10.1145/2366145.2366148.

[24] P. Song *et al.*, "Reconfigurable interlocking furniture," *ACM Trans. Graph.*, vol. 36, no. 6, pp. 1–14, Nov. 2017, doi: 10.1145/3130800.3130803.

[25] S. Kiazyk and A. Lubiw, "Star Unfolding from a Geodesic Curve," *Discrete Comput. Geom.*, vol. 56, no. 4, pp. 1018–1036, Dec. 2016, doi: 10.1007/s00454-016-9795-1.

[26] S. Katz and A. Tal, "Hierarchical Mesh Decomposition using Fuzzy Clustering and Cuts," p. 8.

[27] T. Haenselmann and W. Effelsberg, "Optimal strategies for creating paper models from 3D objects," *Multimed. Syst.*, vol. 18, no. 6, pp. 519–532, Nov. 2012, doi: 10.1007/s00530-012-0273-1.

[28] S. Takahashi, H.-Y. Wu, S. H. Saw, C.-C. Lin, and H.-C. Yen, "Optimized Topological Surgery for Unfolding 3D Meshes," *Comput. Graph. Forum*, vol. 30, no. 7, pp. 2077–2086, Sep. 2011, doi: 10.1111/j.1467-8659.2011.02053.x.

[29] Z. S. GharehTappeh and Q. Peng, "Simplification and unfolding of 3D mesh models: review and evaluation of existing tools," *Procedia CIRP*, vol. 100, pp. 121–126, 2021, doi: 10.1016/j.procir.2021.05.023.

[30] T. Grothe, B. Brockhagen, and J. L. Storck, "Three-dimensional printing resin on different textile substrates using stereolithography: A proof of concept," *J. Eng. Fibers Fabr.*, vol. 15, p. 155892502093344, Jan. 2020, doi: 10.1177/1558925020933440.

[31] S. Chakraborty and M. C. Biswas, "3D printing technology of polymer-fiber composites in textile and fashion industry: A potential roadmap of concept to consumer," *Compos. Struct.*, vol. 248, p. 112562, Sep. 2020, doi: 10.1016/j.compstruct.2020.112562.

[32] University of Central Florida, Institute for Simulation and Training, Prototype Development and 3D Print Lab, Orlando, FL 32826, USA, R. Uysal, J. B. Stubbs, and University of Central Florida, Institute for Simulation and Training, Prototype Development and 3D Print Lab, Orlando, FL 32826, USA, "A New Method of Printing Multi-Material Textiles by Fused Deposition Modelling (FDM)," *TEKSTILEC*, vol. 62, no. 4, pp. 248–257, Nov. 2019, doi: 10.14502/Tekstilec2019.62.248-257.

[33] N. Grimmelsmann, Y. Martens, P. Schäl, H. Meissner, and A. Ehrmann, "Mechanical and Electrical Contacting of Electronic Components on Textiles by 3D Printing," *Procedia Technol.*, vol. 26, pp. 66–71, 2016, doi: https://doi.org/10.1016/j.protcy.2016.08.010.

[34] N. A. Fountas, P. Kostazos, H. Pavlidis, V. Antoniou, D. E. Manolakos, and N. M. Vaxevanidis, "Experimental investigation and statistical modelling for assessing the tensile properties of FDM fabricated parts," *Procedia Struct. Integr.*, vol. 26, pp. 139–146, 2020, doi: 10.1016/j.prostr.2020.06.017.

[35] N. Hill and M. Haghi, "Deposition direction-dependent failure criteria for fused deposition modeling polycarbonate," *Rapid Prototyp. J.*, vol. 20, no. 3, pp. 221–227, Apr. 2014, doi: 10.1108/RPJ-04-2013-0039.

[36] S. Ravindrababu, Y. Govdeli, Z. W. Wong, and E. Kayacan, "Evaluation of the influence of build and print orientations of unmanned aerial vehicle parts fabricated using fused deposition modeling process," *J. Manuf. Process.*, vol. 34, pp. 659–666, Aug. 2018, doi: 10.1016/j.jmapro.2018.07.007.

[37] K. Fayazbakhsh, M. Movahedi, and J. Kalman, "The impact of defects on tensile properties of 3D printed parts manufactured by fused filament fabrication," *Mater. Today Commun.*, vol. 18, pp. 140–148, Mar. 2019, doi: 10.1016/j.mtcomm.2018.12.003.

[38] S. Rohde *et al.*, "Experimental Characterization of the Shear Properties of 3D–Printed ABS and Polycarbonate Parts," *Exp. Mech.*, vol. 58, no. 6, pp. 871–884, Jul. 2018, doi: 10.1007/s11340-017-0343-6.

[39] B. M. Tymrak, M. Kreiger, and J. M. Pearce, "Mechanical properties of components fabricated with open-source 3-D printers under realistic environmental conditions," *Mater. Des.*, vol. 58, pp. 242–246, Jun. 2014, doi: 10.1016/j.matdes.2014.02.038.

[40] R. T. L. Ferreira, I. C. Amatte, T. A. Dutra, and D. Bürger, "Experimental characterization and micrography of 3D printed PLA and PLA reinforced with short carbon fibers," *Compos. Part B Eng.*, vol. 124, pp. 88–100, Sep. 2017, doi: 10.1016/j.compositesb.2017.05.013.

[41] J. M. Chacón, M. A. Caminero, E. García-Plaza, and P. J. Núñez, "Additive manufacturing of PLA structures using fused deposition modelling: Effect of process parameters on mechanical properties and their optimal selection," *Mater. Des.*, vol. 124, pp. 143–157, Jun. 2017, doi: 10.1016/j.matdes.2017.03.065.

[42] "Materials > PLA," *Ultimaker*. https://support.ultimaker.com/hc/en-us/sections/360003504300 (accessed Jun. 18, 2022).

[43] S. A. Tronvoll, N. P. Vedvik, C. W. Elverum, and T. Welo, "A new method for assessing anisotropy in fused deposition modeled parts using computed tomography data," *Int. J. Adv. Manuf. Technol.*, vol. 105, no. 1–4, pp. 47–65, Nov. 2019, doi: 10.1007/s00170-019-04081-7.

[44] N. Grimmelsmann, H. Meissner, and A. Ehrmann, "3D printed auxetic forms on knitted fabrics for adjustable permeability and mechanical properties," *IOP Conf. Ser. Mater. Sci. Eng.*, vol. 137, p. 012011, Jul. 2016, doi: 10.1088/1757-899X/137/1/012011.

[45] "Hangprinter." https://hangprinter.org/

[46] A. M. Verzoni, "DESIGN, ANALYSIS, AND OPTIMIZATION OF COMPACTIBLE ORIGAMI- INSPIRED SHELTERS," p. 332.

[47] T. Heckmann, W. Schwanghart, and J. D. Phillips, “Graph theory—Recent developments of its application in geomorphology,” *Geomorphology*, vol. 243, pp. 130–146, Aug. 2015, doi: 10.1016/j.geomorph.2014.12.024.

[48] “Creality3D.” https://www.creality3dofficial.com/

[49] M. L. Demaine, R. A. Hearn, J. Hoshido, J. Ku, and R. Uehara, “Rectangular Unfoldings of Polycubes,” *J. Inf. Process.*, vol. 28, no. 0, pp. 841–845, 2020, doi: 10.2197/ipsjjip.28.841.

[50] P. M. Dodd, P. F. Damasceno, and S. C. Glotzer, “Universal folding pathways of polyhedron nets,” *Proc. Natl. Acad. Sci.*, vol. 115, no. 29, Jul. 2018, doi: 10.1073/pnas.1722681115.

[51] “Fabric Wholesale Direct.” https://www.fabricwholesaledirect.com/

[52] “Sigma Aldrich.” https://www.sigmaaldrich.com/US/en

APPENDICES

APPENDIX A: MATLAB Script for Computing Raw Data from Pull Tests to Usable Data

```
%%%%%%%%%%%%%%%%%%%%%%%%%%%%%%%%%%%%%%%%%%%%%%%%%%%%%%
%         Ingersoll Pull Testing Results             %
%%%%%%%%%%%%%%%%%%%%%%%%%%%%%%%%%%%%%%%%%%%%%%%%%%%%%%
clc,clf,clear;
%%%%%%%%%%%%%%%%%%%%%%%%%%%%%%%%%%%%%%%%%%%%%%%%%%%%%%%%%%%%%%%%%%%%%%
%%%------- PLEASE CHANGE PATH TO WHERE THE DATA IS LOCATED!--------%%%
%%%%%%%%%%%%%%%%%%%%%%%%%%%%%%%%%%%%%%%%%%%%%%%%%%%%%%%%%%%%%%%%%%%%%%
path ='C:\Users\';
%%%------- ONLY DATA TO BE PROCESSED SHALL BE LOCATED IN DIRECTORY -----%%%
files = dir(fullfile(path,'*.csv'));
info = struct2cell(files(:));
names= info(1,:); fullnames =string(fullfile(path,names));
numfiles = length(names);
clear files info;

%---- Calculate the Areas ----%
%Sigma 1 Area: Nominal Area of Sample
Sig1_Area = 3.14159*25.4*25.4/4;
%Name the File Information is Saved to:
fname='Pull Sample Properties.txt';
f = fopen(fname,'wt');

%%%%%%%%%%%%%%%%%%%%%%%%%%%%
% Initial Text File Header %
%%%%%%%%%%%%%%%%%%%%%%%%%%%%
fprintf(f,'%7s \n','--------------------------------');
fprintf(f,'%7s \n','---    Pull Sample Results   ---');
fprintf(f,'%7s \n','--------------------------------');

%%%%%%%%%%%%%%%%%%%%%%%%%%%
% Primary Data Processing %
%%%%%%%%%%%%%%%%%%%%%%%%%%%
%---- Specimen Loop ----%
for sn = 1:1

        count = 0;
    if (sn==1),range=[1:14];
    end
    for i = range

        %-------------------------------%
        %---- Specimen Data Reading ----%
        %-------------------------------%
        %Load the Filename for this Iteration of the Loop:
        filename = fullnames(i);
        temp = char(names(i));
        temp = temp(1:6);
        %Load the Respective Specimen Data Using CSV Read:
        dataArray = csvread(filename,2,0);
        %---- Load Data into Arrays ----%
```

```
        %Position in inches (mm) from Instron:
        Position = abs((dataArray(:,2)));
        %Shift Position to Begin at the Origin:
        Position = abs(Position - Position(1))*25.4; %convert in to mm
        %Load in pounds (lb) from Instron:
        Load = (dataArray(:,3))*4.4482216; %convert lb to N
```

```
    %---- Strain in Percent (in) from Extensometer ----%
    %Longitudinal Strain:
    Ext_Strain = ((Position));
    %%%%%%%%%%%%%%%%%%%%
    % Data Manipulation %
    %%%%%%%%%%%%%%%%%%%%
    %Convert Load Data to Stress Data:
    Sig1 = Load / Sig1_Area;
    %---- Find the Peak Load ----%
    PeakLoad(i) = max(Load);
    %---- Sigma 1 Strength Calculations ----%
    %Find Sigma 1 Ultimate Stress (Strength):
    Strength_Sig1(i) = max(Sig1);
    %---- Strain Data Manipulation ----%
    %Process Extensometer Strain to Strain:
    Strain = Ext_Strain/(22.5); %Divides by extensometer gage length
    %Find the index of failure:
    %Based on the peak load seen during the test
    index = find(Load == PeakLoad(i));
    %Find the Failure Strain: (micro-strain)
    Fail_Strain(i) = Strain(index);
```

```
    %%%%%%%%%%%%%%%%%%%%%%%%%%%%%%
    % Print Calculations to File %
    %%%%%%%%%%%%%%%%%%%%%%%%%%%%%%
    %---- Specimen Identification ----%
    fprintf(f,'%7s \n','-----------------');
    %fprintf(f,'%7s %7s \n','Specimen',temp(22:24));
    fprintf(f,'%7s \n','-----------------');
    %---- Peak Load ----%
    %Print Peak Load and Strength Values to Text Document:
    fprintf(f,'%7s %5.0f %s \n','Peak Load',(PeakLoad(i)), ' N');
    %---- Strengths ----%
    %Sigma 1 Strength:
    fprintf(f,'%s %5.1f %s \n','Sigma 1',(Strength_Sig1(i)), ' MPa');
    %---- Areas ----%
    %Print Area 1 Value: (Corresponds to Sigma 1)
    fprintf(f,'%6s %5.1f %s \n','Area 1',Sig1_Area, ' mm^2');
    %---- Failure Strain ----%
    %Print Failure Strain: (independent of stress calculations)
    fprintf(f,'%6s %5.0f %s \n','Failure Strain',Fail_Strain(i),...
        ' micro-strain');

    %---- Generate Stress-Strain Plots ----%
    %---- Figures for Data ----%
    if sn == 1
        %Figure for Longitudinal Sttress-Strain:
```

```
            figure(5)
            hold on;
            plot(Strain(1:index),Sig1(1:index));
            xlabel('Strain');
            ylabel('Stress (MPa)');
        end
```

```
        %---- End of Loop Cleanup ----%
        %Clear the Position, Load, dataArray, and index Variables
        %is manually setup to work specifically with given data as to give
        %desired graphs
        if (count == 0)
            Positioncheck0=Position;
            Loadcheck0=Load;
            Stresscheck0=Sig1;
            Straincheck0=Strain;
        elseif (count == 1)
            Positioncheck1=Position;
            Loadcheck1=Load;
            Stresscheck1=Sig1;
            Straincheck1=Strain;
        elseif (count == 2)
            Positioncheck2=Position;
            Loadcheck2=Load;
            Stresscheck2=Sig1;
            Straincheck2=Strain;

            for a= 1:1399

Positionave(a,1)=((Positioncheck0(a,1)+Positioncheck1(a,1)+Positioncheck2(a,1))/3);
                Loadave(a,1)=((Loadcheck0(a,1)+Loadcheck1(a,1)+Loadcheck2(a,1))/3);
                Stressave(a,1)=((Stresscheck0(a,1)+Stresscheck1(a,1)+Stresscheck2(a,1))/3);
                Strainave(a,1)=((Straincheck0(a,1)+Straincheck1(a,1)+Straincheck2(a,1))/3);
            end

            figure(7)
            subplot(2,1,1);
            plot(Positionave(1:index),Loadave(1:index));
            xlabel('Actuator Displacement (mm)');
            ylabel('Applied Load (N)');
            hold on;
            %---- Subplot for Sigma 1 Stress-Strain ----%
            subplot(2,1,2);
            plot(Strainave(1:index),Stressave(1:index));
            xlabel('Strain');
            ylabel('Stress (MPa)');
            hold on;

        elseif (count == 3)
            Positioncheck0=Position;
            Loadcheck0=Load;
            Stresscheck0=Sig1;
            Straincheck0=Strain;
```

```
        elseif (count == 4)
             Positioncheck0=Position;
             Loadcheck0=Load;
             Stresscheck0=Sig1;
             Straincheck0=Strain;

         elseif (count == 5)
             Positioncheck0=Position;
             Loadcheck0=Load;
             Stresscheck0=Sig1;
             Straincheck0=Strain;

             for a= 1:1225

Positionave(a,1)=((Positioncheck0(a,1)+Positioncheck1(a,1)+Positioncheck2(a,1))/3);
                 Loadave(a,1)=((Loadcheck0(a,1)+Loadcheck1(a,1)+Loadcheck2(a,1))/3);
                 Stressave(a,1)=((Stresscheck0(a,1)+Stresscheck1(a,1)+Stresscheck2(a,1))/3);
                 Strainave(a,1)=((Straincheck0(a,1)+Straincheck1(a,1)+Straincheck2(a,1))/3);
             end
             figure(8)
             subplot(2,1,1);
             plot(Positionave(1:index),Loadave(1:index),'--');
             xlabel('Actuator Displacement (mm)');
             ylabel('Applied Load (N)');
             hold on;
             %---- Subplot for Sigma 1 Stress-Strain ----%
             subplot(2,1,2);
             plot(Strainave(1:index),Stressave(1:index),'--');
             xlabel('Strain');
             ylabel('Stress (MPa)');
             hold on;

          elseif (count == 6)
             Positioncheck0=Position;
             Loadcheck0=Load;
             Stresscheck0=Sig1;
             Straincheck0=Strain;
         elseif (count == 7)
             Positioncheck1=Position;
             Loadcheck1=Load;
             Stresscheck1=Sig1;
             Straincheck1=Strain;

             for a= 1:1133
             Positionave(a,1)=((Positioncheck0(a,1)+Positioncheck1(a,1))/2);
             Loadave(a,1)=((Loadcheck0(a,1)+Loadcheck1(a,1))/2);
             Stressave(a,1)=((Stresscheck0(a,1)+Stresscheck1(a,1))/2);
             Strainave(a,1)=((Straincheck0(a,1)+Straincheck1(a,1))/2);
        end

             figure(7)
             subplot(2,1,1);
             plot(Positionave(1:index),Loadave(1:index),'-.');
             xlabel('Actuator Displacement (mm)');
```

```
            ylabel('Applied Load (N)');
            hold on;
            %---- Subplot for Sigma 1 Stress-Strain ----%
            subplot(2,1,2);
            plot(Strainave(1:index),Stressave(1:index),'-.');
            xlabel('Strain');
            ylabel('Stress (MPa)');
            hold on;

        elseif (count == 8)
            Positioncheck0=Position;
            Loadcheck0=Load;
            Stresscheck0=Sig1;
            Straincheck0=Strain;

            for a= 1:1096
                Positionave(a,1)=((Positioncheck0(a,1)));
                Loadave(a,1)=((Loadcheck0(a,1)));
                Stressave(a,1)=((Stresscheck0(a,1)));
                Strainave(a,1)=((Straincheck0(a,1)));
            end

            figure(8)
            subplot(2,1,1);
            plot(Positionave(1:index),Loadave(1:index));
            xlabel('Actuator Displacement (mm)');
            ylabel('Applied Load (N)');
            hold on;
            %---- Subplot for Sigma 1 Stress-Strain ----%
            subplot(2,1,2);
            plot(Strainave(1:index),Stressave(1:index));
            xlabel('Strain');
            ylabel('Stress (MPa)');
            hold on;

        elseif (count == 9)
            Positioncheck0=Position;
            Loadcheck0=Load;
            Stresscheck0=Sig1;
            Straincheck0=Strain;
        elseif (count == 10)
            Positioncheck1=Position;
            Loadcheck1=Load;
            Stresscheck1=Sig1;
            Straincheck1=Strain;
        elseif (count == 11)
            Positioncheck2=Position;
            Loadcheck2=Load;
            Stresscheck2=Sig1;
            Straincheck2=Strain;

            for a= 1:946

Positionave(a,1)=((Positioncheck0(a,1)+Positioncheck1(a,1)+Positioncheck2(a,1))/3);
```

```
            Loadave(a,1)=((Loadcheck0(a,1)+Loadcheck1(a,1)+Loadcheck2(a,1))/3);
            Stressave(a,1)=((Stresscheck0(a,1)+Stresscheck1(a,1)+Stresscheck2(a,1))/3);
            Strainave(a,1)=((Straincheck0(a,1)+Straincheck1(a,1)+Straincheck2(a,1))/3);
        end

        figure(7)
        subplot(2,1,1);
        plot(Positionave(1:index),Loadave(1:index));
        xlabel('Actuator Displacement (mm)');
        ylabel('Applied Load (N)');
        hold on;
        %---- Subplot for Sigma 1 Stress-Strain ----%
        subplot(2,1,2);
        plot(Strainave(1:index),Stressave(1:index));
        xlabel('Strain');
        ylabel('Stress (MPa)');
        hold on;

    elseif (count == 12)
        Positioncheck0=Position;
        Loadcheck0=Load;
        Stresscheck0=Sig1;
        Straincheck0=Strain;
    elseif (count == 13)
        Positioncheck1=Position;
        Loadcheck1=Load;
        Stresscheck1=Sig1;
        Straincheck1=Strain;

        for a= 1:718
            Positionave(a,1)=((Positioncheck0(a,1)+Positioncheck1(a,1))/2);
            Loadave(a,1)=((Loadcheck0(a,1)+Loadcheck1(a,1))/2);
            Stressave(a,1)=((Stresscheck0(a,1)+Stresscheck1(a,1))/2);
            Strainave(a,1)=((Straincheck0(a,1)+Straincheck1(a,1))/2);
        end

        figure(8)
        subplot(2,1,1);
        plot(Positionave(1:index),Loadave(1:index));
        xlabel('Actuator Displacement (mm)');
        ylabel('Applied Load (N)');
        hold on;
        %---- Subplot for Sigma 1 Stress-Strain ----%
        subplot(2,1,2);
        plot(Strainave(1:index),Stressave(1:index));
        xlabel('Strain');
        ylabel('Stress (MPa)');
        hold on;
    end

    clearvars Position Load dataArray index;
    saveas(figure(5),sprintf('Longitudinal_Stress_Strain.emf'));
    saveas(figure(7),sprintf('Averages .emf'));
    saveas(figure(8),sprintf('Averages with Primer.emf'));
```

```
        %Step the counter
        count = count + 1;
        %Save specimen name to the used names vector
        usednames(count) = names(i);
        %-- End Specimen Loop --%

    end

    %---- Clear Variables ----%
    clearvars count

end

%---- Save Figures ----%
        saveas(figure(5),sprintf('Longitudinal_Stress_Strain.emf'));
        saveas(figure(7),sprintf('Averages without Primer.emf'));
        saveas(figure(8),sprintf('Averages with Primer.emf'));
%Close the Text File:
fclose(f);

%%%%%%%%%%%%%%%%%%%%
% Revision History %
%%%%%%%%%%%%%%%%%%%%
%Heaviliy adpated by Maxwell Blais from previous code written by Camerin Seigars for use in
%determining the interfacial strength of a pull sample
```

Published with MATLAB® R2019a

APPENDIX B: MATLAB Script for Computing Raw Data from Peel Tests to Usable Data

```
%%%%%%%%%%%%%%%%%%%%%%%%%%%%%%%%%%%%%%%%%%%%%%%%%%%%%%%%%%%%%%%%%%%%%%%%
%         Instron 3D Print on Fabric Peel Test                %
%%%%%%%%%%%%%%%%%%%%%%%%%%%%%%%%%%%%%%%%%%%%%%%%%%%%%%%%%%%%%%%%%%%%%%%%
clc,clf,clear;
clf(figure(1));
clf(figure(2));
clf(figure(3));
clf(figure(4));

%%%%%%%%%%%%%%%%%%%%%%%%%%%%%%%%%%%%%%%%%%%%%%%%%%%%%%%%%%%%%%%%%%%%%%%%
%------- PLEASE CHANGE PATH TO WHERE THE DATA IS LOCATED!--------%
%%%%%%%%%%%%%%%%%%%%%%%%%%%%%%%%%%%%%%%%%%%%%%%%%%%%%%%%%%%%%%%%%%%%%%%%
path ='C:\Users\;
%%%------- ONLY DATA TO BE PROCESSED SHALL BE LOCATED IN DIRECTORY -----%%%
files = dir(fullfile(path,'*.csv'));
info = struct2cell(files(:));
names= info(1,:);
fullnames = string(fullfile(path,names));
numfiles = length(names);
%clear files info;

%---- Calculate the Areas ----%
%Area in this case is the width and length of peel sample in millimeters
adhesionstress_Area = 25.4*152;
%Name the File Information is Saved to:
fname='Peel Sample Data.txt';
f = fopen(fname,'wt');
%Excel Sheet information is at the end

%
%%%%%%%%%%%%%%%%%%%%%%%%%%%
% Initial Text File Header %
%%%%%%%%%%%%%%%%%%%%%%%%%%%
fprintf(f,'%7s \n','----------------------------------');
fprintf(f,'%7s \n','---           Instron          ---');
fprintf(f,'%7s \n','---    Peel Testing Results    ---');
fprintf(f,'%7s \n','----------------------------------');
```

```
%%%%%%%%%%%%%%%%%%%%%%%%%%%
% Primary Data Processing %
%%%%%%%%%%%%%%%%%%%%%%%%%%%
%---- Specimen Loop ----%
for sn = 1:1
```

```
        count = 1;
    if (sn==1),range=[1:numfiles];  %Change range to amount of files being read at the time
(could be a simpler function
    end
    for i = range
```

```
        %-------------------------------%
        %---- Specimen Data Reading ----%
```

```
%------------------------------%
%Load the Filename for this Iteration of the Loop:
filename = fullnames(i);
%Load the Respective Specimen Data Using CSV Read:
dataArray = readmatrix(filename);
%---- Load Data into Arrays ----%
%Time in seconds (s) from Instron:
Time = abs((dataArray(:,1)));
%Position in inches (mm) from Instron:
Position = abs((dataArray(:,2)));
%Shift Position to Begin at the Origin:
Position = abs(Position - Position(1));
%Load in pounds (lb) from Instron:
Load = (dataArray(:,3));
```

```
%%%%%%%%%%%%%%%%%%%%
% Data Manipulation %
%%%%%%%%%%%%%%%%%%%%
%Convert Load Data to Stress Data:
%Stress Sigma 1: Nominal Longitudinal & Transverse
%N/mm^2
adhesionstress = Load / adhesionstress_Area;
%N/mm
adhesionstrength = Load / (adhesionstress_Area/152);
%---- Find the Peak Load ----%
PeakLoad(i) = max(Load);
%---- Sigma 1 Strength Calculations ----%
%Find Sigma 1 Ultimate Stress (Strength), Likely Unneeded:
Strength_Stress(i) = max(adhesionstress);
%Find Maximum Adhesion Strength Found in N/mm, Likely Unneeded
Adhesion_Strength(i)=max(adhesionstrength);
```

```
%%%%%%%%%%%%%%%%%%%%%%%%%%%%%%
% Print Calculations to File %
%%%%%%%%%%%%%%%%%%%%%%%%%%%%%%
%---- Specimen Identification ----%
fprintf(f,'%7s \n','-----------------');
%fprintf(f,'%7s %7s \n','Specimen',temp(22:24));
fprintf(f,'%7s \n','-----------------');
%---- Peak Load ----%
%Print Peak Load and Strength Values to Text Document:
fprintf(f,'%7s %5.0f %s \n','Peak Load',(PeakLoad(i)), ' N');
%---- Strengths ----%
%Sigma 1 Strength:
fprintf(f,'%s %5.3f %s \n','Sigma 1',(Strength_Stress(i)), ' MPa');

%Max Adhesion Strength:
fprintf(f,'%s %5.2f %s \n','Adhesion Strength',(Adhesion_Strength(i)), ' N/mm');

%---- Areas ----%
%Print Area 1 Value: (Corresponds to Sigma 1)
fprintf(f,'%6s %5.1f %s \n','Area 1',adhesionstress_Area, ' mm^2');
```

```
%%%%%%%%%%%
% Plotting %
```

```
%%%%%%%%%%
%---- Generate Figure with Four Subplots ----%
%---- Figure For Data ----%
figure(sn)
hold on;
%---- Subplot for Load-Displacement ----%
subplot(2,2,1);
plot(Position,Load);
xlabel('Actuator Displacement (mm)');
ylabel('Applied Load (N)');
hold on;
%---- Subplot for Sigma 1 Stress-Strain ----%
subplot(2,2,2);
plot(Position,adhesionstrength);
xlabel('Actuator Displacement (mm)');
ylabel('Adhesion Strength (N/mm)');
hold on;
%---- Subplot for Sigma 2 Stress-Strain ----%
subplot(2,2,3);
plot(Position,adhesionstrength);
xlabel('Actuator Displacement (mm)');
ylabel('Adhesion Strength (N/mm)');
hold on;
%---- Subplot for Sigma 3 Stress-Strain ----%
subplot(2,2,4);
plot(Time,adhesionstrength);
xlabel('Time (s)');
ylabel('Adhesion Strength (N/mm)');
hold on;
%---- Generate Figure with Two Subplots ----%
%---- Figure For Data ----%
figure(2)
hold on;
%---- Subplot for Load-Displacement ----%
subplot(2,1,1);
plot(Position,Load);
xlabel('Actuator Displacement (mm)');
ylabel('Applied Load (N)');
hold on;
%---- Subplot for Sigma 1 Stress-Strain ----%
subplot(2,1,2);
plot(Position,adhesionstrength);
xlabel('Actuator Displacement (mm)');
ylabel('Adhesion Strength (N/mm)');
hold on;
%---- Generate Stress-Strain Plots ----%
%---- Figures for Data ----%
if sn == 1

    %Figure for Time and Adhesion Strength with Peaks:
    figure(3)
    findpeaks(adhesionstrength,Time);
    [maxadhesion, maxtime] = findpeaks(adhesionstrength,Time);
    [maxtimeRows,maxtimeCols] = size(maxtime);
```

```
            startingtime = maxtime(6,1);
            brackettime = (maxtime((maxtimeRows-5),1)-startingtime);
            segmenttime = brackettime/10;

            for LL = [1:9]

                ttime(LL,count) = startingtime + segmenttime * LL;
                dist    = abs(maxtime(:,1) - ttime(LL,count));
                minDist = min(dist);
                minIdx  = find(dist == minDist);
                minIdx(1,1)
                rtime(LL,count) = maxtime(minIdx(1,1));
                pointsadhesion(LL,count) = (maxadhesion(minIdx(1,1)));
            end

            xlabel('Time (s)');
            ylabel('Adhesion Strength (N/mm)');
            hold on;
        end

        if sn == 1
            %Figure for Time and Adhesion Strength with Peaks:
            figure(4)
            plot(Time,adhesionstrength);
            xlabel('Time (s)');
            ylabel('Adhesion Strength (N/mm)');
            hold on;
        end

        %Save specimen name to the used names vector
        usednames(count) = names(i);
        %Add to count for next file
        count = count + 1;

        %-- End Specimen Loop --%

        %---- Save Excel Sheet ----%
    %Sheet Was Specialized for 17 Specific Samples
    %if less samples are used the additional writings have to be commented out
    sheetfile = 'Peel Adhesion Values.xlsx';
    %Cell formating for Excel Sheet
    cell(i) = 11*i-5;
    cellformatname = "%s%d";
    cellformatdata = "%s%d%s%s%d";
    cellplacea(i) = sprintf(cellformatname,'A',cell(i));
    cellplacedata(i) = sprintf(cellformatdata,'A',cell(i)+1,':','B',cell(i)+1);
    cellplacename(i) = sprintf(cellformatdata,'A',cell(i)+2,':','A',cell(i)+2+8);
    cellplaceadhesion(i) = sprintf(cellformatdata,'B',cell(i)+2,':','B',cell(i)+2+8);

    writecell(usednames(1,i),sheetfile,'Sheet',1,'Range', cellplacea(i));

    Text = ["Time (s)","Adhesion Strength (N/mm)"];

    writematrix(Text,sheetfile,'Sheet',1,'Range', cellplacedata(i));
```

```
    writematrix(rtime(1:9,i),sheetfile,'Sheet',1,'Range', cellplacename(i));

    writematrix(pointsadhesion(1:9,i),sheetfile,'Sheet',1,'Range', cellplaceadhesion(i));


    end

    %%%%%%%%%%%%%%%%%%%%%%%%%%%%
    % Final Figure Manipulation %
    %%%%%%%%%%%%%%%%%%%%%%%%%%%%
    %---- Assign Legend to figure ----%
    if sn == 1
    %---- Figure 1 Formatting ----%
    figure(1);
    hold on;
    subplot(2,2,1);
    ax = gca;
    ax.YAxis.Exponent = 0;
    ax.XAxis.Exponent = 0;
    set(gca,'FontSize',10);
    %ylim([0 3]);
    %xlim([0 350]);
    pos=get(gca,'position'); pos(1)=0.85*pos(1); pos(3)=0.85*pos(3);...
       set(gca,'position',pos);
    subplot(2,2,2);
    ax = gca;
    ax.YAxis.Exponent = 0;
    ax.XAxis.Exponent = 0;
    set(gca,'FontSize',10);
    %xlim([0 200]);
    %ylim([0 7]);
    pos=get(gca,'position'); pos(1)=0.85*pos(1); pos(3)=0.85*pos(3);...
        set(gca,'position',pos);
    subplot(2,2,3);
    ax = gca;
    ax.YAxis.Exponent = 0;
    ax.XAxis.Exponent = 0;
    set(gca,'FontSize',10);
    %xlim([0 20000]);
    %ylim([0 7]);
    pos=get(gca,'position'); pos(1)=0.85*pos(1); pos(3)=0.85*pos(3);...
        set(gca,'position',pos);
    subplot(2,2,4);
    ax = gca;
    ax.YAxis.Exponent = 0;
    ax.XAxis.Exponent = 0;
    set(gca,'FontSize',10);
    %ylim([0 7]);
    %xlim([0 160]);
    pos=get(gca,'position'); pos(1)=0.85*pos(1); pos(3)=0.85*pos(3);...
        set(gca,'position',pos);
    set(gcf,'units','inches','Position',[1 1 12 6]);
    legend(usednames,'units','inches','Position',[10.5 3 0.25 1],'Interpreter','none');
```

```
%---- Figure 2 Formatting ----%
figure(2);
hold on;
subplot(2,1,1);
ax = gca;
ax.YAxis.Exponent = 0;
ax.XAxis.Exponent = 0;
set(gca,'FontSize',10);
pos=get(gca,'position'); pos(1)=0.85*pos(1); pos(3)=0.85*pos(3);...
    set(gca,'position',pos);
subplot(2,1,2);
ax = gca;
ax.YAxis.Exponent = 0;
ax.XAxis.Exponent = 0;
set(gca,'FontSize',10);
pos=get(gca,'position'); pos(1)=0.85*pos(1); pos(3)=0.85*pos(3);...
    set(gca,'position',pos);
set(gcf,'units','inches','Position',[14 1 12 6]);
legend(usednames,'units','inches','Position',[10.5 3 0.25 1],'Interpreter','none');
%---- Figure 3 Formatting ----%
figure(3);
hold on;
ax = gca;
 ax.YAxis.Exponent = 0;
 ax.XAxis.Exponent = 0;
set(gca,'FontSize',10);
%ylim([0 7]);
%xlim([0 160]);
pos=get(gca,'position'); pos(1)=0.85*pos(1); pos(3)=0.85*pos(3);...
set(gca,'position',pos);
set(gcf,'units','inches','Position',[1 8 12 6]);
legend(usednames,'units','inches','Position',[10.5 3 0.25 1],'Interpreter','none');

%---- Figure 4 Formatting ----%
figure(4);
hold on;
ax = gca;
 ax.YAxis.Exponent = 0;
 ax.XAxis.Exponent = 0;
set(gca,'FontSize',10);
%ylim([0 7]);
%xlim([0 80]);
pos=get(gca,'position'); pos(1)=0.85*pos(1); pos(3)=0.85*pos(3);...
set(gca,'position',pos);
set(gcf,'units','inches','Position',[14 8 12 6]);
legend(usednames,'units','inches','Position',[10.5 3 0.25 1],'Interpreter','none');

end
```

```
%%%%%%%%%%%%%%%%%%%%%%%%%%
% Mean & COV Calculations %
%%%%%%%%%%%%%%%%%%%%%%%%%%
%Formatting Line:
fprintf(f,'%7s \n','--------------------------------');
```

```
    %Average Properties Label:
    fprintf(f,'%7s \n','Average Properties');
    %Formatting Line:
    fprintf(f,'%7s \n','--------------------------------');

    %Sigma 1 Strength
    fprintf(f,'%s %5.3f %s \n', 'Mean Stress 1: ',...
        (mean(Strength_Stress(range))), ' MPa');
    %Maximum Adhesion Strength
    fprintf(f,'%s %5.2f %s \n', 'Mean Adhesion Strength of All Samples: ',...
        (mean(Adhesion_Strength(range))), ' N/mm');
    %Find the COV on Strength, likely irrelivant:
    COV_S1(sn) = std(Strength_Stress(range))/mean(Strength_Stress(range));
    fprintf(f,'%s %5.1f %s \n', 'Strength 1 COV: ',(COV_S1(sn)*100), ' %');

    %---- Clear Variables ----%
    clearvars count
    Strength = [];

    %Close the Text File:
    fclose(f);
end

%---- Save Figures ----%
saveas(figure(1),sprintf('Longitudinal_4subplots.fig'));
saveas(figure(2),sprintf('Longitudinal_2subplots.fig'));
saveas(figure(3),sprintf('Longitudinal_Strength_Time.fig'));
saveas(figure(4),sprintf('Longitudinal_Strength_Time_NoPeaks.fig'));

disp('File has Finished Uploading');

%Software by Maxwell Blais: 4/5/2022
%For Peel Testing Of 3D Printed Fabric Samples
```

Published with MATLAB® R2019a

BIOGRAPHY OF THE AUTHOR

Maxwell Blais was born in Portland, Maine on May 10th, 1997. He was raised initially in Gorham, Maine and then in Farmington, Maine where he graduated from Mt. Blue High School. Maxwell then attended the University of Maine, majoring in Mechanical Engineering. He received his Bachelor of Science degree in Mechanical Engineering with a minor in mathematics and robotics in 2019, as well as being part of the Francis Crowe Society. Maxwell then went on to work with the Advanced Structures and Composites Center at the University of Maine the summer of 2019. Maxwell Blais is a candidate for the Master of Science degree in Mechanical Engineering from the University of Maine in December 2022.